

NANOSIZED CROSSLINKED PROTEIN AGGREGATES (NANO-CLPA)

By

ANASTASIA ZAKHARYUTA

Submitted to the Graduate School of Engineering and Natural Sciences
in partial fulfillment of
the requirements for the degree of
Doctor of Philosophy

Sabanci University

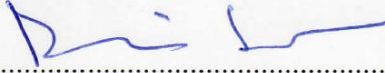
October 2015

NANOSIZED CROSSLINKED PROTEIN AGGREGATES (NANO-CLPA)

APPROVED BY:

Asst. Prof. Dr. Alpay Taralp 
(Thesis Supervisor)

Assoc. Prof. Dr. Batu Erman 

Asst. Prof. Dr. Deniz Sezer 

Prof. Dr. Uğur Sezerman 

Asst. Prof. Dr. Burcu Kaplan Türköz 

DATE OF APPROVAL: 05/10/2015

© Anastasia Zakharyuta 2015

All Rights Reserved

NANOSIZED CROSSLINKED PROTEIN AGGREGATES (NANO-CLPA)

Anastasia Zakharyuta

Biological Sciences and Bioengineering PhD Thesis, 2015

Thesis Supervisor: Alpay Taralp

Keywords: crosslinked protein aggregates, heterogeneous phase catalyst, nanoparticle

Abstract

Kinetic limitations associated with heterogeneous phase reaction for micron size catalyst formulations so far have been addressed by bottom-up approach, which while successful through a number of methods tends to involve laborious procedures, high production costs and is restricted to a limited number of proteins.

This study presents the top-down approach, based on physical downsizing of conveniently fabricated crosslinked protein aggregates (CLPA) or herein developed crosslinked protein lyophilizates (CLPL). This method, while retaining both process convenience/generality and stability advantages associated with crosslinking of CLPA leads to nano-particle formulations of adjustable size, applicable on a wide range of proteins, independent of their purity grade.

Crosslinked protein micron-sized aggregates were prepared by crash precipitation of soluble proteins, alternatively lyophilizates were prepared. The solid proteins were chemically or dehydrothermally crosslinked, forming insoluble powders. The crosslinked

precursors were then nanonized, realized through application of mechanical or hydrodynamic shear, facilitated by an optimal medium.

Herein, conventional CLPA synthesis was optimized as to facilitate subsequent downsizing. Alternative CLPA/CLPL formulations were also developed, addressing challenges posed by particular protein types, addressing suboptimal overall synthesis yields and/or catalytic activity. Various parameters, such as precursor crosslinked material properties, shear rate and time and downsizing medium composition were employed in nanonization procedure optimization. Catalytically active nano-particles on the range of 100-900 nm were generated.

The nanonized aggregates described herein serve to highlight a number of potential advantages in industrial, analytical and biomedical fields. A preliminary *in vitro* study showed successful internalization of nanosized CLPAs in different mammalian cell cultures in the formulation dependant manner, raising hopes for novel systemic and local protein-based therapeutics.

NANO ÇAPRAZ BAĞLI PROTEİN AGREGATLAR (NANO-CLPA)

Anastasia Zakharyuta

Biyoloji Bilimleri ve Biyomühendislik Doktora Tezi, 2015

Tez Danışmanı: Alpay Taralp

Anahtar kelimeler: çapraz bağlı agregalar, heterojen faz katalizi, nanoparçacık

Özet

Şimdiye kadar, mikron boyutta katalizör formülasyon durumundaki heterojen faz tepkimeler ile alakalı kinetik sınırlanmalar aşağıdan-yukarı yaklaşımıyla ele alınmıştır. Bu yaklaşım, mevcut bir takım yöntemlerle başarılı olup, zahmetli prosedürler, yüksek üretim maliyeti ve sınırlı sayıda protein için uygulanabilirliği gibi dezavantajlara sahiptir.

Bu çalışma ilk yukarıdan-aşağı yaklaşımı öne sürmekte ve kolay üretilebilir bilinen çapraz bağlı protein agregatların (CLPA) veya bu çalışma kapsamında geliştirilmiş çapraz bağlı protein liyofilizatların (CLPL) fiziksel olarak boyut ufaltma yöntemine dayanmaktadır. Bu yöntem, CLPA/CLPL'ya özgün çapraz bağlamadan kaynaklanan stabilite, üretim kolaylığı ve genel uygulanabilirlik avantajlarını koruyarak, boyutu ayarlanabilir nano-parçacık oluşumuna yol açmaktadır ve yüksek çeşitlilikte protein türü üzerinde, saflık derecelerinden bağımsız olarak, uygulanabilmektedir.

Mikron boyutta çapraz bağlı protein agregatlar çözünen proteinlerden ani çöktürme ile veya, alternatif olarak, liyofilizasyon yöntemiyle hazırlanmıştır. Oluşan katı formda proteinler, çözünmez tozlar oluşturmak üzere, kimyasal veya dehidrotermal olarak çapraz

bağlanmıştır. Bunun ardından, çapraz bağlı bu ön-malzemeler, uygun ortam içerisinde mekanik veya hidrodinamik makaslama gerilimi uygulanarak nanoboyuta indirgenmiştir.

Çalışma kapsamında, boyut ufaltma sürecini kolaylaştırmak amacıyla bilinen CLPA üretim yöntemleri optimize edilmiştir.

Bunun dışında, belirli protein türlerine özgün üretim verimi ve/veya katalitik aktivite sorunlarını gidermek amacıyla, alternatif CLPA/CLPL formülasyonları geliştirilmiştir. Nanonizasyon süreci optimizasyonu, çapraz bağlı ön-malzeme özellikleri, makaslama gerilim hızı ve süresi ve nanonizasyon ortamı gibi parametreler kullanılarak gerçekleştirilmiştir.

100-900 nm boyut aralığında katalitik olarak aktif nano-parçacıklar üretilmiştir.

Bahsi geçen nanonize edilmiş agregatlar, endüstriyel, analitik ve biyomedikal alanlarda çeşitli potansiyel avantajlara sahiptir. Öncü in vitro çalışması, malzeme formülasyonuna bağlı olarak, nano-CLPA/CLPL'ların farklı memeli hücre kültürlerinde hücre tarafından başarılı bir şekilde alınımı gösterilmiştir. Bu sonuç potansiyel yeni sistemik ve lokal protein bazlı ilaç formülasyonların geliştirilmesine ümit vermektedir.

To my dear parents

Acknowledgements

First of all I would like to express my gratitude to my supervisor, Dr. Alpay Taralp, for all of the guidance and support he has provided. I very much appreciate the time and energy he took to encourage me in both academic and personal matters. His wide and unbiased attitude towards any scientific problem and infinite ideas have been very inspiring and strongly influenced my current approach to scientific research. Furthermore, the opportunity of independent research, that he has encouraged, has helped me shape my confidence as a scientist.

My labmates and dear friends, Senem M. Avaz and Tuğçe Akkaş, have been the constant source of support and motivation. I very much appreciate all their help, contributions.

I am very grateful to all the faculty members, of Natural Science and Engineering Faculty for making multidisciplinary guidance and facilities necessary for my research available. In particular, I would like to thank Dr. Batu Erman, who has provided me with an opportunity and guidance to conduct *in vitro* cell culture studies, which not only proved very beneficial to my work but also has left me with the valuable experience in this field. The members of Dr. Erman's research team have also been very helpful; the guidance of Asma Almutadha and former members Dr. Emre Deniz and Dr. Nazlı Keskin is very much appreciated.

I would like to thank members of my thesis jury, Dr. Burcu Kaplan Türköz, Dr. Uğur Sezerman, Dr. Deniz Sezer, and once again Dr. Batu Erman, first of all, for their time and afford and also for their invaluable insights and guidance.

The graduate team members of Biological Sciences and Bioengineering and Material Science and Engineering Programs have all been very helpful and generous in sharing their knowledge and experience. Particularly, I could not be grateful enough to Bahriye Karakaş, for her significant contribution to this work as well as her selfless support and friendship.

This thesis reflects the research associated with the work kindly supported by TÜBİTAK1001 111M680 Project.

On the more personal note; I can hardly imagine this work completed without invaluable support from my friends, they all have been there for me providing motivation, each in their unique way. Evrim Kurtoğlu, who has always been there to say exactly the right thing at exactly the right time, regardless of the severely different time zones; Esen Doğan, who at times didn't even have to say anything with her wonderful empathy abilities; Alper Durmuş, with his limitless energy, has always been the wonderful source of entertainment and great music at the times of my much needed breaks from work; Bora Köksal's ultimate optimism has kept me going at all times. From the bottom of my heart I wish to thank the Kesici family (Eda, Onur and their parents Ihsan and Nurten), whom I view as my second family, for their invaluable support at all times.

I am very grateful to Emrah Süvari for his utter patience, warm support and encouragement throughout the most difficult times of my work.

Last but not least, I would like to thank my whole family, for their constant unconditional love and support. My parents, Fenia and Vyacheslav, have always provided me with inspiration as individuals in general, and scientists in particular, which has encouraged and challenged me to realize my potential. I am forever grateful to my parents, and I would like to dedicate my thesis to them.

Table of Contents

1. Introduction	1
1.1. Protein Immobilization Formulations	1
1.1.1. Protein immobilization rationale	1
1.1.2. Crosslinking	2
1.2. Crosslinked Protein Crystals (CLPC) and Aggregates (CLPA)	4
1.3. Goal of This Study: nano-CLPA	6
2. Crosslinked Protein Aggregates (CLPA) Optimization Using Conventional Techniques and Introduction of Crosslinked Protein Lyophilizates (CLPL) Synthesis	9
2.1. Introduction and Rationale	9
2.2. Materials	12
2.3. General Methods	13
2.3.1. CLPA and CLPL synthesis	13
2.3.2. Characterization	18
2.4. Results and Discussion	21
2.4.1. Preliminary methodology studies	21
2.4.2. Optimization of precursor protein solutions in terms of CLPA synthesis yield and catalytic activity	24
2.4.3. Optimization of aggregation method and protocol in terms of CLPA synthesis and catalytic activity	29
2.4.4. Optimization of crosslinking method and protocol in terms of CLPA synthesis yield and catalytic activity	33
2.4.5. Special case CLPA optimization and Introduction of CLPL	44
3. Generation and Characterization of Nano-CLPA and Nano-CLPL Materials	50
3.1. Introduction and Rationale	50
3.2. Materials	51
3.3. General Methods	52
3.3.1. Nano-CLPA generation	53
3.3.2. Analysis	54
3.4. Results and Discussion	56
3.4.1. Initial methodology development	56

3.4.2.	Optimization of nanonization conditions in terms of nanonization yield and size reduction efficiency and consequent final product catalytic activity.....	67
3.4.3.	Optimization of CLPA synthesis steps in terms of nanonization yield, size and final product catalytic activity.....	82
3.4.4.	Stability of nano-CLPA.....	92
3.4.5.	Applicability of the scale up process.....	94
4.	Nano/Micro-CLEA Formulations for Potential Biomedical Applications.....	96
4.1.	Introduction and Rationale.....	96
4.2.	Materials.....	97
4.3.	Methods.....	97
4.3.1.	Synthesis of albumin, lysozyme, hemoglobin, lysozyme/hemoglobin co-aggregate and alpha-galactosidase CLPA.....	97
4.3.2.	<i>In Vitro</i> Cell Culture Study.....	99
4.3.3.	Characterization.....	102
4.4.	Results and Discussion.....	103
4.4.1.	Lysozyme, hemoglobin and lysozyme/hemoglobin co-aggregate nano-CLPA 103	
4.4.2.	<i>in vitro</i> internalization study on the model of albumin and alpa-galactosidase nano-CLPA.....	112
5.	Conclusion.....	133
	REFERENCES.....	135

List of Figures

Figure 1.1: Protein functional groups at physiological pH.....	2
Figure 1.2: Reaction of amino functionalized species with bifunctional aldehyde	3
Figure 1.3: Reaction of carbodiimides through carboxyl group activation of peptide carboxyl residues, with subsequent amino residue conjugation	4
Figure 1.4: Dehydrothermal crosslinking mode of juxtaposed protein functional groups	7
Figure 2.1: General review of crash precipitation step efficiency.....	22
Figure 2.2: General review of aggregation method effect on relative catalytic activity of CLPA	23
Figure 2.3: General review of crosslinking method effect on relative catalytic activity of CLPA	24
Figure 2.4: Precursor solution effect on CLPA catalytic activity. Trypsin CLPA (aggregated in acetone, glutaraldehyde crosslinked).....	25
Figure 2.5: Precursor solution effect on CLPA catalytic activity. Chymotrypsin CLPA (aggregated 2-propanol, glutaraldehyde crosslinked).....	27
Figure 2.6: Precursor solution effect on crosslinking yield. Trypsin CLPA (aggregated in acetone, glutaraldehyde crosslinked).....	28
Figure 2.7: Aggregation medium effect on aggregation (up) and crosslinking yield (down).Albumin CLPA (pH 7.4 precursor solution, glutaraldehyde crosslinked).....	30
Figure 2.8: Aggregation medium effect on aggregation (up) and crosslinking yield (down). Trypsin CLPA (glutaraldehyde crosslinked).....	31
Figure 2.9: Aggregation medium effect on CLPA catalytic activity. Trypsin CLPA (glutaraldehyde crosslinked).....	33
Figure 2.10: Effect of crosslinking method on CLPA catalytic activity. Trypsin CLPA (pH 4.5 precursor solution, aggregated in 2-propanol).....	35
Figure 2.11: Effect of crosslinking method on CLPA catalytic activity. Chymotrypsin CLPA (pH 7.4 precursor solution, aggregated in 2-propanol)	36
Figure 2.12: Effect of crosslinking reagent (glutaraldehyde) and pH on CLPA catalytic activity. Trypsin CLPA (pH 4.5 precursor solution, aggregated in 2-propanol).....	37
Figure 2.13: Effect of crosslinking reagent (dextran polyaldehyde) and pH on CLPA catalytic activity. Trypsin CLPA (pH 4.5 precursor solution, aggregated in 2-propanol) ...	38

Figure 2.14: Crosslinking degree effect on CLPA catalytic activity. Trypsin CLPA (pH 4.5 precursor solution, aggregated in 2-propanol, crosslinker glutaraldehyde)	
* numbers 1-8 represent amount of crosslinker applied: 1. $1,064 \times 10^{-6}$; 2. $2,12 \times 10^{-6}$;	
3. $0,53 \times 10^{-5}$; 4. $1,06 \times 10^{-5}$; 5. $2,12 \times 10^{-5}$; 6. $3,18 \times 10^{-5}$; 7. $4,24 \times 10^{-5}$; 8. $6,36 \times 10^{-5}$ mol per mg protein	39
Figure 2.15: FTIR spectra of glutaraldehyde crosslinked albumin CLPA. *0 represents native lyophilized albumin and numbers 2-8 represent amount of crosslinker applied: 2. $2,12 \times 10^{-6}$; 4. $1,06 \times 10^{-5}$; 6. $3,18 \times 10^{-5}$; 8. $6,36 \times 10^{-5}$ mol per mg protein	41
Figure 2.16: Ratio of IR band intensities versus crosslinking degree. Glutaraldehyde crosslinked albumin CLPA. * 0 represents native lyophilized albumin and numbers 2-8 represent amount of crosslinker applied: 2. $2,12 \times 10^{-6}$; 3. $0,53 \times 10^{-5}$; 4. $1,06 \times 10^{-5}$; 5. $2,12 \times 10^{-5}$; 6. $3,18 \times 10^{-5}$; 7. $4,24 \times 10^{-5}$; 8. $6,36 \times 10^{-5}$ mol per mg protein	42
Figure 2.17: FTIR spectra of 1. Native lyophilized albumin and 2. Dehydrothermally 3. Glutaraldehyde 4. Dextran polyaldehyde 5. Carbodiimide crosslinked albumin CLPA.....	43
Figure 2.18: Catalytic activity of urease CLPA obtained by “precursor solution pre-crosslink assisted” method.....	45
Figure 2.19: Catalytic activity of urease CLPL	46
Figure 2.20: Catalytic activity of trypsin CLPL	48
Figure 2.21: Catalytic activity of chymotrypsin CLPL	49
Figure 3.1: Flow chart summarizing the overall synthesis and optimization process	52
Figure 3.2: Raw DLS data presentation of crosslinked lysozyme aggregates (a) before and (b) after nanonization with 5 mg/ml potassium iodide	57
Figure 3.3: SEM images of lysozyme (a) CLPA, (b) homogenized and (c) grinded nano-CLPA	58
Figure 3.4: Preliminary review of nanonization method effect relative catalytic activity of CLPA	62
Figure 3.5: Effect of additive incorporation in the homogenization medium on nanonization yield. (Albumin CLPA was homogenized at 20 krpm, 30 min)	64
Figure 3.6: Effect of homogenization time on nanonization efficiency. (Albumin CLPA was homogenized at 20 krpm)	65

Figure 3.7: Effect of homogenization speed on nanonization efficiency. (Albumin CLPA was homogenized for 30 min)	66
Figure 3.8: Effect of glycerol incorporation in aqueous homogenization medium on nanonization efficiency and nano-particle generation yield. (Albumin CLPA was homogenized at 20 krpm, 30 min)	70
Figure 3.9: Effect of ethanol incorporation in homogenization medium on nanonization efficiency and nano-particle generation yield. (Albumin CLPA was homogenized at 20 krpm, 30 min)	72
Figure 3.10: Effect of homogenization speed on nanonization efficiency of albumin CLPA. (homogenized in 30 wt% glycerol for 30 min).....	75
Figure 3.11: Effect of homogenization speed on nanonization efficiency of trypsin CLPA. (homogenized in 50 wt% glycerol for 30 min).....	76
Figure 3.12: Effect of homogenization speed on nanonization efficiency of Savinase® CLEA (CLEA Technologies). (Homogenized in 50 wt% glycerol for 30 min).....	77
Figure 3.13: Effect of homogenization speed on nanonization efficiency of albumin CLPA. (Homogenized in 30 wt% glycerol at 20 krpm)	78
Figure 3.14: Visualization of sample placement prior to homogenization.....	79
Figure 3.15: Effect of particle size on catalytic activity of trypsin CLPA. (sub-optimally formulated CLPA)	81
Figure 3.16: Effect of particle size on catalytic activity of Savinase® CLEA (CLEA Technologies).....	82
Figure 3.17: Comparison of chemically and dehydrothermally crosslinked CLPA nanonization results	84
Figure 3.18: Precursor solution effect on 300 nm nano-CLPA catalytic activity. Trypsin CLPA (aggregated in acetone, glutaraldehyde crosslinked).....	85
Figure 3.19: Aggregation medium effect on 300 nm nano-CLPA catalytic activity. Trypsin CLPA (glutaraldehyde crosslinked).....	86
Figure 3.20: Crosslinking reagent (glutaraldehyde) pH effect on 300 nm nano-CLPA catalytic activity. Trypsin CLPA (pH 4.5 precursor solution, aggregated in 2-propanol) ...	88
Figure 3.21: Crosslinking reagent (dextran polyaldehyde) pH effect on 300 nm nano-CLPA catalytic activity. Trypsin CLPA (pH 4.5 precursor solution, aggregated in 2-propanol) ...	89

Figure 3.22: Effect of particle size on catalytic activity of trypsin CLPL.....	90
Figure 3.23: Effect of precursor CLPA crosslinking degree on nanonization efficiency. (Albumin CLPA homogenized in 50 wt% glycerol at 20 krpm).....	91
Figure 3.24: Effect of precursor CLPA crosslinking degree on catalytic activity of 300nm trypsin nano-CLPA.	92
Figure 3.25: Comparison of scale up and laboratory scale nano-CLPA synthesis efficiency	95
Figure 4.1: Crosslinking method effect on 200 nm hemoglobin nano-CLPA catalytic activity.	104
Figure 4.2: Effect of homogenization speed on size reduction and resultant catalytic activity of dextran polyaldehyde crosslinked hemoglobin CLPA. (CLPA was homogenized in 30 wt% glycerol for 30 min).....	105
Figure 4.3: Crosslinking method effect on 150 nm lysozyme nano-CLPA catalytic activity	107
Figure 4.4: Effect of homogenization speed on size reduction and resultant catalytic activity of dextran polyaldehyde crosslinked lysozyme CLPA. (CLPA was homogenized in 30 wt% glycerol for 30 min)	108
Figure 4.5: Assessment of substrate size versus catalyst particle size relationship on model of dextran polyaldehyde crosslinked lysozyme CLPA. Method 1.: Fluorimetric analysis of small substrate degradation; Method 2.: Optical density detection of bacterial wall degradation. (please see Methods section for detail).....	109
Figure 4.6: Comparison of hemoglobin, lysozyme and hemoglobin/lysozyme CLPA size reduction and resultant activity trends	111
Figure 4.7: Internalization upon incubation with albumin nano-CLPA. HeLa cell culture (glutaraldehyde crosslinked, homogenized in glycerol medium to establish size of 400 nm particle size).....	116
Figure 4.8: Co-localization analysis illustration upon incubation with albumin nano-CLPA and lysosomal staining dye. HeLa cell culture	116
Figure 4.9: Size dependant internalization of albumin nano-particles. HeLa cell culture..	117
Figure 4.10: Internalization of PEGilated albumin nano-CLPA observed HeLa cell culture	119

Figure 4.11: Internalization of PEGilated albumin nano-CLPA observed NIH3T3 cell culture	120
Figure 4.12: Internalization of nano-CLPA upon homogenization in glycerol (left) and ethanol (right). HeLa cell culture.....	122
Figure 4.13: Confocal microscope images of internalized albumin (left) and alpha-galactosidase (centered) nano-CLPA presented against control cells (right) in HCT116 cell culture	123
Figure 4.14: Confocal microscope images of internalized albumin (left) and alpha-galactosidase (centered) nano-CLPA presented against control cells (right) in NIH/3T3 cell culture	123
Figure 4.15: Confocal microscope images of internalized albumin (left) and alpha-galactosidase (centered) nano-CLPA presented against control cells (right) in HEK293 cell culture	124
Figure 4.16: Dosage dependent effect of albumin nano-CLPA on HeLa cell proliferation	125
Figure 4.17: Dosage dependent effect of alpha-galactosidase nano-CLPA on HeLa cell proliferation	126
Figure 4.18: Dosage dependent effect of albumin nano-CLPA on HCT116 cell proliferation	127
Figure 4.19: Dosage dependent effect of alpha-galactosidase nano-CLPA on HCT116 cell proliferation	128
Figure 4.20: Dosage dependent effect of albumin nano-CLPA on NIH/3T3 cell proliferation	129
Figure 4.21: Dosage dependent effect of alpha-galactosidase nano-CLPA on NIH/3T3 cell proliferation	130
Figure 4.22: Dosage dependent effect of albumin nano-CLPA on HEK293 cell proliferation	131
Figure 4.23: Dosage dependent effect of alpha-galactosidase nano-CLPA on HEK293 cell proliferation	132

1. Introduction

1.1. Protein Immobilization Formulations

1.1.1. Protein immobilization rationale

Various protein-based formulations are being routinely used in a wide range of industrial, analytical and biomedical fields¹. The general goal of various immobilization techniques developed over years is to overcome drawbacks of free enzymes as materials such as, low stability under various conditions prescribed by the nature of a given application, short shelf life and lack of reusability^{2,3}. In the particular case of drug delivery formulations, reduced bioavailability by enzymatic degradation or renal filtration, and low cellular uptake efficiency and specificity are crucial points of interest, which merit constant improvement. The existing approaches to immobilization can be generally categorized as physical adsorption, encapsulation, surface immobilization and crosslinking^{4,5}. The later involves covalent bonding of protein alone, or aided by grafting with supplementary protein and/or other organic polymer, and forms the technique of interest in this study falls into the latter category.

1.1.2. Crosslinking

Crosslinking is the process of chemically joining two or more molecules by a covalent bond. Covalent modification and crosslinking of proteins is facilitated through chemical reagent capable of reacting with the specific functional groups naturally present in proteins structure. These groups are constituted of protein amino acid side chains, namely are amino-, carboxy- and sulfhydryl (Figure 1.1).

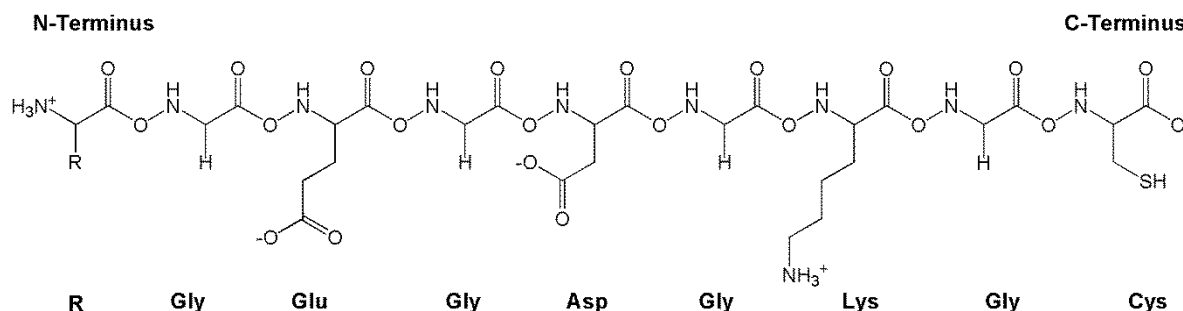


Figure 1.1: Protein functional groups at physiological pH

Sulfhydryl group modification is a widely used method especially where more specific modification modes are required, but will not be further discussed herein⁶

The charged amino acid side chains are generally more abundantly located at the interior of a globular protein, rendering them a susceptible target for intermolecular conjugation. Modification oriented at these functional groups is not specific and mentioned location relatively protects resultant conjugates from dramatic conformational alterations. That being said, improperly-chosen or sub-optimally utilized crosslinkers could knock-out residues important to binding or catalysis without altering the protein global structure, yielding an apparent reduction of overall activity⁷.

Primary amines are present at the N-terminus of a polypeptide chain (α -amine) and in the side chain of lysine (Lys) residues (ϵ -amine). These are subject to modification with N-hydroxy succinimide esters, imidoesters and aldehydes. For the purposes of inter-protein conjugation, bifunctional crosslinking reagents are employed. Aldehyde functional crosslinking reagents were utilized in this study.

Formaldehyde and glutaraldehyde are one of the most abundantly used crosslinking reagent intended for various applications⁸. These are also highly toxic and due to small molecular size can readily penetrate the protein interior and lead to extensive modifications directly affecting areas responsible for catalyst or binding, leading to permanent degradation of catalytic activity. Larger molecular weight alternatives have been preferred in protein modification, due to decreased toxicity and higher specificity towards surface modification. The aldehyde alternative of choice in this study is dextran polyaldehyde, conventionally applied in biomedical applications due its relatively low toxicity⁹. The reaction mechanism of aldehydes with amino residues is demonstrated briefly on Figure 1.2.

The dehydration upon formation of Schiff bases intermediate is reversible and reduction with sodium cyanoborohydride or sodium borohydride is necessary under most reaction conditions. Sodium cyanoborohydride is widely used where milder reduction conditions, but is highly toxic. More reactive sodium borohydride has been used throughout this study. The mechanism illustrated herein is very simplified, in reality glutaraldehyde species in aqueous solutions greatly vary, undergoing aldol condensation to form unsaturated polyaldehyde species. Furthermore, different proposed reaction mechanisms are likely to contribute the overall product crosslinking, particularly varying with pH of glutaraldehyde solution with relation to dominating aqueous species^{10,11}.

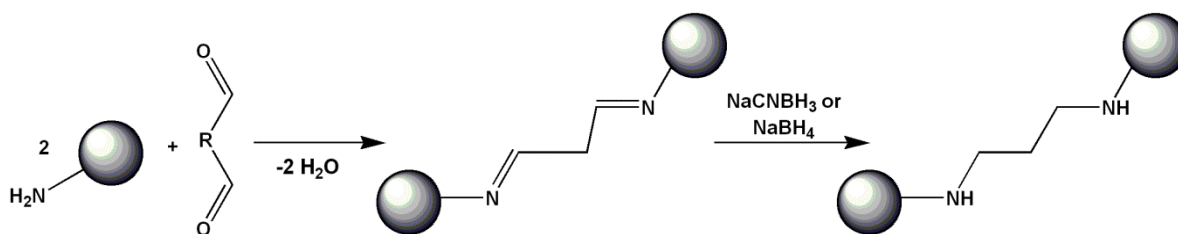


Figure 1.2: Reaction of amino functionalized species with bifunctional aldehyde

Carboxylic functional (-COOH) residues are present at the C-terminus of a polypeptide chain and in the side chains of aspartic acid (Asp) and glutamic acid (Glu). Carboxyls are reactive towards carbodiimides⁷. On the contrary to the described reactions incorporation of carbodiimide reagents leads to zero-length amide bond formation between the reagent activated carboxyl residue and a juxtaposed amino group (Figure 1.3). This method is widely applied in peptide synthesis, but low efficiency is expected upon diffusion

challenged large substrates, due to instability of activated O-acylisourea intermediate. Incorporation of N-hydroxysuccinimide or its analogues stabilizes the carboxyl intermediate, therefore increasing the possible time frame of the potential conjugation.

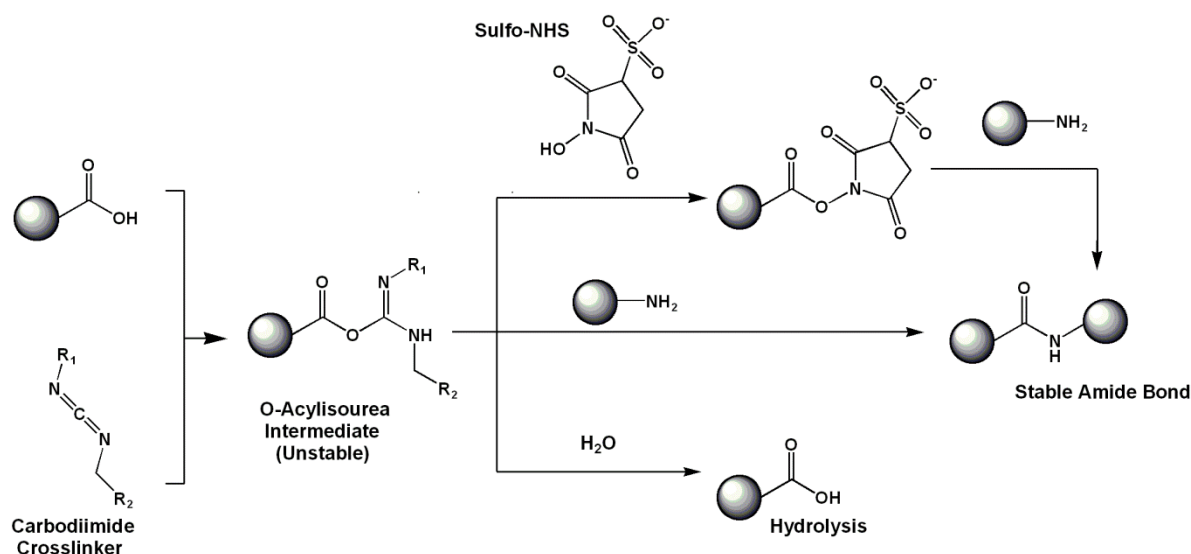


Figure 1.3: Reaction of carbodiimides through carboxyl group activation of peptide carboxyl residues, with subsequent amino residue conjugation

Protein structure and function are closely interconnected, and any possible alterations induced by reagent modification must be taken into account. While non specific crosslinking of proteins in aqueous solution is widely applied, it often isn't optimal and leads to dramatic catalytic activity loss. This issue has been very successfully addressed by introduction of crosslinked protein crystals and aggregates.

1.2. Crosslinked Protein Crystals (CLPC) and Aggregates (CLPA)

Out of conventional crosslinked enzyme formulations, Crosslinked Enzyme Crystals (CLEC), developed by Quioco *et. al.*¹² in 1964, formed and remained the most efficient

example in terms of stability and catalytic performance. Technique was initially developed in an attempt to obtain a stable enzyme crystal formulation for X-ray diffraction studies. During this study it has become apparent that such formulations retained biocatalytic activity, while gaining greatly enhanced mechanical, chemical and thermal stability. Nevertheless, further development of the technique aiming enhanced biocatalyst formulations has not been improved significantly until last two decades, when Vertex Pharmaceuticals have rendered this catalyst commercially available, for a number of proteins¹³.

CLEC provide a very stable formulation with advantage of very pure enzyme content, which implies high catalyst to weight ratio¹⁴⁻¹⁷. That being said, formulations involve a very laborious synthesis process, requires only enzymes of very high purity, and results in low yields, which also implies very high costs of large scale productions. This technique is limited to only certain (crystallizable) enzymes.

Addressing most of the described drawbacks, crosslinked enzyme aggregate technology has been pioneered by Roger Sheldon et. al. CLEA retain very good stability while based on a very general user friendly synthesis process which can also be applied to a very wide range of proteins^{18,19}

The principle of the technique lies within stabilization of proteins in form of aggregates, achieved by crash precipitation. Apparently, the tertiary structural alteration of proteins sterically locked in the relatively rigid aggregate state is prevented throughout the course of chemical modification, resulting in rather robust catalytically active material²⁰. Furthermore, aggregation process serves as a purification step, and is applicable on industrial grade proteins.

The increase in catalytic activity observed in various CLEC and CLEA formulations could be rationalized through neighbor- and crosslinker-induced restrictions of conformational freedom, which would reduce the protein's entropy per unit time. The end result would be Gibbs ground state elevation of individual proteins in the CLPA, yielding more reactive catalysts. While potentially degrading effect of a crosslinking reagent cannot be dismissed, in the optimized formulations it does not appear to dominate.

1.3. Goal of This Study: nano-CLPA

The topic of this study has been inspired by the described CLEC and CLPA materials.

The micron and greater size catalyst introduces an assortment of problems foreign to individual proteins, such as mass transport limitations, reduced access to catalytic centers, restricted catalytic turnover due to crosslinking, and poor bioabsorptivity²¹

When considering solid state catalyst systems it should be noted that Michaelis-Menten analysis only yields apparent values, due to heterogeneous reaction environment. The reaction rate is limited by mass transport and diffusion, reduced access to catalytic centers and restricted catalytic turnover due to crosslinking. Heterogeneous size distribution of particles also leads to unpredictable/poorly reproducible reaction rates. The particle size is particularly important in the case of biomedical applications, which imply cellular internalization. These require very well defined nano-scale particles, depending on the aimed behavior²².

As described earlier, while forming a golden standard of immobilized protein formulations CLECs synthesis is very laborious and resultant particle size is very hard to obtain under 500nm²³. Furthermore, user friendly CLEA synthesis process results in the micron scale end product.

One approach to mitigate these issues has rested on limiting the particle size to the nanoscale so as to optimize substrate turnover, while retaining all the stability advantages associated with crosslinking²⁴. Accordingly, individual protein units have been brought together by way of various bottom-up approaches, yielding nanoscale enzyme particles. While effective, such attempts have generally proven very laborious, expensive, protein-specific, lossy, and impractical towards various target proteins^{25,26}. In contrast, herein this issue is addressed with a generalized procedure suitable for wide range of proteins and applications – Namely, physical nanonization of crosslinked protein aggregate particles. The principle lies within limiting the particle size to the nanoscale so as to optimize substrate turnover, while retaining all the stability advantages associated with crosslinking.

This method should also be nicely applicable to CLEC formulations, but has not been yet attempted. Up till now protein nano-particle formulations have only been attempted by bottom-up approach, technique presented herein is unique in sense that it is based on very general and practical size reduction method.

Depicting the first top-down approach in this area, the success of this strategy rests on nanonizing macroscopic precursors via several means, namely application mechanical and hydrodynamic shear, under optimized media conditions.

In the course of this study conventional CLEA approach was pursued in synthesis of precursor materials. Optimization of these processes has been performed aiming to better accommodate following downsizing procedure. Furthermore, alternative formulations have been developed.

Dehydrothermal crosslinking of lyophilizates strategy, developed in house, is demonstrated on Figure 1.4. Dehydrothermal crosslinking yields zero-length inter-protein amide bonds by thermally dehydrating inter-protein ammonium carboxylate salt bridges under vacuum-assisted conditions. The salt bridges undergoing transformation are made to juxtapose beforehand during the lyophilization step. The thermal stability imparted to proteins in the dry state and the anoxic processing conditions ensure good retention of bioactivity^{27,28}.

Dehydrothermal crosslinking is particularly attractive in preparing biomaterials, since the reagent-free approach eliminates toxicity concerns relating to the use of exogenous chemicals.

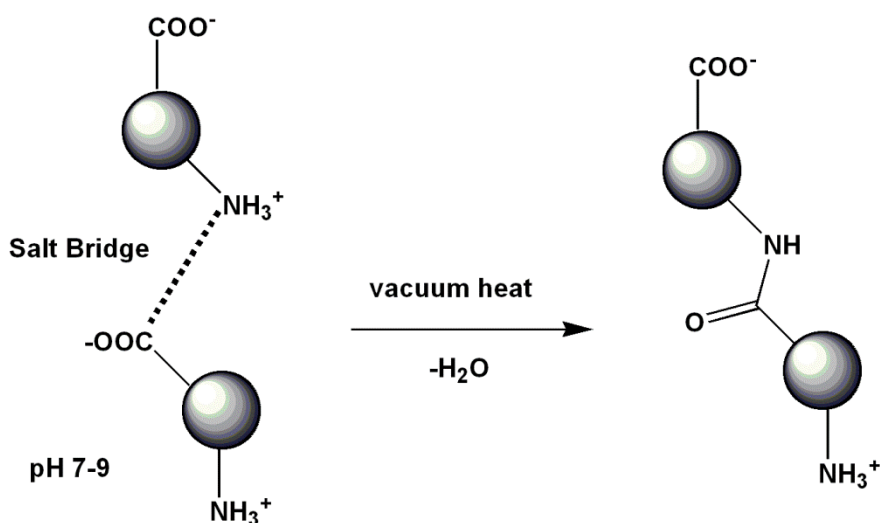


Figure 1.4: Dehydrothermal crosslinking mode of juxtaposed protein functional groups

The “pH memory”, a term coined to signify the retention of functional group ionization states over the course of lyophilization, has allowed one to optimize many water-free, “pH-dependent” chemical transformations of a lyophilized material by appropriately adjusting the pH of the protein solution prior to lyophilization^{29,30}.

Furthermore, inspired by the efficiency of the lyophilizate approach above, chemical crosslinking of lyophilizates in organic media was attempted on challenging protein formulations where dehydrothermal method efficiency failed to yield plausibly, giving rise to yet another convenient alternative: crosslinked protein lyophilizate (CLPL) formulations. Nano-CLEA formulations are aimed to provide a beneficial alternative to conventional protein formulation as well establish new potential products.

Industrial nanoCLEA could address already widely explored fields such as detergent, textile, leather industry, food, animal feed industry and biodiesel production and waste treatment. Those of course are mainly hydrolytic enzymes and the starting material for some of the applications can be very crude. In terms of organic synthesis, novel greener catalysis, involving much milder conditions are being attempted, with less hazardous reagent, to achieve industrially important small organics synthesis. Stability of the nanoCLEA under extreme temperature, pH, and organic solvents conditions makes it a very plausible potential catalyst. In analytical field products such as, sensory and diagnostic test enzymes, chromatography media, artificial antibodies are targeted.

Potential biomedical applications along with biosensors³¹ also include both systemic and local therapeutics, aiming topical and internal delivery systems^{32,33}.

2. Crosslinked Protein Aggregates (CLPA) Optimization Using Conventional Techniques and Introduction of Crosslinked Protein Lyophilizates (CLPL) Synthesis

2.1. Introduction and Rationale

This chapter aims to describe a general methodology leading to crosslinked protein aggregates (CLPA) as well as techniques to optimize specific products on the basis of protein type. It further introduces the concept of crosslinked protein lyophilizates (CLPL), which have been developed over the course of this study.

Initial studies performed on a number of proteins are briefly described in this chapter to exemplify each step of the overall work. Optimization of the method has been described in detail on protein models including albumin, trypsin and chymotrypsin. Albumin was chosen as an initial model due to its stability and ease of manipulation. Trypsin and chymotrypsin were chosen to model the catalysis of proteins transformed into their respective CLPAs. Their successful preparation as CLPAs also served to highlight the facility of this method in handling autolytic proteins in particular, and forecast similar benefits in handling all proteins with limited solution-state stability. The CLPA method was also modified to successfully process exceptionally user-unfriendly models such as urease, which afforded poor aggregation recoveries, low crosslinking yields and near-zero retention of bioactivity when processed using established CLPA fabrication methods. In addressing the technical challenges posed by urease, an alternative general aggregation-crosslinking method was envisaged to bypass similar intrinsic challenges posed by other user-unfriendly proteins. The outcome of that research yielded crosslinked protein lyophilizates, i.e., CLPL,

whose success primarily rested on an alternative route to enforce protein aggregation. The promise of the CLPL method has since been demonstrated on several protein systems.

The preparation and optimization of CLPAs in this thesis are based on revisions and additions to original work as described by Sheldon *et al.* Some aspects include:

Aggregation via salting-out or use of anti-solvent

Aggregation is normally achieved through crash precipitation of an aqueous protein solution. To achieve this end, the protein solution is delivered to a stirred vessel containing a suitable high salt aqueous medium or miscible organic antisolvent. Typical media used to crash-precipitate have included concentrated aqueous ammonium sulfate, polymers and acetone. Long-established alternatives to precipitate protein, such as isoelectric point precipitations, have proved lower yielding when used alone. Where appropriate, these techniques can be integrated into the crash precipitation step in order to optimize aggregation. For instance, for optimal results, the solution pH value can be matched to the protein pI immediately before salting-out is conducted.

Aggregation enforced by lyophilization

Later described in this work, the use of lyophilization instead of crash precipitation has been established as the method of choice to handle proteins, which showed poor aggregation out of solution or intolerance to normal aggregation conditions as marked by a dramatic loss of activity. Since material loss cannot occur during freezing and drying, it was rationalized that the protein aggregate could be successfully and quantitatively obtained out of solution through lyophilization in cases where crash precipitation did not give the desired result. The one downside of lyophilization over conventional crash-precipitation is the extra time and equipment needed to dry the material. As part of the lyophilization procedure, optimally formulated protein solutions were lyophilized and later immersed in a medium – generally an organic solvent - to facilitate the subsequent crosslinking step (*vide infra*). The benefits of aggregation via lyophilization were readily apparent in terms of the ease of aggregate recovery and process optimization, high overall yields, predictable bioactivity, and easy handling of the dried products for further manipulation.

Crosslinking

Covalent crosslinking was achieved via conventional techniques, which utilized reaction of protein side chain or terminal functional groups as a means to afford the insoluble crosslinked aggregate. These non-specific techniques primarily target the surface-exposed and thus chemically reactive amino- and carboxyl- residues. Some reagents and factors have been listed below, which prompt covalent crosslinking.

Aldehydes

Glutaraldehyde is the most commonly used crosslinking reagent in general as well as aldehyde. Its crosslinking efficiency is generally high for proteins undergoing reaction under homogeneous phase conditions as well as for aggregated protein powders dispersed in solvent. In proteins with low surface lysyl group content, dextran polyaldehyde has shown higher yields. Dextran polyaldehyde also provides for milder reaction conditions and reduced toxicity risks, thus explaining its preferred use in many biomedical applications. Yet another important rationale supporting its use over glutaraldehyde is its greater steric bulk. This trait could presumably limit its approach to the active center of enzymes, thus reducing the likelihood of deactivation via inadvertent reaction with a lysyl residue involved in binding or catalysis. Aldehyde crosslinked protein-protein aggregates are joined through bridging reagent moieties.

Carbodiimides

Carbodiimides are condensation agents, which act through initial carboxyl group activation, leading to zero-length inter-protein amide bonds. Since the o-acylisourea intermediate is hydrolytically unstable, crosslinking is often aided by adding auxiliary agents such as hydroxysuccinimide. Once the o-acylisourea is attacked, hydroxysuccinimide forms a hydrolytically stable active ester with the carboxyl residue, thereby prolonging the time available for conjugation with amino groups. In our experience, the crosslinking of protein powders dispersed in solvent proved less efficient than classical homogeneous phase reactions. Adding hydroxysuccinimide to the dispersion proved very useful to ameliorate the low crosslinking yields.

Dehydrothermal crosslinking

The dehydrothermal crosslinking method was developed in-house. Dehydrothermal crosslinking yields zero-length inter-protein amide bonds by thermally dehydrating inter-

protein ammonium carboxylate salt bridges under vacuum-assisted conditions. The salt bridges undergoing transformation are made to juxtapose beforehand during the crash-precipitation/lyophilization step. The thermal stability imparted to proteins in the dry state and the anoxic processing conditions ensure good retention of bioactivity. Dehydrothermal crosslinking is particularly attractive in preparing biomaterials, since the reagent-free approach eliminates toxicity concerns relating to the use of exogenous chemicals. Dehydrothermal crosslinking should not be confused with “dehydrothermal processing”, which is a common method practiced on ceramic materials.

The study described in this chapter highlights new optimization techniques and alternative routes to conventional CLPA material synthesis. Furthermore, the principles and methods expressed herein will form the groundwork leading to the development of nano-CLPAs and nano-CLPLs, which are described in the following chapter. In particular, the material synthesized in this chapter will serve as the product precursor of the following chapter, yielding nano-sized particles over the course of nanonization. The specific physico-chemical traits of the precursor material will also reflect the choice of method and optimization strategy used in the downsizing process.

2.2. Materials

Bovine Serum Albumin was obtained from Sigma-Aldrich. Bovine Serum Albumin, heat shock fraction, pH 7, $\geq 98\%$

Trypsin was obtained from PAN Biotech GmbH. Trypsin powder (1 : 250) porcine origin

Chymotrypsin was obtained from Sigma-Aldrich. α -Chymotrypsin from bovine pancreas, Type II, lyophilized powder, ≥ 40 units/mg protein

Jack Bean Urease was obtained from Sigma-Aldrich. Urease from *Canavalia ensiformis* (Jack bean), Type IX, powder, 50,000-100,000 units/g solid

Henn Egg Lysozyme was obtained from Sigma-Aldrich. Lysozyme from chicken egg white lyophilized powder, protein $\geq 90\%$, $\geq 40,000$ units/mg protein

Bovine Hemoglobin was obtained from Sigma-Aldrich. Hemoglobin from bovine blood, suitable for protease substrate, substrate powder

All other reagents were obtained from commercial suppliers as analytical grade and were used without further purification.

2.3. General Methods

In a typical preparation, soluble monomeric protein starting materials were crash precipitated or lyophilized, forming macroscopic aggregates. These soft solids were chemically directly in aggregation medium or dehydrothermally crosslinked. Choice of initial solution composition, aggregation and crosslinking steps were conducted in a manner permitting retention, and in many cases, improvement of biological activity.

Material was further characterized to establish the optimal synthesis conditions in terms of overall synthesis yield efficiency and biological activity.

2.3.1. CLPA and CLPL synthesis

2.3.1.1. Precursor protein solutions

All protein solutions were prepared by mild agitation at 4 °C. Final protein concentrations in solution were verified either spectrophotometrically (using molar extinction coefficient,

280nm) or by recording the weight of the lyophilized protein of known initial volume depending on the further procedure.

Protein solutions described in this chapter were generally of the following composition:

Protein(s)	Concentration (mg/ml)	Solution composition	pH
Albumin	100-200	100mM sodium acetate buffer	5,6
		100mM sodium phosphate buffer	7,4
Trypsin	50-100	10mM CaCl ₂ in hydrochloric acid solution	3
		10mM CaCl ₂ in hydrochloric acid solution	4,5
		10mM CaCl ₂ in 10mM sodium acetate buffer	5,6
		10mM CaCl ₂ in 10mM Tris buffer	7,4
		10mM CaCl ₂ in 10mM Tris buffer	9,2
Trypsin/ Albumin	50/50	10mM CaCl ₂ in hydrochloric acid solution	3
		10mM CaCl ₂ in hydrochloric acid solution	4,5
		10mM CaCl ₂ in 10mM sodium acetate buffer	5,6
		10mM CaCl ₂ in 10mM Tris buffer	7,4
		10mM CaCl ₂ in 10mM Tris buffer	9,2
Chymotrypsin	50	10mM CaCl ₂ in hydrochloric acid solution	3
		10mM CaCl ₂ in hydrochloric acid solution	4,5
		10mM CaCl ₂ in 10mM sodium acetate buffer	5,6
		10mM CaCl ₂ in 10mM Tris buffer	7,4
		10mM CaCl ₂ in 10mM Tris buffer	9,2
Urease	25-100	100mM sodium phosphate buffer	7,4
Urease/Albumin	10-50/50-100	100mM sodium phosphate buffer	7.4

2.3.1.2. Precipitation

Precipitation procedures were performed with freshly prepared protein solution at 4 °C, through lyophilization or crash precipitation.

Lyophilization: Protein solutions were submerged into liquid nitrogen, and freshly frozen material was lyophilized using Christ brand ALPHA 1-2 LDplus laboratory scale freeze-dryer (Martin Christ Gefriertrocknungsanlagen GmbH, Germany) (0.02-0.04mbar, 12h).

Crash Precipitation: Protein solutions were dropwise added into a saturated ammonium sulfate solution (salting out) or an anti-solvent under constant stirring conditions at v:v ratio of 1:9 and left to stir for 20-30 min at 400-550 rpm, at 4 °C. Anti-solvents described here were methanol, ethanol, acetone, 1-propanol, 2-propanol, 2-butanol, dimethylformamide and dioxane.

*All preparations involving dioxane were performed at room temperature.

2.3.1.3. Crosslinking

Chemical crosslinking:

Chemical crosslinking of crash-precipitated aggregates was conducted directly in the stirred aggregation medium by adding a chemical crosslinking reagent to suspensions of protein solution previously incubated with salting-out agent or anti-solvent. To covalently crosslink protein lyophilizates, in case of CLPL synthesis, lyophilized powders were immersed in an anti-solvent containing crosslinker.

Glutaraldehyde

Glutaraldehyde was applied at concentrations of 0.106×10^{-6} – 6.36×10^{-5} mol per mg protein (dry weight equivalent). Listed below are the amounts of glutaraldehyde used in each trial:

1. 1.064×10^{-6} mol per mg protein
2. 2.12×10^{-6} mol per mg protein
3. 0.53×10^{-5} mol per mg protein
4. 1.06×10^{-5} mol per mg protein

5. 2.12×10^{-5} mol per mg protein
6. 3.18×10^{-5} mol per mg protein
7. 4.24×10^{-5} mol per mg protein
8. 6.36×10^{-5} mol per mg protein

Glutaraldehyde is typically stored and sold at slightly acidic pH values, which serves to reduce its optimal reactivity. In this work, commercial glutaraldehyde stocks (25wt%, pH 5) were directly used without pH adjustment. Alternatively, water-diluted stocks (12.5wt%, adjusted to pH 9.2 using 0.1M sodium carbonate buffer and pH 7.4 using 0.1M sodium phosphate buffer) were used. Suspension was incubated for 20h while stirring (400 rpm) at 4°C, if not stated otherwise in the text. Crosslinked material was isolated from reaction medium by centrifugation (4krpm) and incubated in 0.1 % sodium borohydride solution (at volume equivalent to the aggregation medium used) at mild agitation (200 rpm). Once all imines were presumably reduced (30 min), the crosslinked material was washed thrice with double distilled water and dried under vacuum prior to storage (RT).

Dextran Polyaldehyde

Dextran polyaldehyde was synthesized in house according to the following procedure¹⁰: Dextran 1.65 g was dissolved in 80 mL of water, and 3.85 g sodium metaperiodate were added. The resulting solution was stirred at room temperature during 90 min. Subsequently, the solution was dialyzed five times, using a MW cutoff of 10 KDa against 5 L of water each time at room temperature during 2 hrs and under stirring. The final volume of the dextran polyaldehyde was 87 mL.

Dextran polyaldehyde was applied at concentration of 0.38 mg or 0.76 mg per mg protein (dry weight equivalent) for all samples, if not stated otherwise in the text. Suspension was incubated for 20h while stirring (400 rpm) at 4°C, if not stated otherwise in the text. Crosslinked material was isolated from reaction medium by centrifugation (4 krpm) and incubated in 0.1 % sodium borohydride solution (at volume equivalent to the aggregation medium used) at mild agitation (200 rpm). Once all imines were presumably reduced (30 min), the crosslinked material was washed thrice with double distilled water and dried under vacuum prior to storage (RT).

Carbodiimides

1-ethyl-3(3-dimethylaminopropyl)carbodiimide (EDC) and N,N'-dicyclohexylcarbodiimide (DCC) crosslinking was attempted. EDC was applied at 5.2×10^{-6} – 3.1×10^{-5} mol and DCC at 3.8×10^{-6} – 1.9×10^{-5} mol concentrations per mg protein (dry weight equivalent), with/out prior addition of N-hydroxysuccinimide (1.4×10^{-5} – 2.8×10^{-5} mol). EDC was applied to ammonium sulfate aggregated suspensions, while CDC was applied to dimethyl formamide and 2-propanol aggregated suspensions. Suspension was incubated for 20h while stirring (400 rpm) at 4°C, if not stated otherwise in the text. Crosslinked material was isolated from reaction medium by centrifugation (4 krpm) and incubated in 0.1 wt% sodium borohydride solution (at volume equivalent to the aggregation medium used) for 30 min at mild agitation (200 rpm). Reduced material was washed thrice with double distilled water.

***In vacuo* Dehydrothermal Crosslinking:**

Precursor solutions were flash frozen in liquid nitrogen and lyophilized (0.02-0.04mbar, 12-48h) without applying external cooling. Prior to *in vacuo* heating, lyophilizates were incubated (RT, 8-12h) in a partially-evacuated desiccator containing solid ammonium carbonate (5g), in order to adjust the ionization states to promote efficient crosslinking.

A make-shift apparatus consisting of a lyophilizer vessel, and a heat-variable oil-bath, was employed to drive the *in vacuo* crosslinking. Pretreated as described, the protein lyophilizates were transferred into the glass vessel and incubated under constant evacuation (100°C, 0.2-0.6mbar, 14-20h) with the vessel partially submerged in the oil-bath. The act of continuously evacuating the vessel combined with heating hastened the loss of previously non-desorbed water as well as water arising from the crosslinking reactions.

2.3.2. Characterization

2.3.2.1. Determination of aggregation and crosslinking yields

Aggregation yield

Protein solutions were dropwise added into a saturated ammonium sulfate solution (salting out) or an anti-solvent under constant stirring conditions at v:v ratio of 1:9 and left to stir for 20-30 min at 400-550 rpm, at 4 °C, in pre-weighted 50 ml falcon tubes. The formed suspensions were centrifuged (4 krpm) and supernatants were removed. The remaining precipitate was dried and weighted.

Corresponding precursor protein solution was lyophilized in the pre-weighted eppendorf tube and weighted. The weight of lyophilizate was used as reference in place of protein concentration. The aggregation yield was calculated according to the following equation (2.1):

$$\text{Aggregation Yield (\%)} = \frac{W_a}{W_l} \times 100\% \quad (2.1)$$

Where W_a and W_l are dry weights of aggregate and lyophilizate respectively.

All presented data was the mean value of experimental results performed in triplicates.

Crosslinking yield

Crosslinking was conducted as described above in the pre-weighted 50 ml falcon tubes and subsequently reduced with sodium borohydride, where applicable. Formed CLPA was washed thrice with distilled water, centrifuged (4 krpm) and resultant precipitate was dried. The crosslinking yield was calculated according to the following equation (2.2):

$$\text{Crosslinking Yield (\%)} = \frac{W_{clpa} - W_{xl}}{W_a} \times 100\% \quad (2.2)$$

Where W_{clpa} and W_a are dry weights of CLPA and precursor aggregate respectively. W_{xl} is the calculated dry weight of crosslinking reagent applied.

All presented data was the mean value of experimental results performed in triplicates.

2.3.2.2. ATR-FTIR molecular structure analysis (*amide area fluctuations)

Attenuated total reflectance Fourier Transform Infrared Spectroscopy (ATR-FTIR) was used to directly monitor changes of dipole moment in amide and other regions as a function of protocol (crosslinker type, amount, crosslinking time and temperature) in case of chemical reagent crosslinking and as a function of crosslinking time in case of dehydrothermal crosslinking. The data was then related to changes in material hydratability and protein-protein interactions within the material. Prior to analysis, the crosslinked and control material were simultaneously pre-incubated (overnight, RT) in a partially-evacuated desiccator containing distilled water in order to normalize the hydration level of each sample. The vacuum was broken, and ATR-FTIR spectra were acquired. 34 consecutive scans were acquired per sample, and the averaged result was baseline-corrected. Lyophilizates were clamped along the observation window of an ATR accessory, and spectra were obtained from 550 to 4000 cm^{-1} at a resolution of 0.5 cm^{-1} .

2.3.2.3. Relative bioactivity assays

Proteases

Relative catalytic activity of proteases was detected by digestion of gelatin incubated for two hours at 37°C, agitated at 450 rpm. Ninhydrin analysis was performed using spent buffer/ninhydrin/isopropanol comprising 100:1:99 [v/w/v] (70°C, 30min). Color yields were analyzed spectrophotometrically (570nm). Native protease solution measurements were assigned a value of 100% and CLPA measurements were calculated relative to this value.

Urease

Urease relative catalytic activity was detected by urea degradation upon 30 min incubation at 37°C, agitated at 450 rpm. Ninhydrin analysis was performed using spent buffer/ninhydrin/isopropanol comprising 100:1:99 [v/w/v] (70°C, 30min). Color yields

were analyzed spectrophotometrically (570nm). Native urease solution measurements were assigned a value of 100% and CLPA measurements were calculated relative to this value.

Lysozyme

Preliminary studies were performed using the assay based on the disruption of cell wall peptidoglycans, resulting in lysis of the bacteria and loss of optical density.

Micrococcus luteus (ATCC 4698) cells were grown in trypticase soy agar (ATCC medium 18) medium. In a typical assay, control native lysozyme solution and CLPA suspensions, were diluted to a concentration of 0.4 mg/mL. For each sample, an aliquot (100 μ l) was transferred to 900 μ l of cell suspension with an optical density of 0.6A (450 nm). Changes of optical density were recorded at each 15-s time interval. The average activity of each sample was calculated by averaging every 15-s measurement acquired over the first 3 min. Native protein solution measurements were assigned a value of 100% and CLPA measurements were calculated relative to this value.

Hemoglobin

The assay used was a variant of a published procedure³⁴. In particular, this method was based on the ability of hemoglobin to catalyze the reaction between o-phenylenediamine and hydrogen peroxide to form 2,3-diaminophenazine.

The reaction was initiated by addition of hydrogen peroxide (2×10^{-3} mM) to a stirred native hemoglobin solution or suspension containing hemoglobin CLPA and o-phenylenediamine (4×10^{-3} mM). Product formation was spectrophotometrically detected at 425 nm after one hour of incubation at room temperature, agitated at 450 rpm. All dilutions were performed in 100mM phosphate buffer, pH 7.4. Native protein solution measurements were assigned a value of 100% and CLPA measurements were calculated relative to this value.

2.4. Results and Discussion

The results herein are presented in the chronologic manner. The preliminary results are briefly presented first, in order to demonstrate the general behavior of CLPA material on a wider range of proteins. It also serves to highlight the challenges and goals of the study and rationalize the following optimization approach. Further description of process optimization is presented on the model of albumin, trypsin and chymotrypsin. Optimization of CLPA product comes down to synchronization of optimum conditions for three main factors: precursor solution formulation, precipitation method and crosslinking method.

2.4.1. Preliminary methodology studies

Preliminary methodology screening was performed on albumin, pepsin, trypsin, chymotrypsin, lysosyme, hemoglobin, pancreatic lipase, urease and industrial grade mixed enzymes (Maps Enzymes) using Sheldon et al work as the directive. The conventional approach has proved satisfactory to some extent in all cases, with an exception of urease, which has therefore required thorough optimization discussed in later on, as the most challenging case.

It has become evident from the initial screening, just as described in the corresponding literature³⁵, that the choice of the technique and solvent is target protein dependent, affecting both aggregation yield and catalytic activity of the end product.

For most of the trial proteins aggregation yield efficiency has not posed an issue (Figure 2.1.), while crosslinking in the given medium often was found to be a target for further optimization, in terms of synthesis efficiency yield.

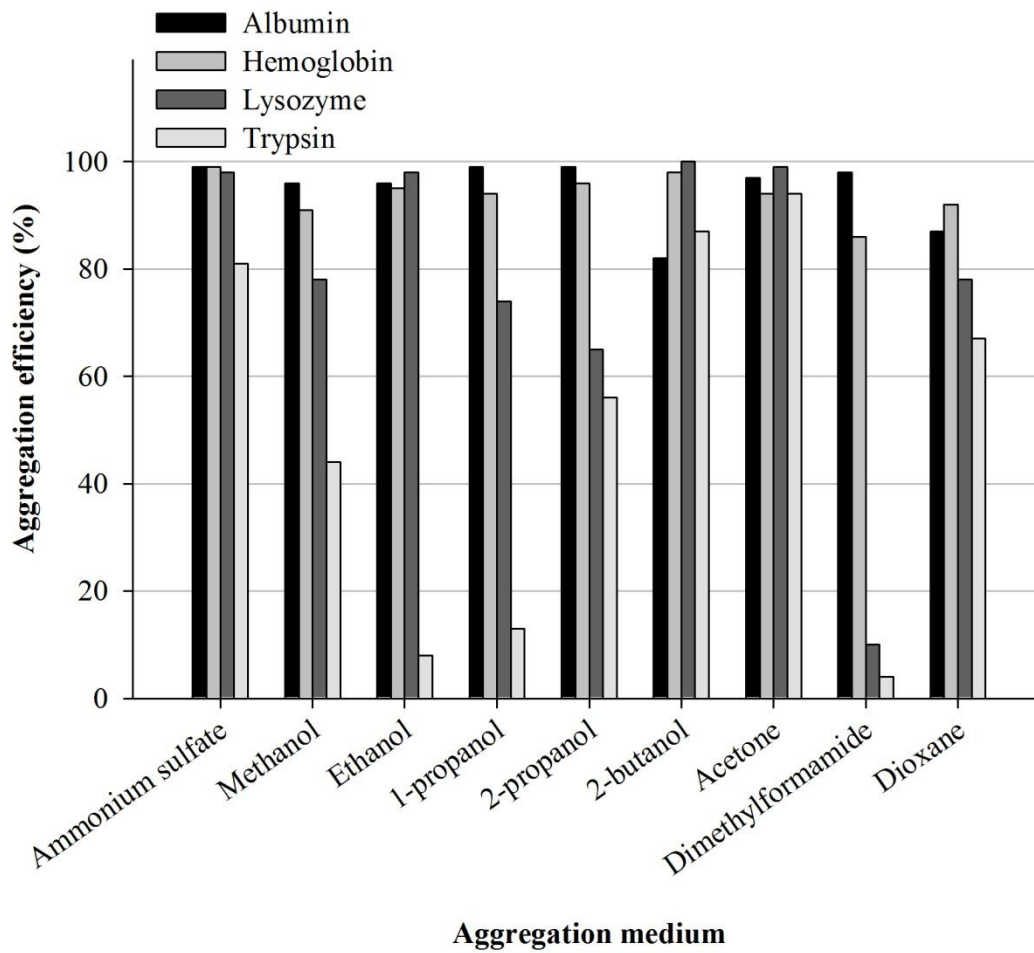


Figure 0.1: General review of crash precipitation step efficiency.

That being said, not surprisingly aggregation method had a dramatic effect on catalytic activity of the final product, in a protein type specific manner (Figure 2.2).

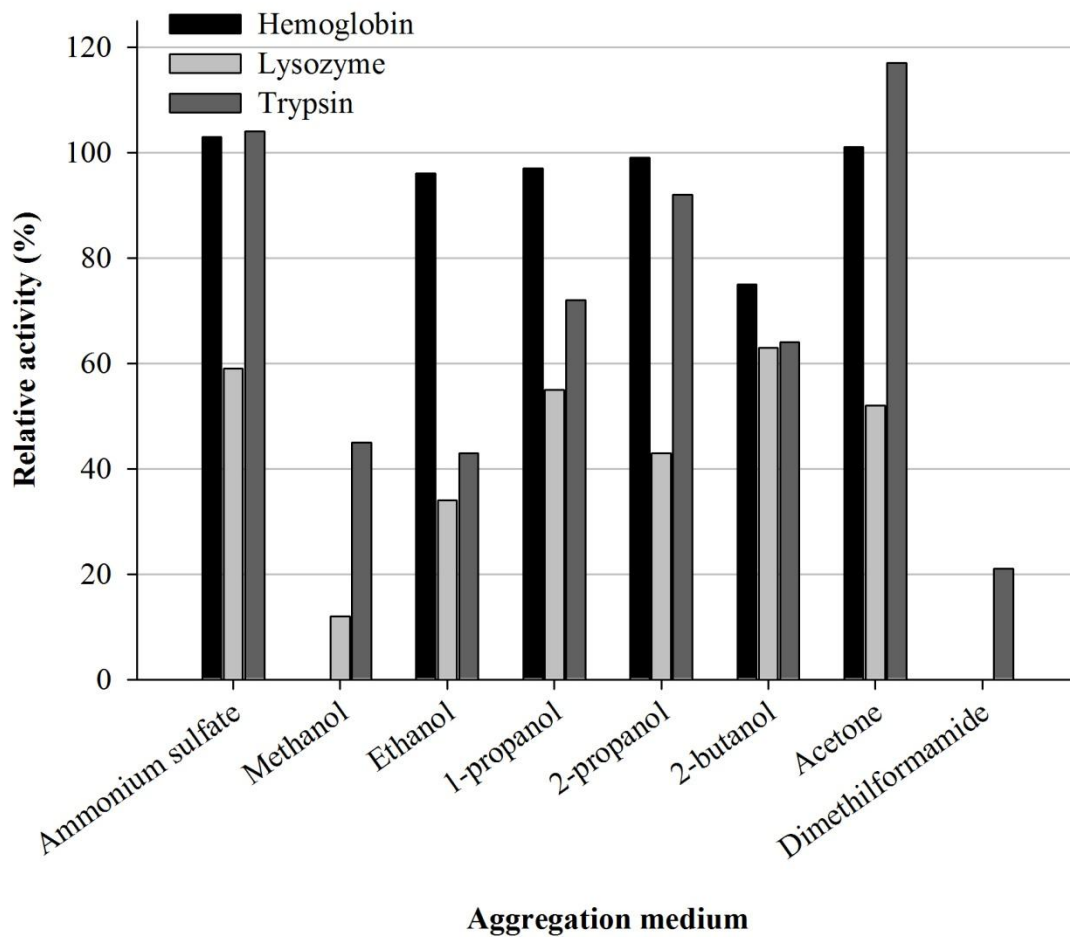


Figure 0.2: General review of aggregation method effect on relative catalytic activity of CLPA

Subsequent crosslinking is strongly dependent on the previous steps in terms of efficiency. The obtained CLPA activity varied strongly both with the method of choice and crosslinking degree and as all other is protein type specific (Figure 2.3).

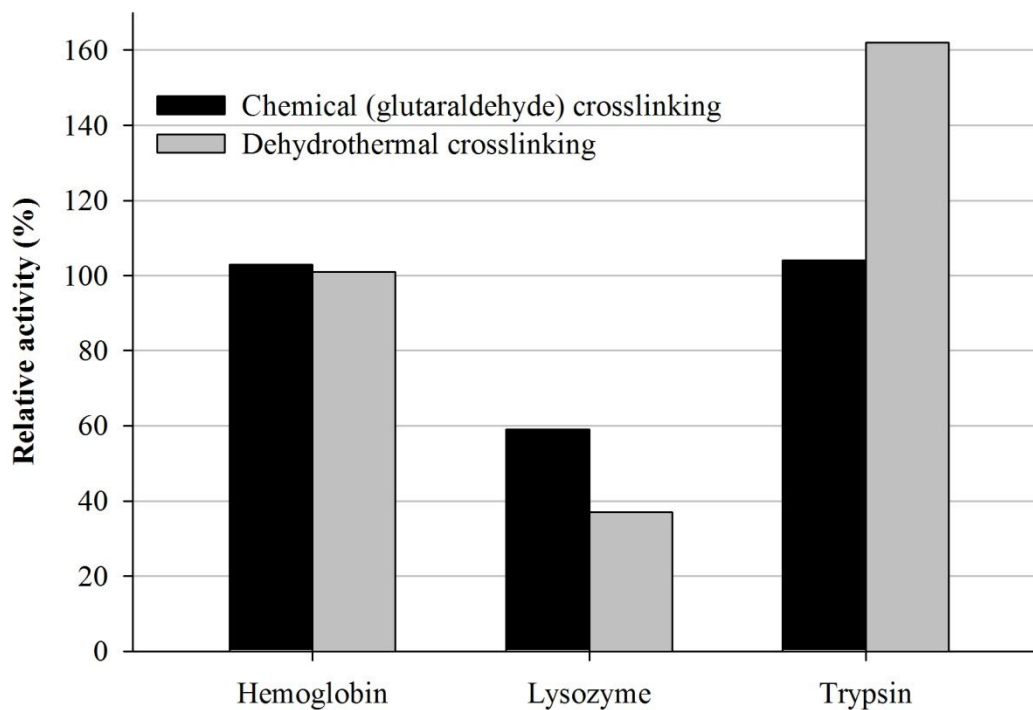


Figure 0.3: General review of crosslinking method effect on relative catalytic activity of CLPA

2.4.2. Optimization of precursor protein solutions in terms of CLPA synthesis yield and catalytic activity

2.4.2.1. Stability of the protein in solution state

Trypsin model formed a very good model for CLPA optimizations, due to its vulnerability in solution state. Particularly, because solution formulations used were of high concentration (50-100 mg/mL), the somewhat prolonged process of obtaining a stable solution was intercepted by the rapid autolysis. The preliminary studies conducted on trypsin CLPA were performed in 10-100mM buffer solutions at various pH values. The

catalytic activity of the final product in these formulations gave very poor results in terms of result reproducibility, all being under 100% with respect to the native enzyme (results not shown). Neutral to high pH formulations in particular, resulted in dramatically diminished activity, while acidic formulation resulted in final product activity approaching 100%. The conventional stabilization approach of co-precipitation with albumin has been attempted and resulted in further diminished catalytic activity yields, which was rationalized by the decrease in accessible catalytically operational surface area. Addition of 10-100mM calcium chloride to the precursor solution formulations has evidently aided in stabilizing the protein, leading to increased consistency of the results and increased activity (Figure 2.4).

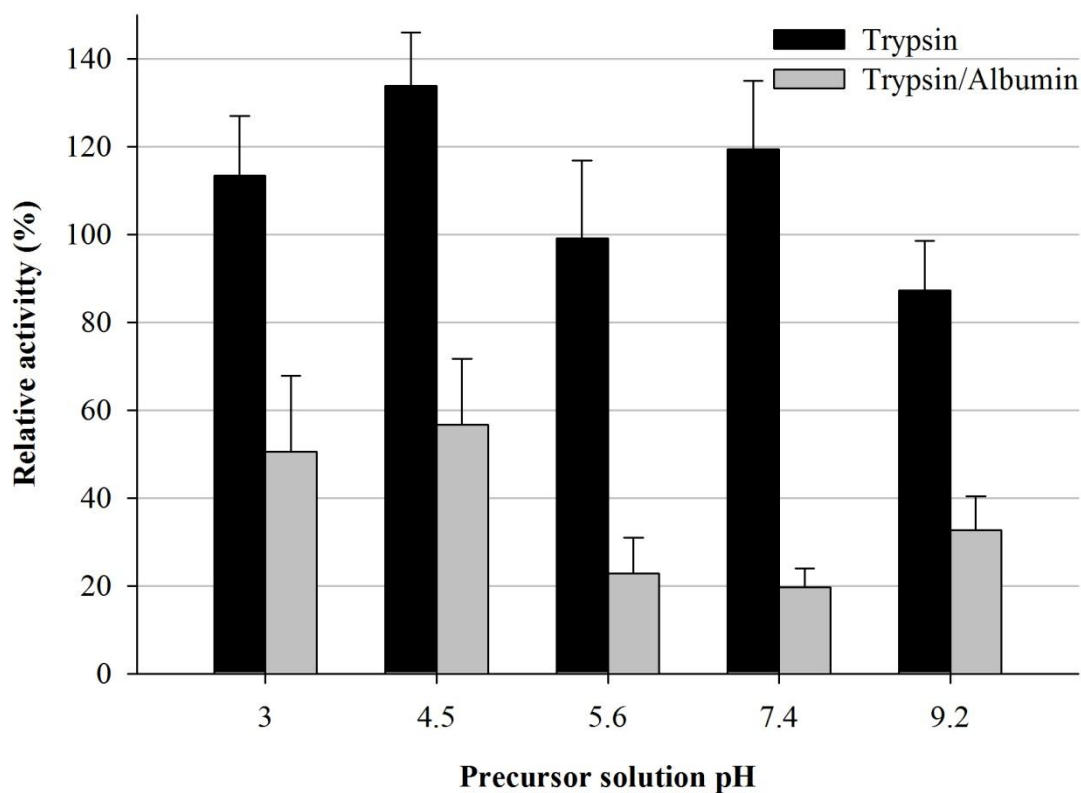


Figure 0.4: Precursor solution effect on CLPA catalytic activity. Trypsin CLPA (aggregated in acetone, glutaraldehyde crosslinked)

The precursor solution related catalytic activity results appear counterintuitive, in terms of initial rationalization that aggregates, as lyophilizates²⁹ would preserve the ionization states dictated by the precursor solution and therefore would perform optimally when aggregated under conditions corresponding to the enzyme's optimum pH and ionic strength. As can be observed from Figure 2.4 highest catalytic activity yield for trypsin CLPA was obtained at pH 4.5. It may be presumed that this point is optimal in terms of stabilization of the enzyme prior to aggregation, while still preserving the operational catalytic site state. Relatively lower activity yield at higher pH points appears to be the result of elevated autolysis in the solution state. In these improved formulation trypsin/albumin co-aggregated CLPA yields have increased insignificantly, further leading to the conclusion that while addition of albumin indeed increased the stability of trypsin in the solution state, significant decrease in the catalytic surface area accessible to the substrate is the predominant factor. It must be emphasized here, that the substrate in question, gelatin, due to its large molecular size poses a dramatic diffusion and catalytic site accessibility limitations, as compared to trypsin specific amino acid/peptide substrates such as N-benzoyl-L-arginine and N-glutaryl-L-phenylalanine derivatives etc., which have not been used in this study. These limitations must be taken into account in over viewing the catalytic activity yields obtained.

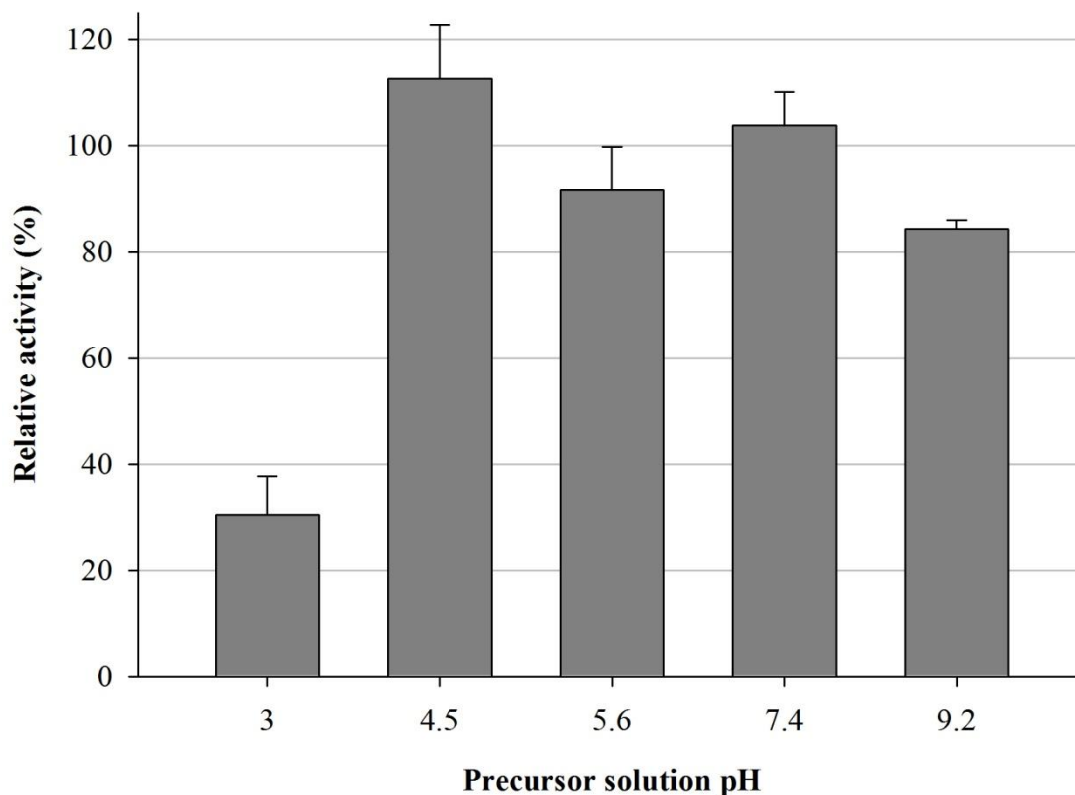


Figure 0.5: Precursor solution effect on CLPA catalytic activity. Chymotrypsin CLPA (aggregated 2-propanol, glutaraldehyde crosslinked)

Predictably, in case of chymotrypsin CLPA, the catalytic activity yield to precursor solution relationship was found similar but less pronounced, since this protease is relatively more stable in the solution state than trypsin (Figure 2.5).

2.4.2.2. Facilitation of further synthesis steps

No statistically significant relationship was found between aggregation yields and precursor protein solution formulations. The precursor solution pH, on the other hand, was found to greatly affect the chemical crosslinking yields for all attempted protein types, where lysine oriented modification methods were applied (Figure 2.6). The result was not surprising given reversibility of glutaraldehyde reactions below pH 7, which would decrease the

number of effective crosslinks formed even with incorporation of borohydride reduction¹¹. This has posed a challenge considering higher activity yields of trypsin CLPA at lower pH conditions; this problem was addressed later on and is discussed in Section 2.4.5. Solution conditions have not posed an issue in case of dehydrothermal crosslinking, owed to the ionization state equilibration procedure applied to lyophilizates prior to crosslinking procedure.

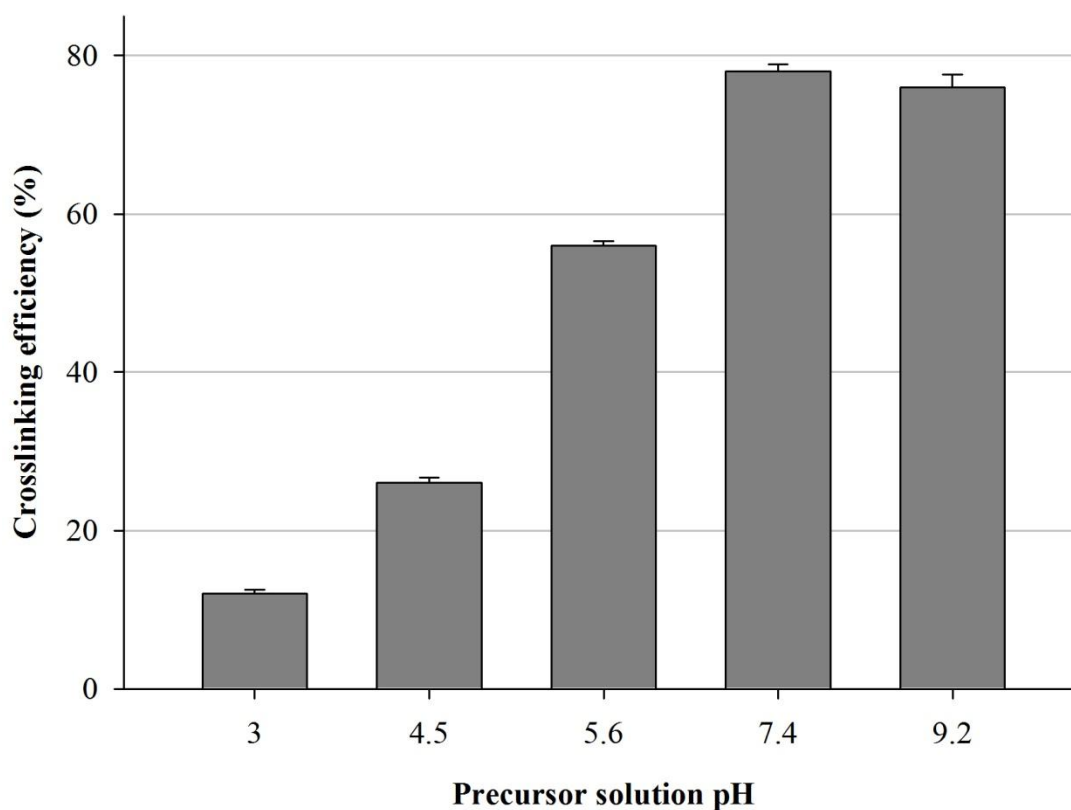


Figure 0.6: Precursor solution effect on crosslinking yield. Trypsin CLPA (aggregated in acetone, glutaraldehyde crosslinked)

2.4.3. Optimization of aggregation method and protocol in terms of CLPA synthesis and catalytic activity

As was demonstrated on the preliminary results, optimization of aggregation yield is protein specific, but generally is easily achieved. Since the synthesis process dictates crosslinking process performed upon aggregation without replacing the medium, choice of aggregation medium significantly influences the crosslinking yield. It can be generalized that, medium containing functional groups competing (ammonium sulfate solution, acetone) for crosslinker reagent somewhat reduces the crosslinking yield, which is partially compensated by coincidental effectiveness of aggregation in these media. Albumin primarily due to abundant surface lysine content is very readily crosslinked, compared to all other attempted protein types; hence the described relationship is minor in case of albumin CLPA (Figure 2.7).

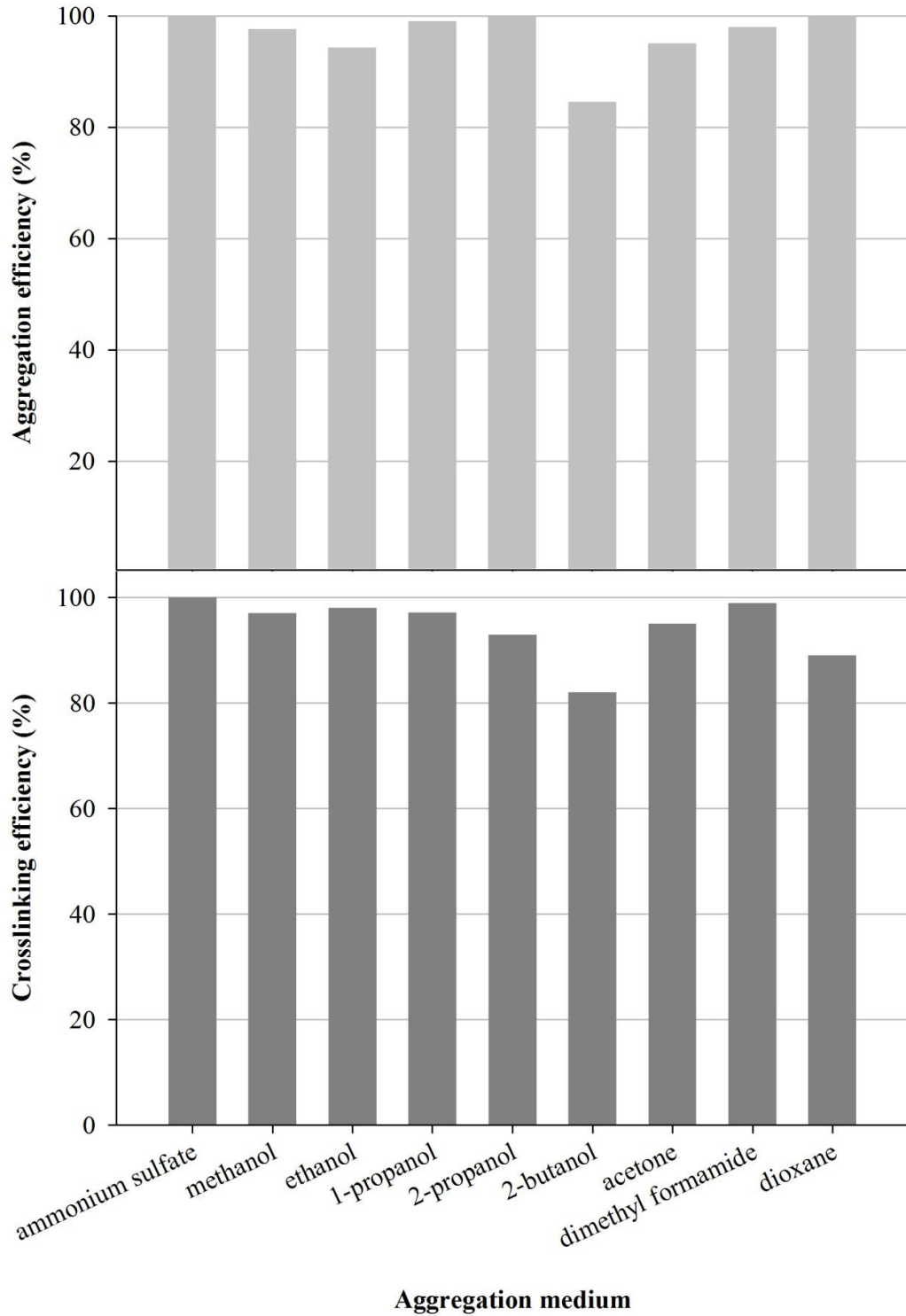


Figure 0.7: Aggregation medium effect on aggregation (up) and crosslinking yield (down).Albumin CLPA (pH 7.4 precursor solution, glutaraldehyde crosslinked)

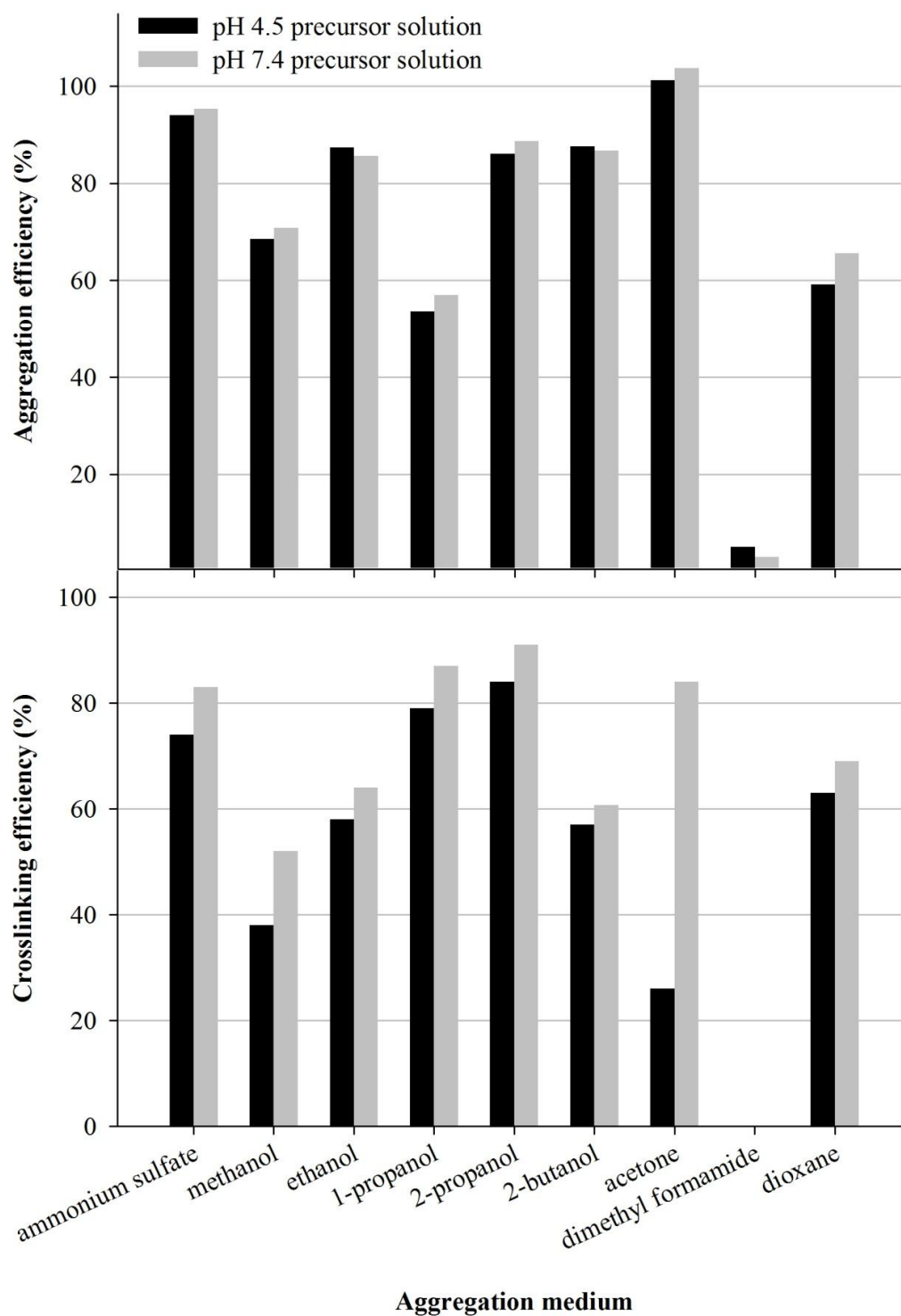


Figure 0.8: Aggregation medium effect on aggregation (up) and crosslinking yield (down).
 Trypsin CLPA (glutaraldehyde crosslinked)

As can be observed from Figure 2.8, the relationship between aggregation medium and crosslinking yield is much more pronounced in case of trypsin CLPA, a closely similar pattern is applied to chymotrypsin CLPA (results not shown). Due to plausible catalytic activity output combined with the high crosslinking yield, 2-propanol was generally the aggregation medium of choice for further trypsin and chymotrypsin CLPA formulations. Effect of aggregation medium on the catalytic activity of CLPA is demonstrated herein on trypsin (Figure 2.9), with once again a very close pattern applied to chymotrypsin (results not shown). It is generally observed from the literature³⁶ and results included in preliminary discussion, that the effect of aggregation medium on catalytic activity is strongly protein type specific and is difficult to generalize. It can be noted that ammonium sulfate precipitation method is relatively mild, and has been widely used for protein purification procedures, which is also applicable in case of crash precipitation. In particular cases where ammonium sulfate might act as an enzyme inhibitor, it can be readily replaced by an alternative inorganic salt with suitable ionic species.

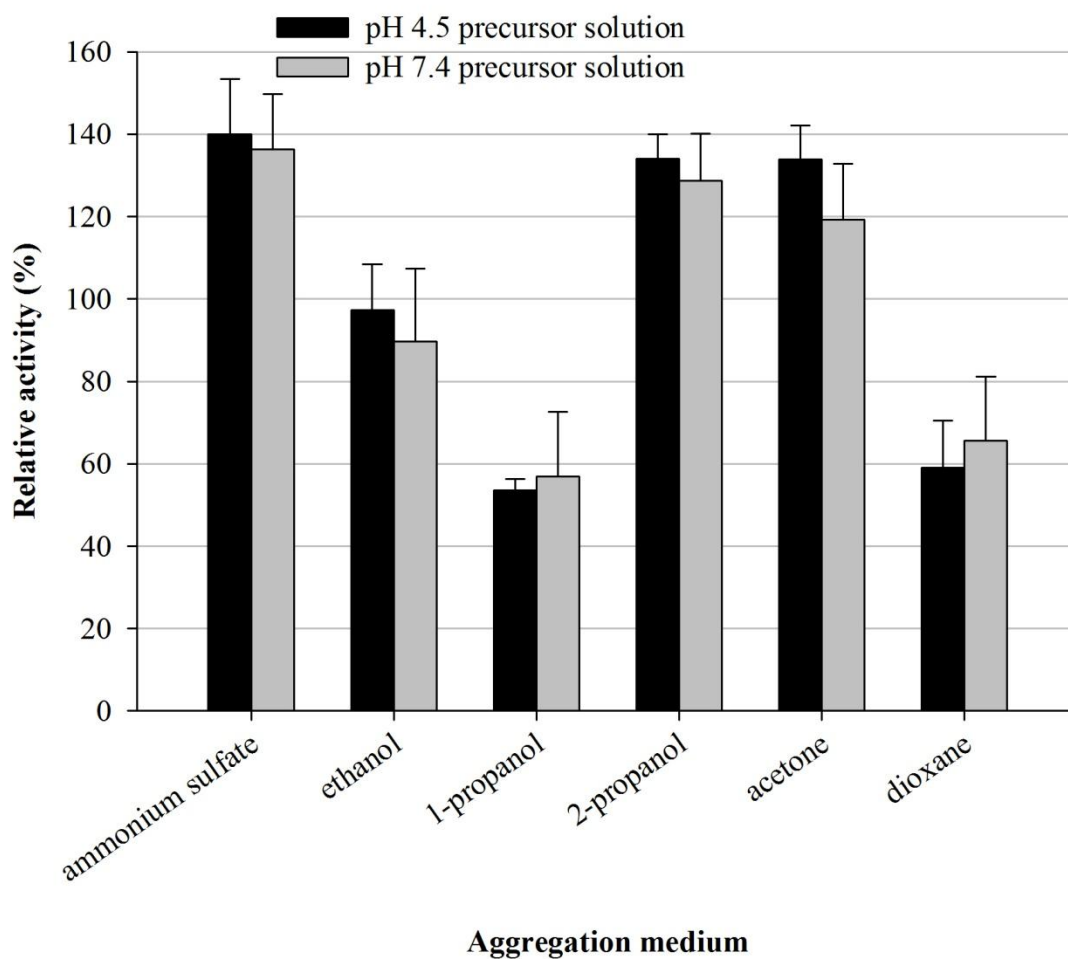


Figure 0.9: Aggregation medium effect on CLPA catalytic activity. Trypsin CLPA (glutaraldehyde crosslinked)

2.4.4. Optimization of crosslinking method and protocol in terms of CLPA synthesis yield and catalytic activity

The crosslinking method choice dominantly dictates the catalytic activity of CLPA and is, as other synthesis steps, protein type specific.

Figure 2.10 presents crosslinking method comparison on the example of trypsin. It is common to expect higher catalytic yields from milder dextran polyaldehyde crosslinking as compared to glutaraldehyde, as is widely mentioned in literature¹⁰. Nevertheless, the activity yield in this case was observed to be statistically insignificant. It can be assumed that steric effect plays a significant role here: as was earlier observed in case of co-precipitation with albumin, the change in accessible catalytic area greatly influences the resultant activity. Much bulkier dextran polyaldehyde, while presumably preserving the catalytic site altering, is increasing the density of the aggregate network, therefore limiting accessibility.

All protocol variants of carbodiimide crosslinking in all attempted protein types resulted in the most poor activity yields relative to other crosslinking techniques employed. The method was optimized to satisfy the average crosslinking yield expectation, by adjusting carbodiimide to hydroxysuccinimide ratio in the reaction, but since the resultant CLPA catalytic activity appeared below average the method was not further investigated and still remains subject to optimization. One of potential reasons for unsatisfactory activity yields, given that the amount the carbodiimide necessary to provide the structural integrity also led to excessive intra-molecular modification. This scenario is also probable because of the relatively small size of carbodiimide reagent, which could access and modify the catalytic site residue of a certain protein fraction. Furthermore additional zero-length bonding, combined with the tightened network of the aggregate could lead to restriction of substrate accessibility. Further optimization of this method could potentially be particularly advantageous in protein types with low available surface lysine content, alone or in combination with primary amine oriented crosslinking reagents.

Dehydrothermal crosslinking, coinciding with preliminary results, yielded highest catalytic activity. The results are not surprising, given the lyophilizate dictated high porosity of the crosslinked product, facilitating substrate accessibility. Furthermore as it has been shown before, this technique appears relatively mild, due to probably much fewer crosslink formations, which are sufficient to obtain high synthesis yield of the insoluble product, as compared to chemical crosslinking. Reagent free method furthermore eliminates risk of catalytic site modification, as in case of small crosslinking reagents.

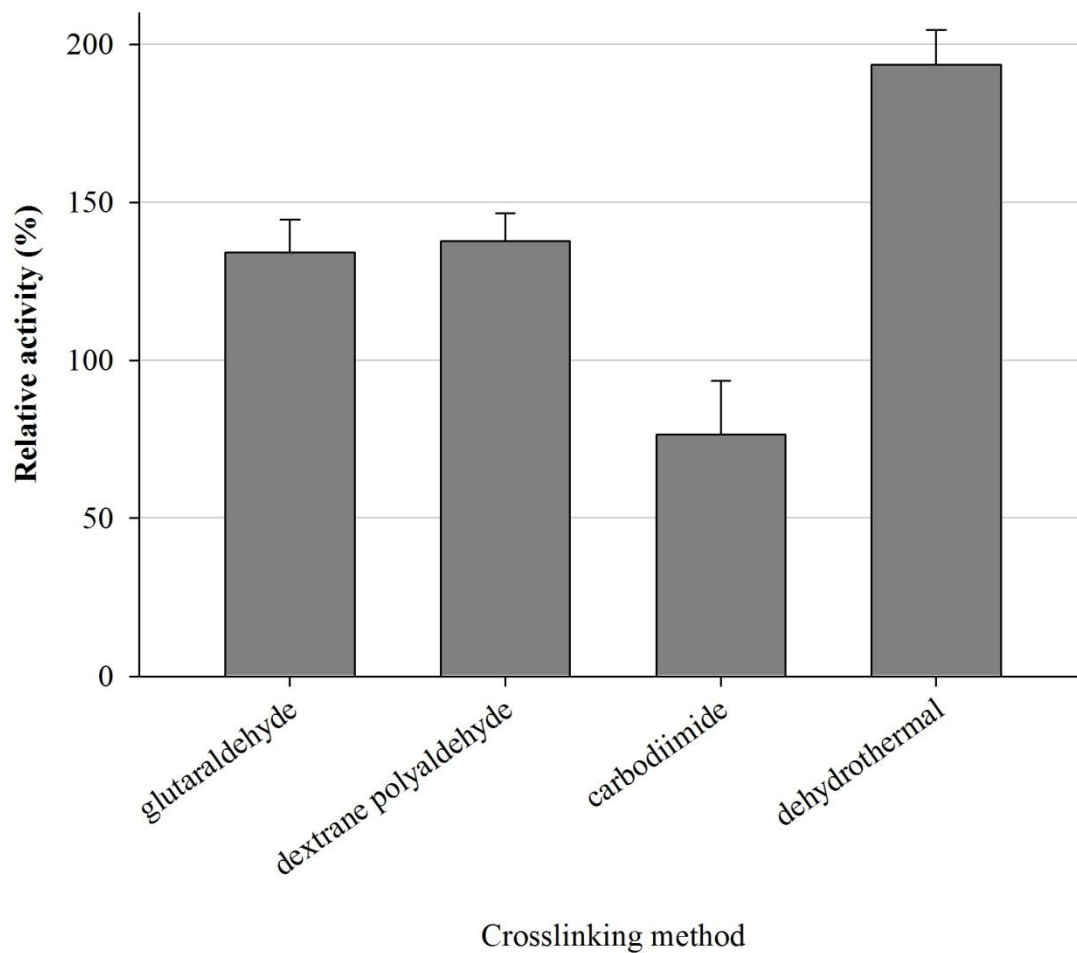


Figure 0.10: Effect of crosslinking method on CLPA catalytic activity. Trypsin CLPA (pH 4.5 precursor solution, aggregated in 2-propanol)

The similar effect was observed on the example of chymotrypsin (Figure 2.11)

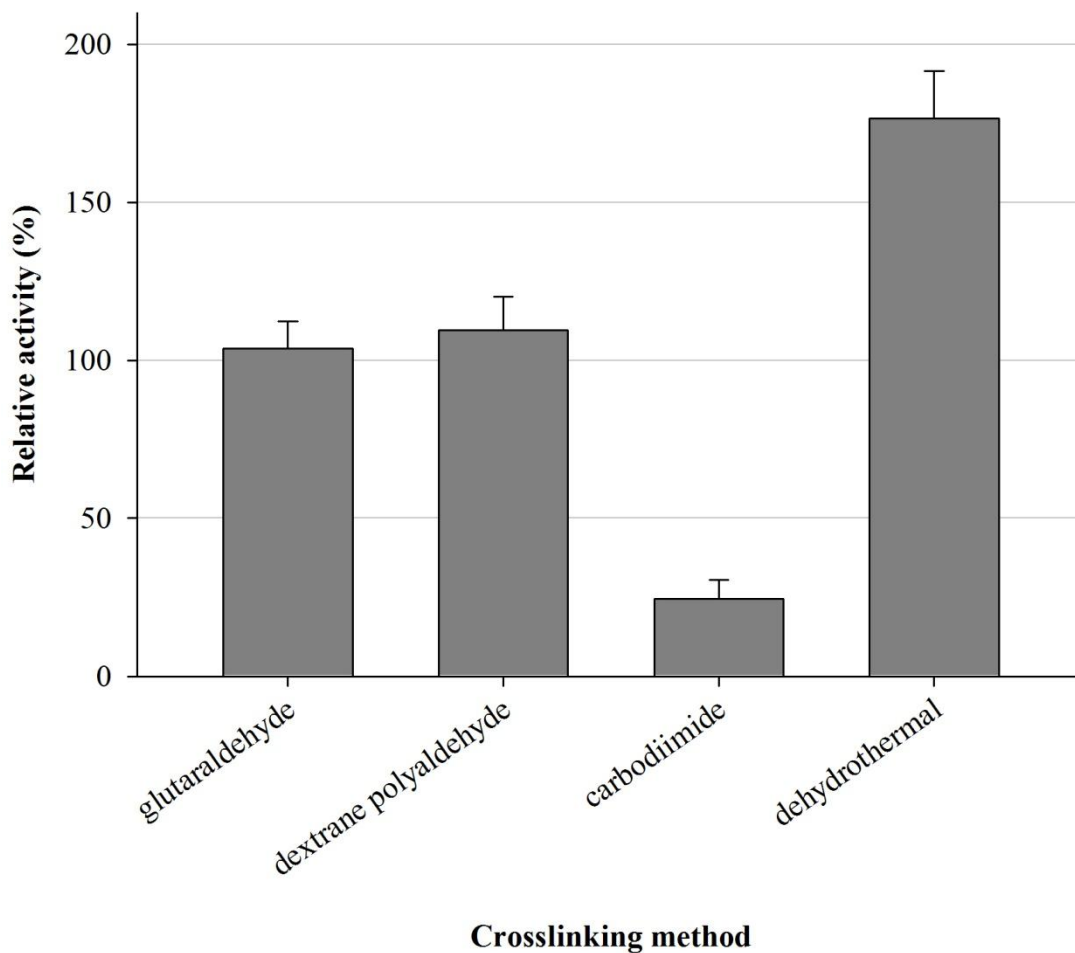


Figure 0.11: Effect of crosslinking method on CLPA catalytic activity. Chymotrypsin CLPA (pH 7.4 precursor solution, aggregated in 2-propanol)

Initial pH of the used crosslinking reagent has had a significant effect on catalytic activity, while resulting in only minor fluctuations in CLPA synthesis yield. The effect of glutaraldehyde and dextran polyaldehyde initial pH on trypsin CLPA activity is demonstrated on Figures 2.12 and 2.13 respectively.

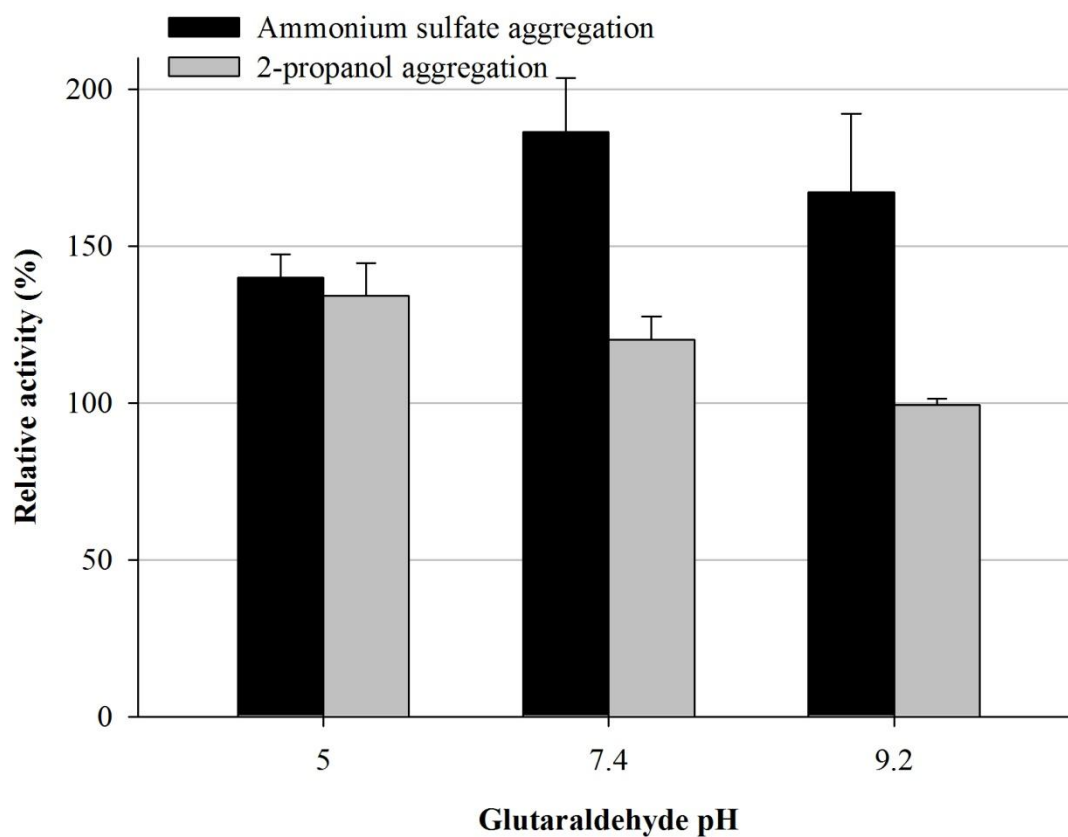


Figure 0.12: Effect of crosslinking reagent (glutaraldehyde) and pH on CLPA catalytic activity. Trypsin CLPA (pH 4.5 precursor solution, aggregated in 2-propanol)

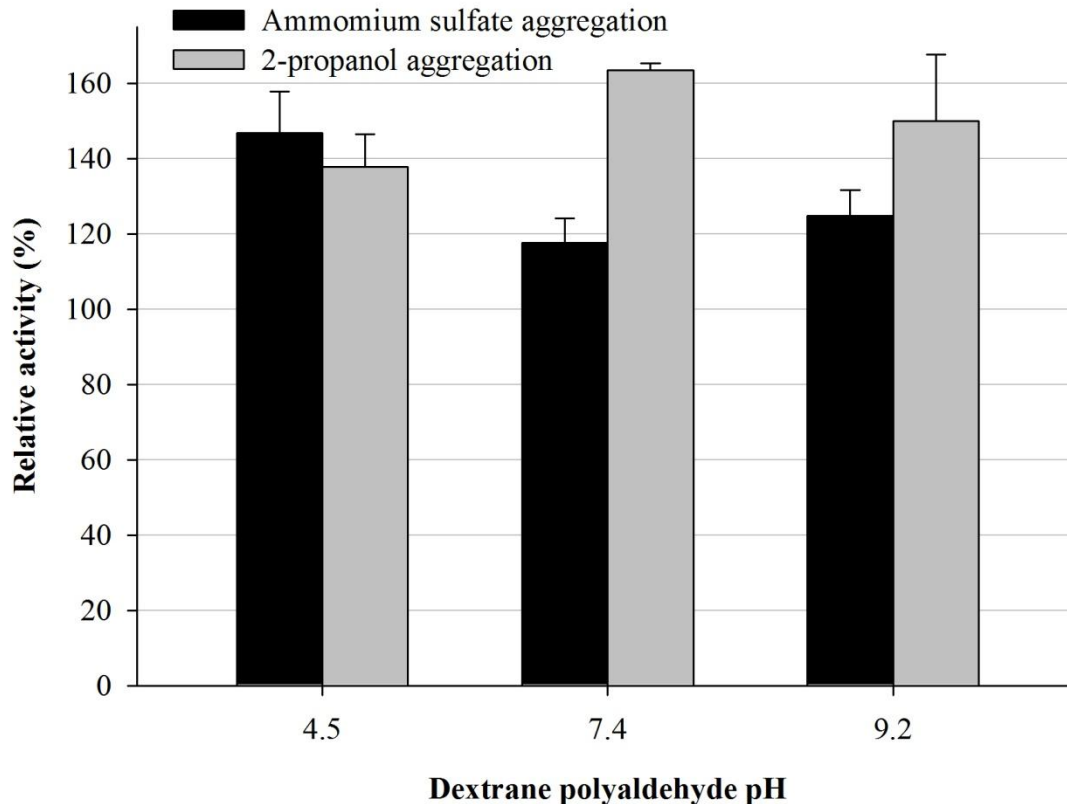


Figure 0.13: Effect of crosslinking reagent (dextran polyaldehyde) and pH on CLPA catalytic activity. Trypsin CLPA (pH 4.5 precursor solution, aggregated in 2-propanol)

While synthesis yield increases with increasing crosslinking extent, there obviously exists an optimum crosslinking degree in terms of catalytic activity. Clearly, optimization should be made, utilizing the amount of reagent necessary for structural integrity and recovery of insoluble aggregate, while taking the catalytic activity of the resultant product into account. Among the proteins attempted for CLPA synthesis albumin has been most readily crosslinked example. Figure 2.14 demonstrates glutaraldehyde amount effect on synthesis yield and resultant catalytic activity on of trypsin CLPA, which provides an average example of globular protein crosslinking. Methods 4. and 5. (1.06×10^{-5} and 2.12×10^{-5} mol of glutaraldehyde per mg protein respectively) were generally employed in all data provided in this and next chapter, providing the optimum yield to catalytic activity relationship.

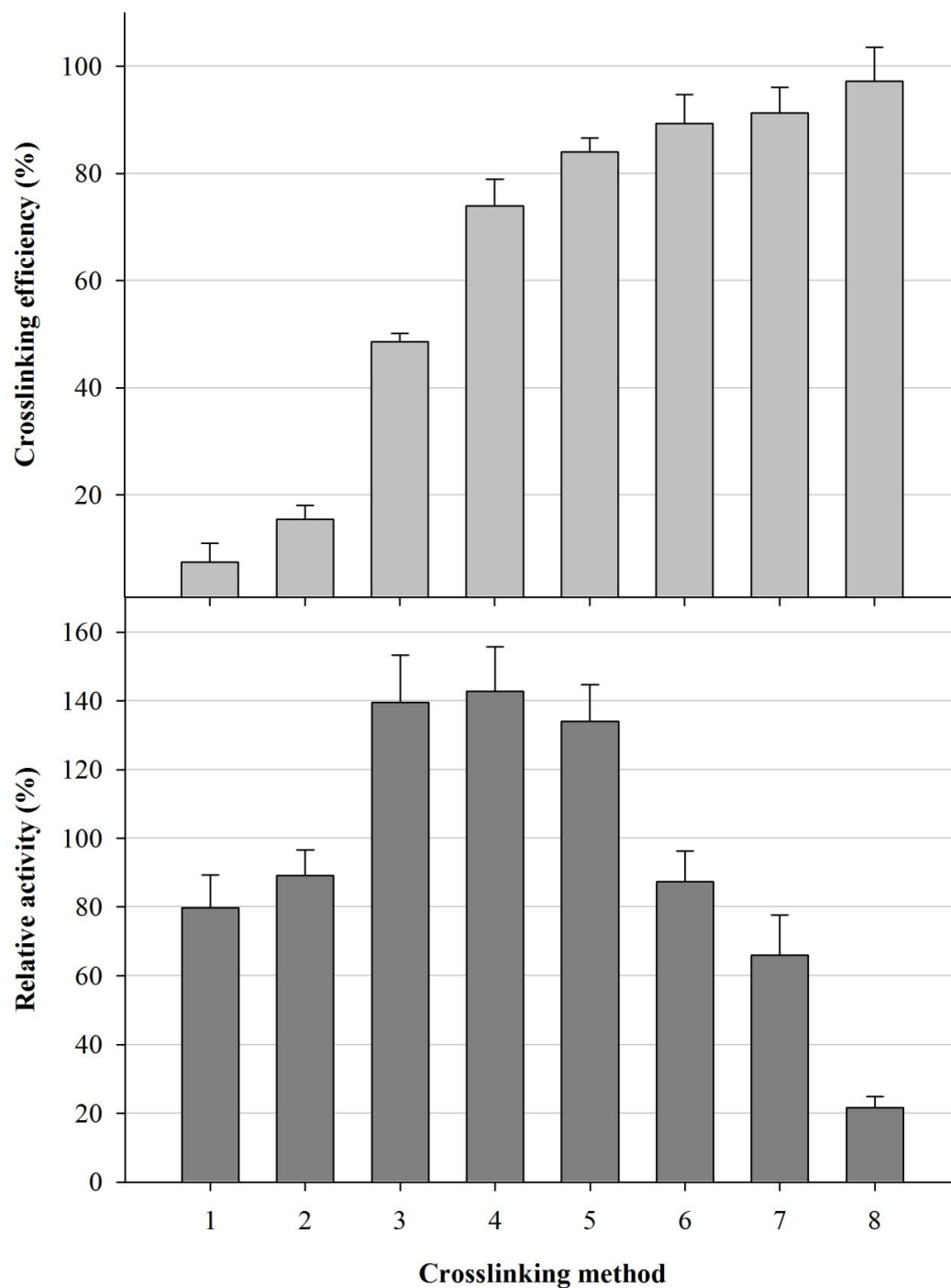


Figure 0.14: Crosslinking degree effect on CLPA catalytic activity. Trypsin CLPA (pH 4.5 precursor solution, aggregated in 2-propanol, crosslinker glutaraldehyde)

* numbers 1-8 represent amount of crosslinker applied: 1. $1,064 \times 10^{-6}$; 2. $2,12 \times 10^{-6}$; 3. $0,53 \times 10^{-5}$; 4. $1,06 \times 10^{-5}$; 5. $2,12 \times 10^{-5}$; 6. $3,18 \times 10^{-5}$; 7. $4,24 \times 10^{-5}$; 8. $6,36 \times 10^{-5}$ mol per mg protein

Attenuated total reflectance Fourier Transform Infrared Spectroscopy (ATR-FTIR) was used to directly monitor changes of dipole moment in amide and other regions as a function of crosslinking degree and to compare structural changes implemented by different crosslinking methods. The data was then related to changes in protein-protein interactions within the aggregate/lyophilizate.

Since IR spectral intensities are influenced by sample population, peak intensity ratios within each sample spectrum were analyzed with respect to the adjacent minima values, rendering the analyses independent of the sample amount. IR could be effectively used herein to probe the material structure and any relative changes upon crosslinking, particularly with regard to the secondary structure. Among the signals acquired, changes of amide I/II intensity are compared in detail.

Herein, amide I (i.e., C=O stretching, 1650 cm^{-1}) and II (i.e., N-H bending, 1540 cm^{-1}) bands appeared to display a minor relative difference of intensity. The structural change in protein depending on the crosslinking degree was monitored on the basis of this spectroscopic difference, which showed a definite change in the ratio of amide I and II band intensities with the increasing amount of crosslinking reagent (Figure 2.15).

These changes appeared to reflect incremental secondary structural changes as a function of crosslinking degree. Presented graphically (Figure 2.16, up), the relative increase of the amide I versus amide II band intensity can be observed with increasing crosslinker reagent amount. Small but certain relative changes in bond polarization pointed to hydrogen bond redistribution.

Observed were spectral differences most likely related to minor covalent changes, i.e., changes which likely influenced structural compliancy, the course of re-hydration, and protein-protein hydrogen bonding. A gradual “tightening” of the inter-protein structure was envisaged, as such a scenario would reflect not only the incremental formation of crosslinks but also the spectroscopic changes. Altered non-covalent inter-protein bonding would also almost certainly be expected to contribute to the observed spectral profile of this “tightened” protein model³⁷. The increasingly pronounced band corresponding to alkane C-H bending ($1350\text{-}1480\text{ cm}^{-1}$) further supports the model³⁸.

Furthermore, the reversal of C-O stretching (around 1100 cm^{-1}) and amide II band has been detected after a certain crosslinking degree (Figure 2.16, down), coinciding with the drop of catalytic activity discussed earlier on the example of trypsin (Figure 2.14). These changes might be pointing out the accumulation of excess glutaraldehyde, possibly polymerized into ether containing species.

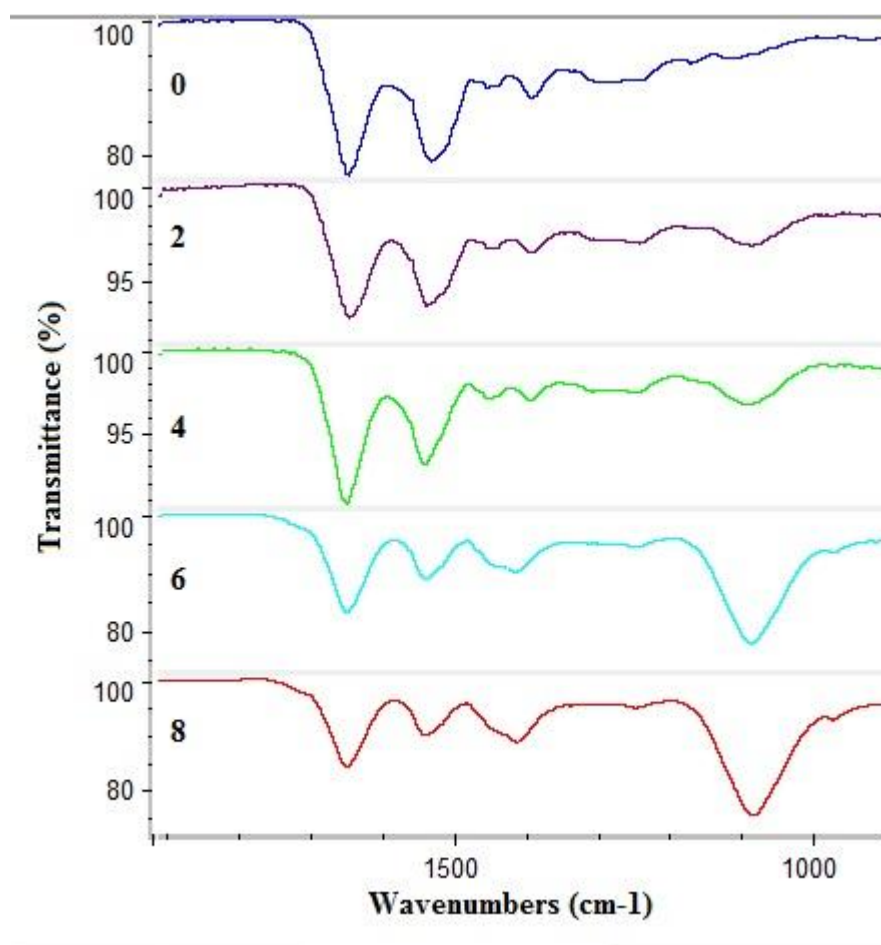


Figure 0.15: FTIR spectra of glutaraldehyde crosslinked albumin CLPA. *0 represents native lyophilized albumin and numbers 2-8 represent amount of crosslinker applied: 2. $2,12 \times 10^{-6}$; 4. $1,06 \times 10^{-5}$; 6. $3,18 \times 10^{-5}$; 8. $6,36 \times 10^{-5}$ mol per mg protein

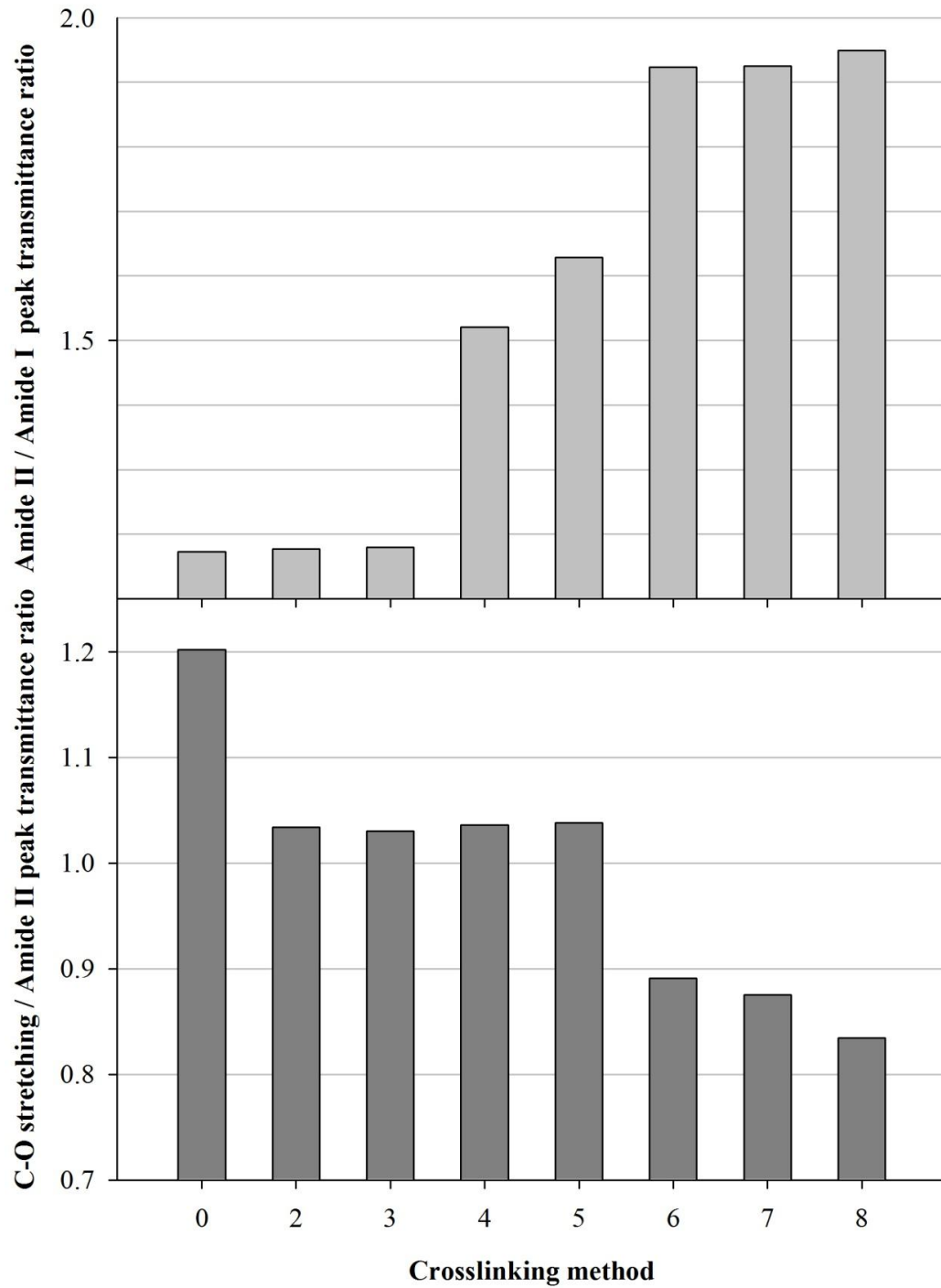


Figure 0.16: Ratio of IR band intensities versus crosslinking degree. Glutaraldehyde crosslinked albumin CLPA. * 0 represents native lyophilized albumin and numbers 2-8 represent amount of crosslinker applied: 2. $2,12 \times 10^{-6}$; 3. $0,53 \times 10^{-5}$; 4. $1,06 \times 10^{-5}$; 5. $2,12 \times 10^{-5}$; 6. $3,18 \times 10^{-5}$; 7. $4,24 \times 10^{-5}$; 8. $6,36 \times 10^{-5}$ mol per mg protein

Figure 2.17 represents qualitative comparison of IR spectra obtained from CLPA crosslinked using different methods. Keeping with discussion above it can be observed that dehydrothermal crosslinking (Figure 2.17-2) gave rise to much milder structural changes compared to chemical crosslinking methods.

Dextran polyaldehyde crosslinked CLPA (Figure 2.17-4) while resembles glutaraldehyde crosslinked (Figure 2.17-3) spectrum, clearly reflects polymer incorporation (C-O stretching peak)

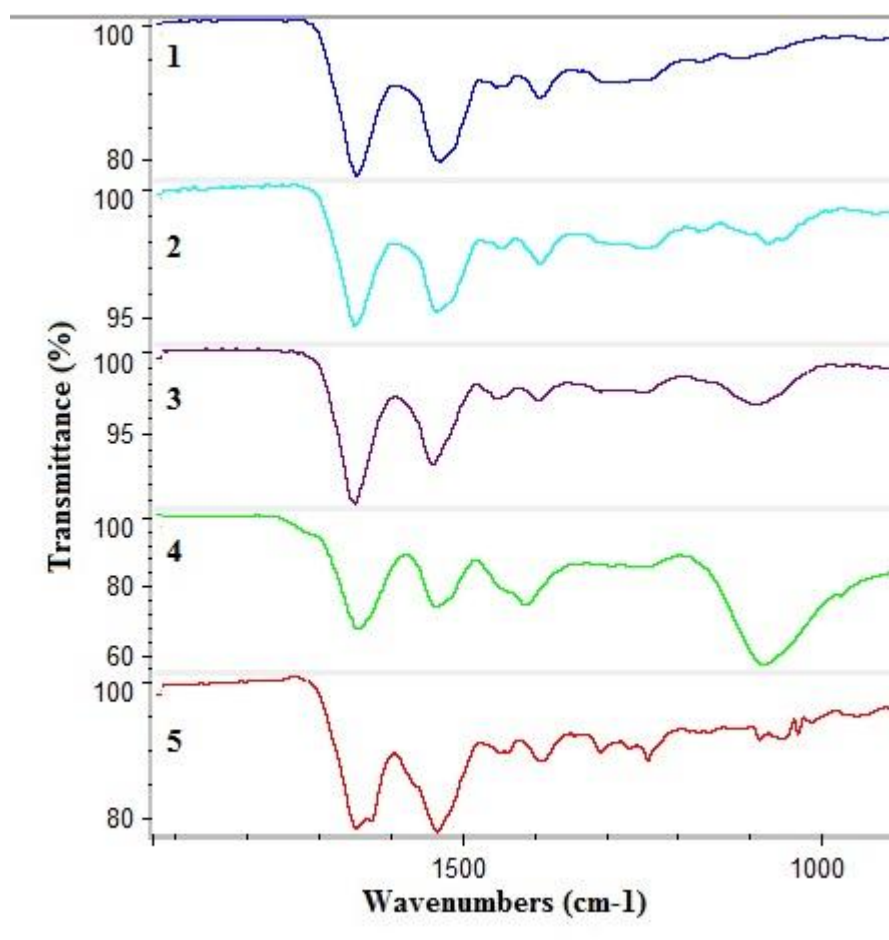


Figure 0.17: FTIR spectra of 1. Native lyophilized albumin and 2. Dehydrothermally 3. Glutaraldehyde 4. Dextran polyaldehyde 5. Carbodiimide crosslinked albumin CLPA

2.4.5. Special case CLPA optimization and Introduction of CLPL

The challenges confronted while attempting urease CLPA synthesis have led to development of alternative/supplementary methodology.

In the case of urease conventional methods for both aggregation and crosslinking have failed. The highest precursor solution achieved was 50 mg/mL in 10 mM pH 7.4 phosphate buffer. Out of precipitation medium trials, acetone and dioxane provided the highest yield, which did not exceed 10%. Any of the above described crosslinked methods further decreased the yield, resulting in the trace amount of CLPA formation. Dehydrothermal crosslinking method was attempted in order to overstep the aggregation problem, but did not result in any significant yield. That could be presumed to occur due to the lack of sufficient number of free surface lysine residues in urease structure.

Co-precipitation with albumin at different urease to albumin weight ratios was attempted aiming to both improve aggregation and provide additional lysine residues to aid inter-protein crosslink formation yield. This has led to slight improvements: It could be safely assumed that aggregation and crosslinking of urease fraction was still way below 20%. Saturated ammonium sulfate solution, acetone and dioxane precipitations provided highest CLPA yield. The catalytic activity measurements on these samples still showed negligible results, acetone precipitation leading to complete loss of activity. Crosslinking with pH 9.2 adjusted glutaraldehyde reagent appeared the most efficient.

The first breakthrough was achieved by applying “solution pre-crosslinking assisted” method, this was performed in order to capture urease out of solution state, making use of few inter-protein crosslinks formed. One tenth of the regular crosslinking reagent amount was applied to urease/albumin solution 1-5 minutes prior to precipitation. This application has finally led to some reproducible results, with while still much below average increased catalytic performance (Figure 2.18).

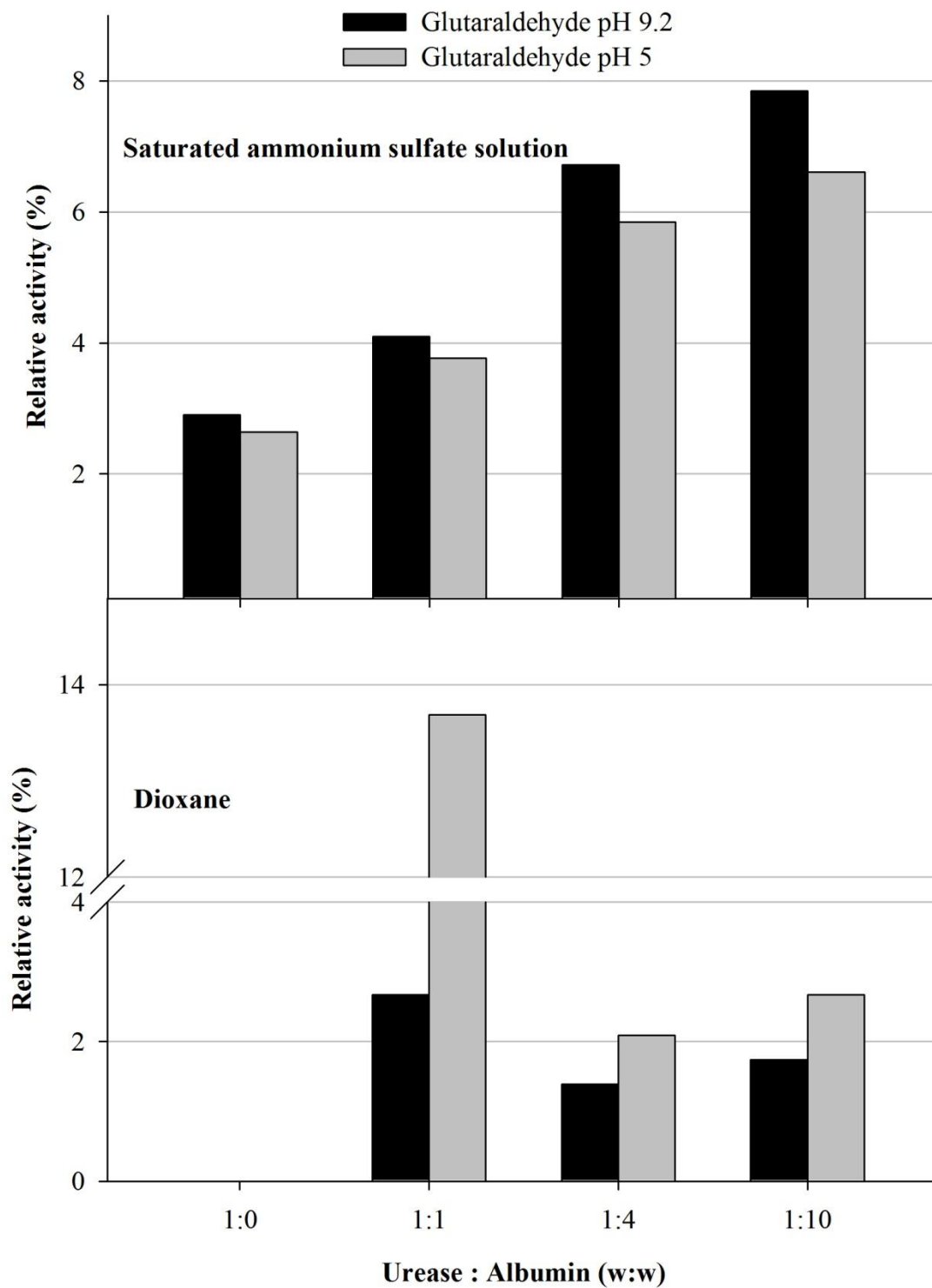


Figure 0.18: Catalytic activity of urease CLPA obtained by “precursor solution pre-crosslink assisted” method

While, dehydrothermal crosslinking method did not succeed, it became obvious that lyophilization was the only feasible way of efficient capturing with high yield. This realization has led to the idea of chemically crosslinked protein lyophilizates (CLPL) synthesis, and was carried out as follows:

Same precursor urease solution formulations were lyophilized and submerged in a crosslinking reagent containing anti-solvent. Choice of an anti-solvent was made out of those facilitating highest yield in previous aggregation attempts.

Figure 2.19 demonstrates much improved catalytic activity yields obtained by the described method. Crosslinking efficiency, on the other hand, remained the subject to further optimization, yielding 10-30 % with the developed technique. All further synthesis optimization and utilization of urease CLPL material is within the scope of another ongoing Doctorate Thesis.

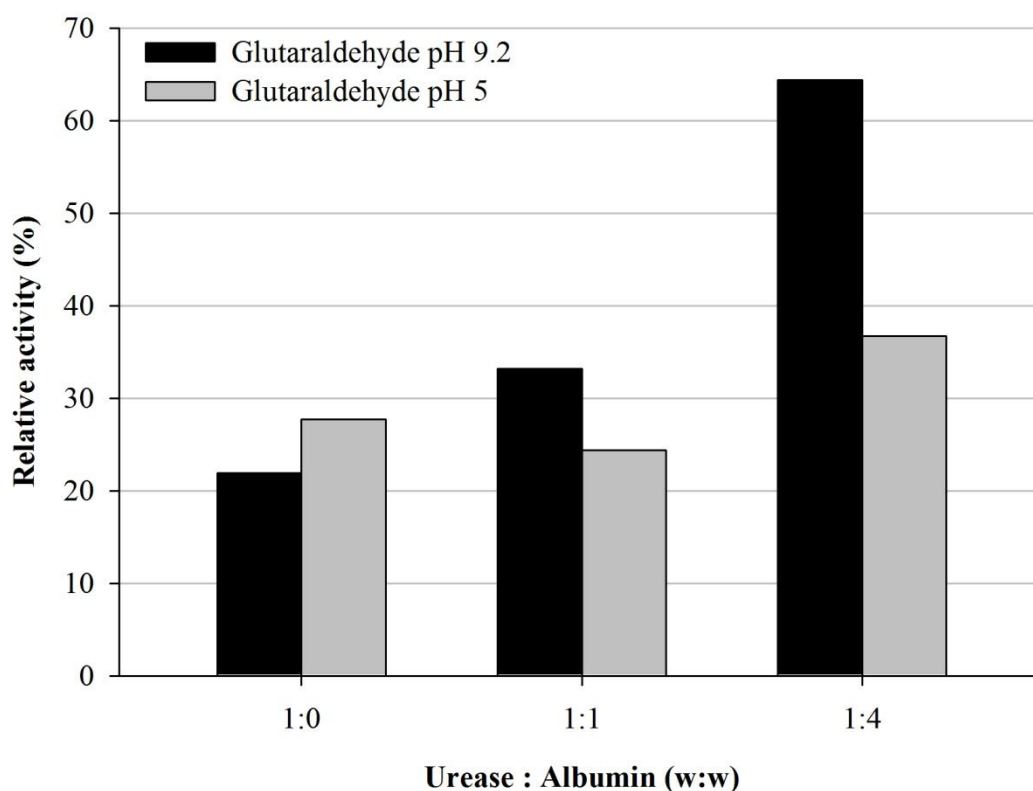


Figure 0.19: Catalytic activity of urease CLPL

The technique developed herein, on the most challenging example of urease, has led to solutions for issues mentioned earlier in the text, particularly related to all

aggregation/crosslinking yields below 100%. Herein it was applied in further optimization of less challenging proteins, aiming to address the drawbacks of earlier developed methods. The earlier discussed issue of crosslinking yield of trypsin and chymotrypsin CLPA formulation, especially in the case of low pH precursor solutions was completely resolved, making use of ionization state adjustment applied to lyophilizates prior to crosslinking, same way as employed in dehydrothermal crosslinking technique. Protein lyophilizates prepared in this manner were immersed in crosslinker reagent containing 2-propanol. This technique led to 98-100% synthesis yield with statistically insignificant fluctuation between different precursor solutions.

Significant change in the crosslinker type effect as compared to corresponding CLPA formulations was observed in cases of both trypsin (Figure 2.20) and chymotrypsin CLPL. Glutaraldehyde crosslinking led to almost complete catalytic deactivation, while much improved catalytic yields were detected in dextran polyaldehyde crosslinked CLPL, as compared to corresponding CLPA. It is assumed that the dense aggregate network has aided in protection of CLPA from excessive intra-protein modification, while much higher porosity bearing lyophilizates were intolerably affected. On the other hand, less bulky morphology has led to decreased accessibility limitations observed in dextran polyaldehyde crosslinked CLPA, resulting in significantly improved catalytic activity, particularly in the case of chymotrypsin (Figure 2.21).

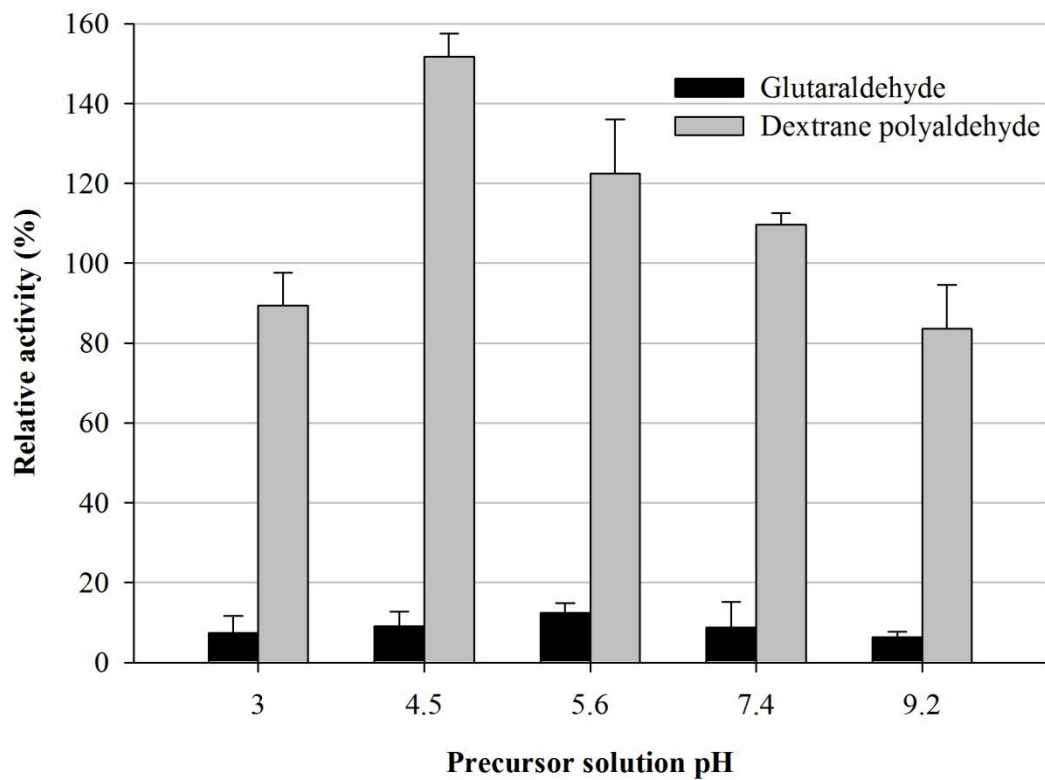


Figure 0.20: Catalytic activity of trypsin CLPL

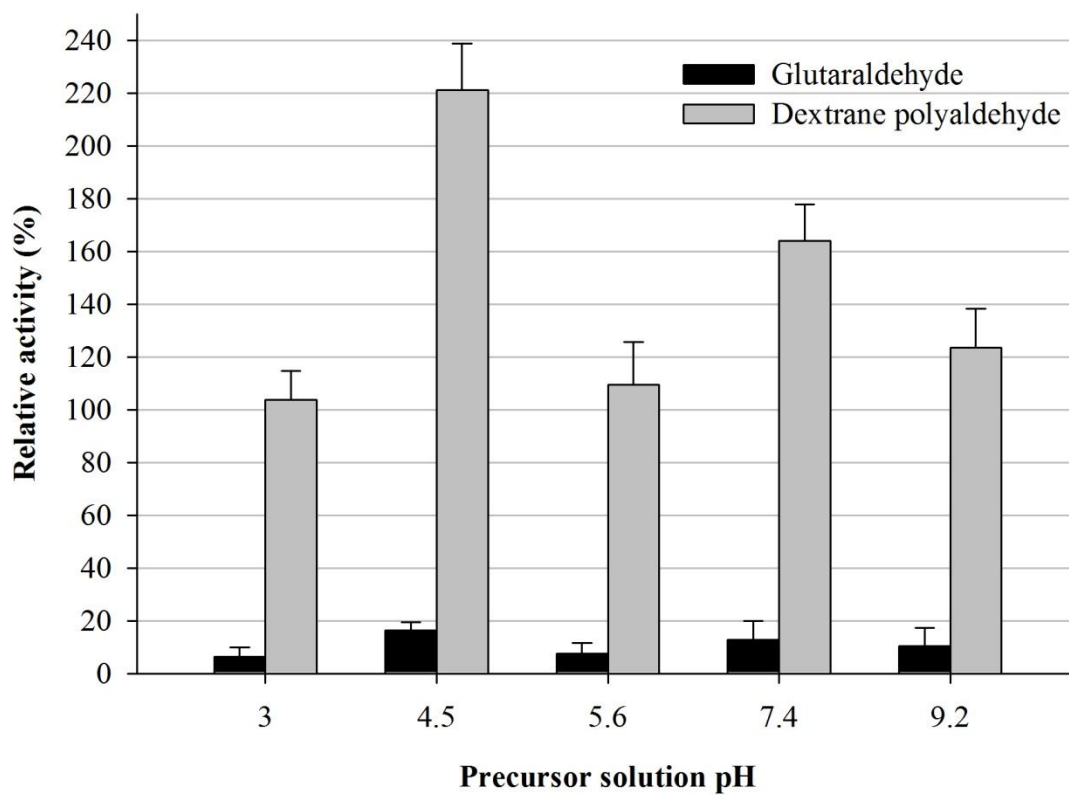


Figure 0.21: Catalytic activity of chymotrypsin CLPL

3. Generation and Characterization of Nano-CLPA and Nano-CLPL Materials

3.1. Introduction and Rationale

This chapter aims to describe general methodology of nano-CLPA generation technique developed herein as a function of nanonization conditions with respect to precursor CLPA protein type and synthesis protocol.

As opposed to the previous chapter methodologies described herein are not based on any existing study and form an entirely novel top-down approach to generation of nano-sized protein catalysts, namely physical downsizing of macroscopic CLPA/CLPL precursors, as opposed to conventional bottom up approach. The macroscopic material is downsized by direct application of mechanic or hydrodynamic shear force in an optimized medium. The general method developed herein attempts to address concerns familiar to heterogeneous-phase aqueous, as well as nonaqueous, enzymatic processes such as mass transport and diffusion limitations, reduced access to catalytic centers, restricted catalytic turnover arising from crosslink-prompted structural rigidity or poor coordination. Under optimized conditions, the resultant nano-particle catalyst was consistently more active than its crosslinked precursor, showing that in addition to the processing history, the apparent activity for a given amount of protein also depended on particle size when transcending from the micron to sub-micron scale.

The scope of this Chapter is focused on the methodology development and optimization, rather than fundamental kinetic study of heterogeneous nano-particle catalyst system, which would form the main subject of the future work.

The technique has been applied to all protein CLPA/CLPL described in Chapter 2, therefore demonstrating general applicability of the method. Methodology optimization is typically described on a model of albumin and trypsin and chymotrypsin. Following the

pattern of Chapter 2, albumin has been chosen as an initial model due to its stability and ease of manipulation. The trypsin and chymotrypsin models were in order to investigate the catalytic activity of CLPA and nano-CLPA formulations, while also serving as an example of handling a protein with low solution state stability, in this case due to high autolysis activity. Furthermore, commercially obtained Savinase® CLEA (CLEA Technologies) has been used in nano-CLPA fabrication in order to compare a conventionally available protein formulation with its nano-CLPA alternative developed in house.

Generation of nano-particles of the defined size in the range of 100-900 nm was successfully achieved herein, aiming to be utilized in a wide range of industrial, analytical and biomedical applications. The emphasis of the work conducted was to establish the general methodology and guidelines to achieve any particle size of the CLPA formulation in question in the range of 100-900 nm size with maximum yield and homogeneity, rather than discussing specific application requirements.

3.2. Materials

Sample of Savinase® CLEA was provided by CLEA Technologies.

Other proteins were obtained as described in Chapter 2.

All other reagents were obtained from commercial suppliers as analytical grade and were used without further purification.

3.3. General Methods

CLPA and CLPL formulations were synthesized via techniques optimized/developed in Chapter 2. The aggregation and crosslinking steps were conducted in a manner that facilitated effective nanonization, while permitting retention, and in many cases, improvement of biological activity. Subsequent to crosslinking, nanonization was realized through hydrodynamic shear or mechanical shear. Grinding aids were typically added to facilitate nanonization and retention of the highest possible bioactivity.

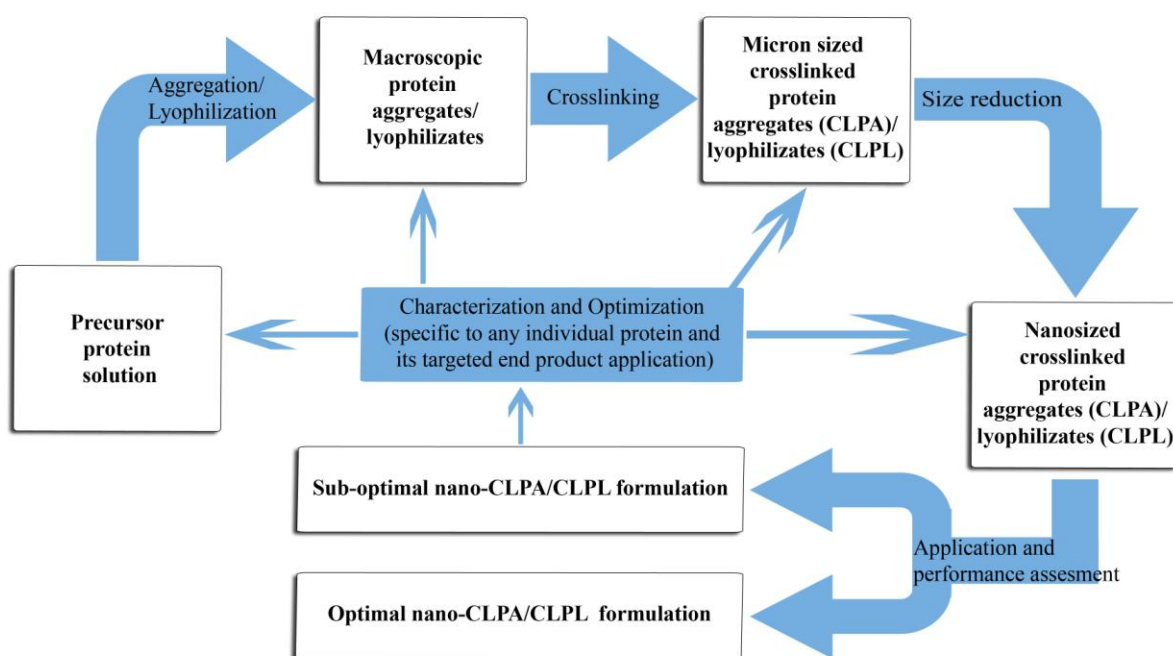


Figure 3.1: Flow chart summarizing the overall synthesis and optimization process

3.3.1. Nano-CLPA generation

Precursor CLPA formulations were synthesized as described in Chapter 2. All nanonization procedures should be viewed upon as a function of the given precursor formulation, both as protein type and CLPA synthesis steps, as signified throughout the discussion.

3.3.1.1. Mechanical shear

Mechanical shear application was performed in an agate mortar with shear force applied by hand. Alternatively Gelimat compounder was employed in initial and scale up downsizing experiments at a rate of 2-6 krpm for the duration of 5-30 min. Sucrose or potassium chloride was used as an additive at 1:1 or 1:2 additive:CLPA weight ratio.

3.3.1.2. Hydrodynamic shear

Preliminary homogenization procedures were performed in standard laboratory scale homogenizer at 1-10 mg CLPA per 1 ml medium. Homogenization medium was composed of aqueous solutions of sucrose or potassium chloride at concentrations varying at 0-10 mg/ml. Homogenization was performed at a rate of 2-6 krpm for the duration of 5-30 min.

Further homogenization procedures were performed in SilentCrusher M homogenizer (Heidolph Instruments GmbH & Co.KG) at a 2.5 mg protein per 1 ml medium.

Homogenization medium was composed of 0-70 wt% aqueous glycerol solution or 70-100 wt% ethanol. Sucrose or potassium chloride was used as additive at 0-10 mg/ml concentrations. Homogenization was performed at a rate of 5-20 krpm for the duration of 5-30 min.

CLPA was typically dried and weighted prior to being transferred into homogenization medium, where not specified otherwise.

3.3.2. Analysis

3.3.2.1. Scanning electron microscopic (SEM) structural analysis

CLPA powder was subjected to treatment in an Emitech brand K950X model carbon coater. An approximate coating thickness of 2-3nm was targeted. The processed samples were loaded into the vacuum chamber of a ZEISS brand LEO SUPRA 35VP model SEM with GEMINI column. An electron gun voltage of 2kV was employed throughout the analyses.

3.3.2.2. Dynamic light scattering (DLS) particle size analysis

For initial screening (data presented in section 3.4.1), 1ml homogenized samples were centrifuged at 1krpm to separate from residual micron sized particles prior to DLS analysis, all further data obtained was collected without centrifugation step. The sample was diluted 10 fold in medium corresponding to their homogenization conditions. DLS data was collected on samples equilibrated at 25 °C in 2ml disposable cuvettes, as a result of 3 consecutive scans, Malvern Zetasizer NANO ZS. Absorption of each sample was measured at 633 nm and included in DLS measurement protocol. Particle refractive index of 1,5 was assumed for all CLPA samples and refractive index of corresponding medium were included in the protocol. Data was analyzed using protein analysis model, Malvern Zetasizer software.

3.3.2.3. Determination of nanonization yield

Nanonization yield was established by centrifugation (0,7-2 krpm, 5-10 min) of the 2ml aliquot of homogenized suspension in the pre-weighted eppendorf tube. Formed precipitate

was isolated, washed thrice, vacuum dried and weighted. The nanonization yield was calculated according to the following equation (3.1):

$$\text{Nanonization Yield (\%)} = 100\% - \frac{W_p}{W_t} \times 100\% \quad (3.1)$$

Where W_p and W_t are dry weights of precipitate obtained upon centrifugation and total weight of CLPA in the 2ml suspension aliquot prior to homogenization (dry weight equivalent) respectively. All presented data was the mean value of experimental results repeated 6 times.

Supernatant obtained from centrifugation was used in order to establish centrifugation conditions necessary to isolate the submicron fraction of the homogenized suspension. The process was conducted interactively with DLS measurements, starting with 5min 0,7 krpm centrifugation conditions and increasing the speed and time of centrifugation after each measurement until no residual micron sized particles could be detected. This fine tuning procedure had to be performed for every sample separately. The centrifugation conditions determined in this manner were used in the nanonization yield determination described above.

3.3.2.4. Relative bioactivity assays

Relative catalytic activity measurements were performed as described in Chapter 2. Methods. Where applicable, nano-CLPA in homogenization medium was dialyzed 4-5 times (depending on the viscosity of homogenization medium), for at least 4 hours each, against buffer solution prescribed for the given analysis, using a MW cutoff of 10 KDa,

3.4. Results and Discussion

In the similar manner to chapter 2 herein the nano-CLPA generation procedure is described in two parts. First, the initial screening is briefly described, therefore providing a short history of the methodology development process, followed by detailed description of process optimization on the model of albumin, trypsin and chymotrypsin.

3.4.1. Initial methodology development

Feasibility and ease of physical downsizing method has been demonstrated on the first attempt. Surprisingly nanoparticle content could even be obtained while using an agate mortar with shear pressure applied by hand. The very simple mechanical down-sizing method proved convenient in providing rapid proof of down-sized, catalytically competent material, and instrumental in revealing the embrittled quality of crosslinked aggregates. However, down-sizing proved impossible to reproduce, as shear was being applied manually. In contrast, the post-nanonization traits of CLPAs subjected to machine-calibrated homogenization proved reproducible, providing a convenient basis to systematically explore the nanonization phenomena in terms of a range of applied shear, amongst other parameters.

Gelimat compounder was successfully used for mechanical shear application, but due to the technical limitations could only be employed in scale up pilot trials, with the minimum overall weight of 100g material.

Alternatively homogenizer was used for application of hydrodynamic shear. Figure 3.2 presents a DLS measurement of supernatant (1krpm) (a) lysozyme CLPA suspended (b) lysozyme CLPA suspended and homogenized in 5mg/ml potassium iodide solution. This data provided evidence of nanoparticle content generation upon nanonization procedure,

since only residual monomeric lysozyme particles can be observed in the unprocessed CLPA sample.

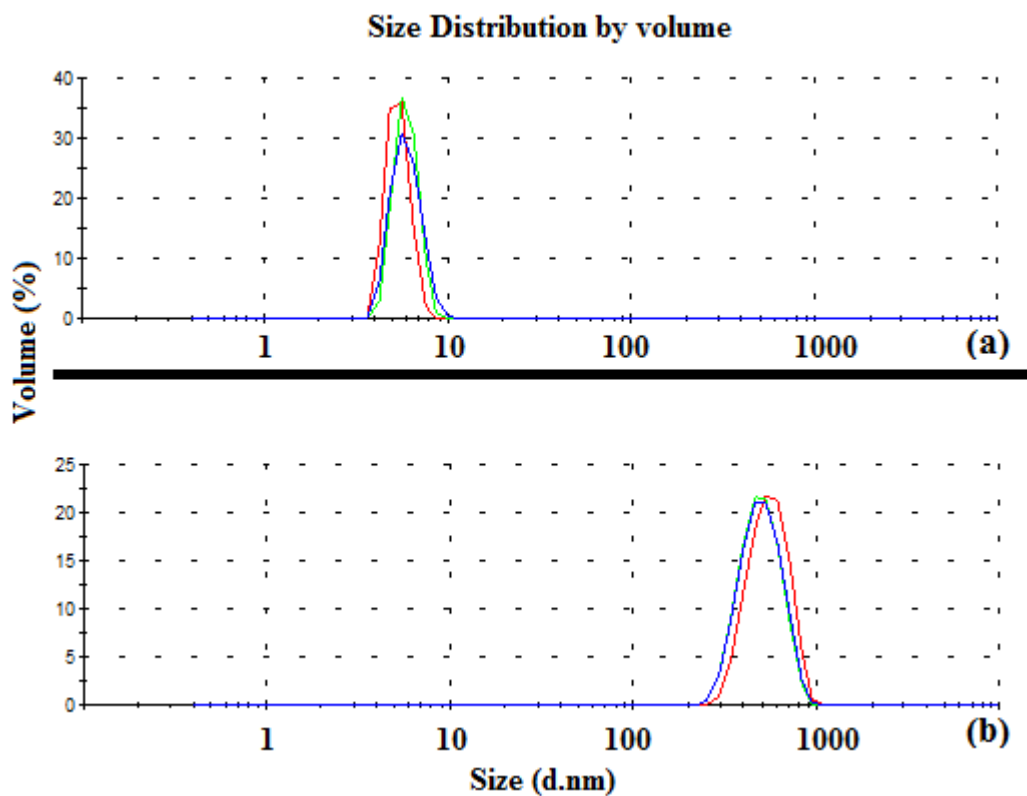


Figure 3.2: Raw DLS data presentation of crosslinked lysozyme aggregates (a) before and (b) after nanonization with 5 mg/ml potassium iodide

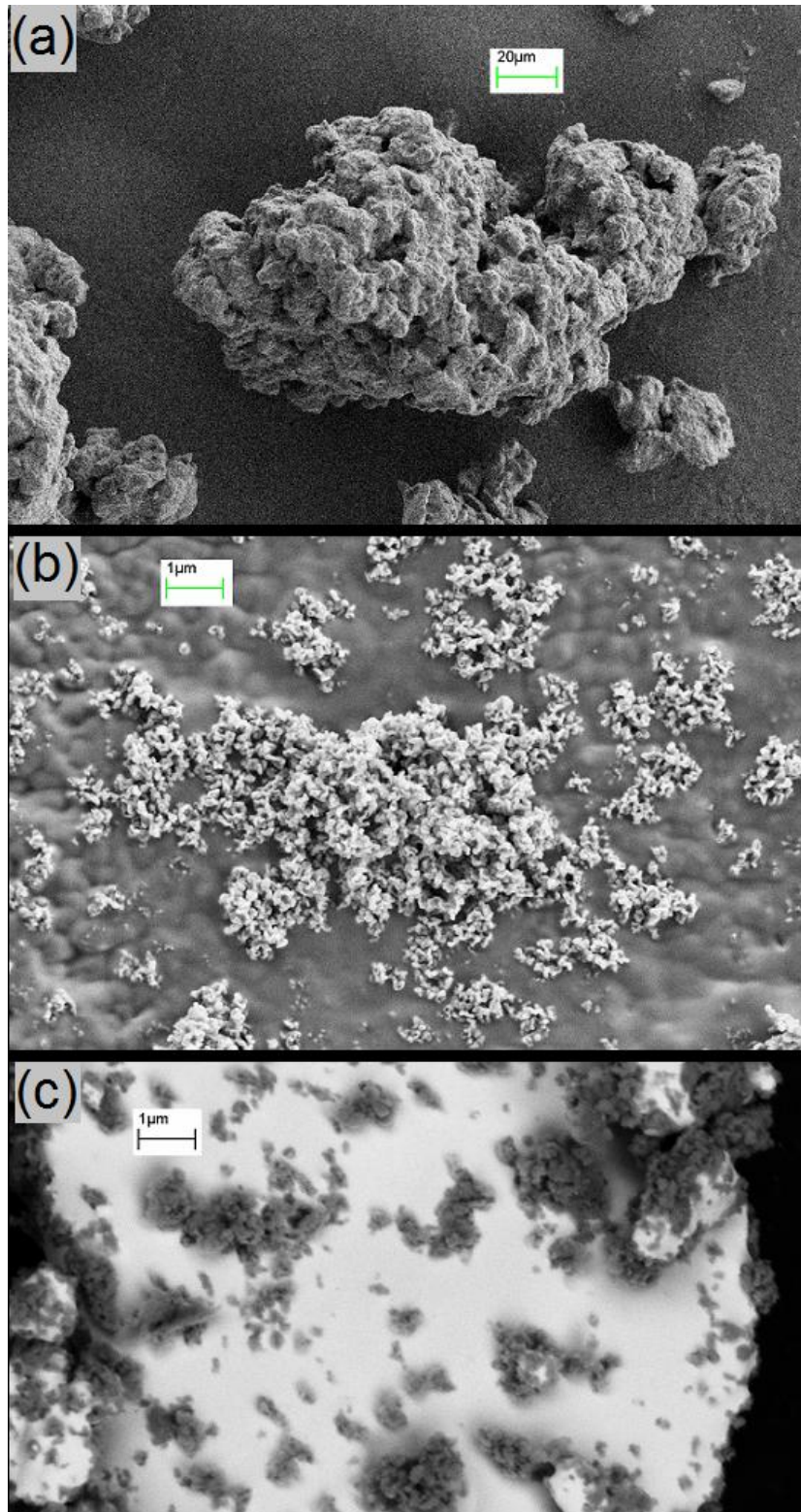


Figure 3.3: SEM images of lysozyme (a) CLPA, (b) homogenized and (c) grinded nano-CLPA

Figure 3.3 presents the preliminary SEM imagery results illustrating the morphology and approximate size order of crosslinked lysozyme precursor material (a), hydrodynamically nanonized crosslinked precursor (b), and mechanically nanonized crosslinked precursor (c). The precursor lysozyme material appeared micron-sized, while material subjected to shear appeared nano-sized and highly polydisperse. In contrast to crosslinked precursor material, noncrosslinked lysozyme aggregates readily dissolved under homogenization conditions, and yielded unretractable smears during manual mechanical shearing. Material prepared using other proteins types displayed the same trend (SEM results not shown). In targeting various particle sizes, the average size and distribution obtained clearly showed protein type variability.

Furthermore, even in the initial trials it could be detected that, irrespective of protein type, the CLPA preparation method and subsequent size-reduction conditions influenced nanonization.

Unlike particle size, catalytic activity was less predictable. As plethora of literature implies catalytic activity was influenced by the processing history leading to CLPA formation, namely, the methods used to aggregate and crosslink protein. The basis of their influence on activity rested on providing conditions, which would permit retention of catalytically-competent structure and sufficient conformational flexibility over the course of the solute-to-solid phase transition and crosslinking step, which was discussed in length in previous Chapter.

The nano-CLEAs were consistently more active than their crosslinked precursors, showing that in addition to the processing history, the apparent activity for a given amount of protein also depended on particle size when transcending from the micron to sub-micron scale. Since nanonization was not anticipated to invoke static or dynamic alterations to the network arrangement, the improved rates also confirmed a gradual transition from diffusion-control to reaction-control in proceeding from micron- to submicron-sized particles. While the generality of this transition has not been confirmed here directly, the predominance of diffusion at the multi-micron scale was clear in any case.

Still, the predominance of diffusion-control was not overwhelming as could have been anticipated particularly for high molecular weight substrates. Previous work on micron-sized crosslinked enzyme crystals¹⁷, which showed that substrate diffusion or active-site

access were not drastic determinants of overall activity as previously feared, contributing only marginally to changes of activity compared to more important factors such as protein rigidity. Enormous substrates notwithstanding, apparent rate differences between native state and nano-CLPAs were not likely diffusion-related. Rather, the underlying factors would relate to the protein itself. In aqueous media, these would include shifted pH optima and other stereoelectronic effects, protein-crosslinker compatibility, and reduced conformational freedom. Indeed, protein-protein juxtapositioning has been shown to perturb pKa value and nucleophilicity, which could prove advantageous or otherwise³⁹. Improperly-chosen or sub-optimally utilized crosslinkers could knock-out residues important to binding or catalysis without altering the protein global structure, yielding an apparent reduction of overall activity. Ironically, neighbor- and crosslinker-induced restrictions of conformational freedom will also reduce the protein's entropy per unit time. The end result would be Gibbs ground state elevation of individual proteins in the CLPA, yielding more reactive catalysts. While the weight-averaged contributions of these terms are subject to variability, it would appear, given the net rise of activity that catalytic losses due to crosslinking had not substantially contributed in the case of the optimized nano-CLPA formulations attempted herein.

Further supporting this claim, most of the catalytic activity yields described here and throughout optimization results, appear very closely related to results obtained for the corresponding precursor macroscopic CLPA. The consistent yield increase does not conceal the distinct pattern dictated by CLPA formulation, demonstrated in the previous Chapter.

While bond rupture was not confirmed, covalent changes inevitably accompanied the nanonization process, given the established chemistry of aldehyde-based reductive crosslinking. Barring that fraction of broken bonds, which failed to yield two nanoaggregates from one, all proteins directly involved in bond rupture would necessarily define the outermost shell of the resultant aggregate. With a shell thickness comparable to the typical protein diameter of 3-5nm, a typical nanoaggregate of 500nm diameter would contain at least 105 catalytically competent proteins in the underlying layers. Hence, activity losses related to bond rupture were presumably insubstantial as opposed to serious.

That being said the mechanical behavior implemented by the nature precursor CLPA, greatly affected both nanonization efficiency and applicability of nanonization in terms of stability under shear applied, some not able to withstand the high shear conditions. Both are discussed within the scope of nanonization procedure optimization.

Initial trials with shear speed approximately equal to that of Gelimat compounder resulted in similar output both in terms of particle size and final activity of the resultant nano-CLPA (Figure 3.4), showing comparability of the two techniques. All of the trials resulted in nano particle content formation and increase in relative catalytic activity compared to the micron sized precursors. That being said, size distribution homogeneity and overall nanoparticle content efficiency appeared higher with application of mechanical shear (up to 70%). While a very low percentage of particles in initial formulations of homogenization medium was nanonized (up to 10%). Yet, due to the described material amount limitations, Gelimat compounder grinding could not be used for initial screening purposes and was only later on applied on industrial grade enzyme mixtures (MAPS enzymes) to prove applicability of a scale up process.

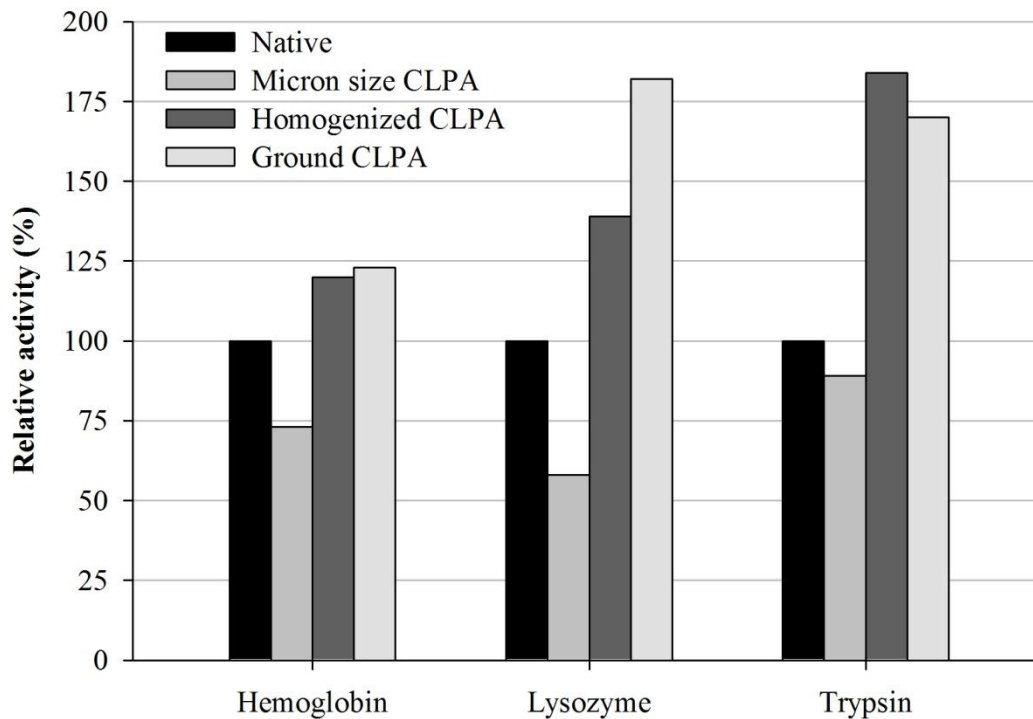


Figure 3.4: Preliminary review of nanonization method effect relative catalytic activity of CLPA

Figure 3.4 expresses the relative activity of native lysozyme, trypsin, and hemoglobin, as well as their micron-sized CLPAs and nanonized CLPAs. Bioactivity for the particular experimental protocol adopted in these preliminary experiments was least in the micron-sized CLPAs, intermediate in the native soluble protein, and highest in the nano-CLPAs. The most dramatic drop in proceeding from native to micron-sized CPLA was in lysozyme, with 60% relative activity being observed. The result is not surprising, given the enormous size of the substrate in the assay employed here, based on the digestion bacterial wall. The other two protein CLPAs showed approximately higher relative activity. Activity in the nano-CPLAs slightly varied amongst the three proteins, reflecting relative activity increases ranging from 40-85% compared to native protein. Activity tested comparable amongst the two nanonization methods for a given protein. The above trend could not be generalized, as other proteins, or sub-optimally prepared nano-CLPA variants of a particular protein, yielded higher activity in the native state compared to the corresponding nano-CLPA

(discussed later in the chapter). It was true for all proteins tested that nano-CLPAs gave higher conversions than the corresponding micron-sized CLPA. The extent of this improvement for the particular protein, was very strongly dependent on the size of the substrate employed, increasingly pronounced with large substrates. This can be observed from the insignificant fluctuation of hemoglobin CLPA upon nanonization.

The shear speed of Gelimat compounder and homogenizer employed in these initial trials could only be controlled approximately, with an error reaching 1krpm.

For all further optimization purposes homogenization method was employed. These initial trials have been conducted on all of the proteins described in Chapter 2. Homogenizer employed at this point (SilentCrusher M homogenizer, Heidolph Instruments GmbH & Co.KG) has facilitated much higher operational precision and time with applicable shear speed up to 25 krpm.

Parameter that could conclusively be tested at this point was the effect of additives on overall nanonization efficiency and size distribution (Figure 3.5). As has been initially rationalized, addition of salts and small sugars was found to facilitate the nanonization of relatively soft CLPA material, serving as grinding aid. The negligible nanonization yield was recorded in additive free medium, for both grinding and homogenization experiments. On the other hand, concentration of additives had an effect to a much less significant extent than could be expected. Furthermore, amongst the attempted additives, the nature of additive had negligible effect on the efficiency of nanonization. Addition of 2,5-5 mg/ml of both potassium chloride and sucrose appeared to yield highest nanonization efficiency and these concentrations of additives in homogenization medium were used in all further trials, unless otherwise specified in the text.

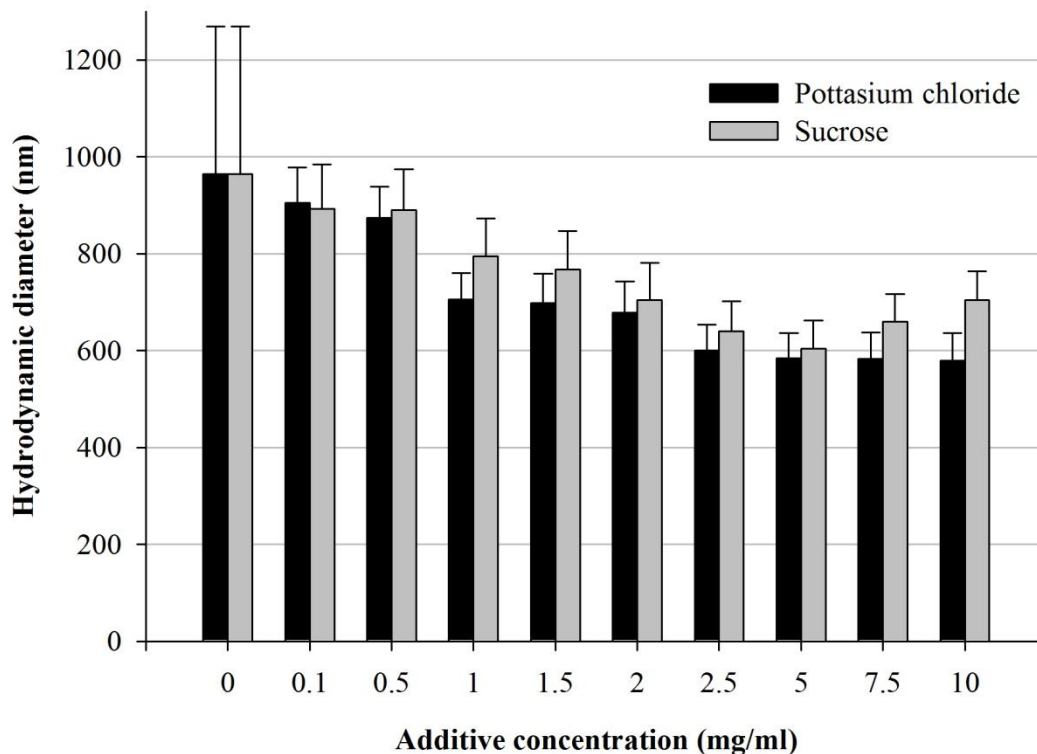


Figure 3.5: Effect of additive incorporation in the homogenization medium on nanonization yield. (Albumin CLPA was homogenized at 20 krpm, 30 min)

The other major role of additives was in arresting irreversible agglomeration of the particles after homogenization, as was shown by the dialysis of particles against double distilled water upon homogenization, which resulted in highly unstable suspension as detected by DLS analysis (results not shown). The use of relatively high ionic strength buffers (PBS) for dialysis has proven sufficient for relative stabilization of the nanoparticle preparations, avoiding irreversible agglomeration of the particle resuspendable upon agitation⁴⁰.

In order to investigate the homogenization speed and time as parameters, experiments were conducted in the range of time (5-30 min) and speed (5-20 krpm) in medium consisting of 5 mg/ml potassium chloride in double distilled water. The general effect of homogenization speed and time could be summarized here. As demonstrated on Figure 3.6 nanonization could be achieved after periods as short as 5 min, but in order to achieve higher size distribution homogeneity longer homogenizations time were required. While some decrease in overall particle size was observed with increasing homogenization time, this parameter is

best used to optimize size homogeneity quality, rather than size fine tuning parameter. On the contrary homogenization speed formed the main parameter in adjusting the desired particle size. With the systematic pattern of higher shear rates generate lower size particles (Figure 3.7).

While somewhat enhanced, the overall nanonization efficiency rarely exceeded 20 % with still highly heterogeneous size distribution of the nanonized fraction.

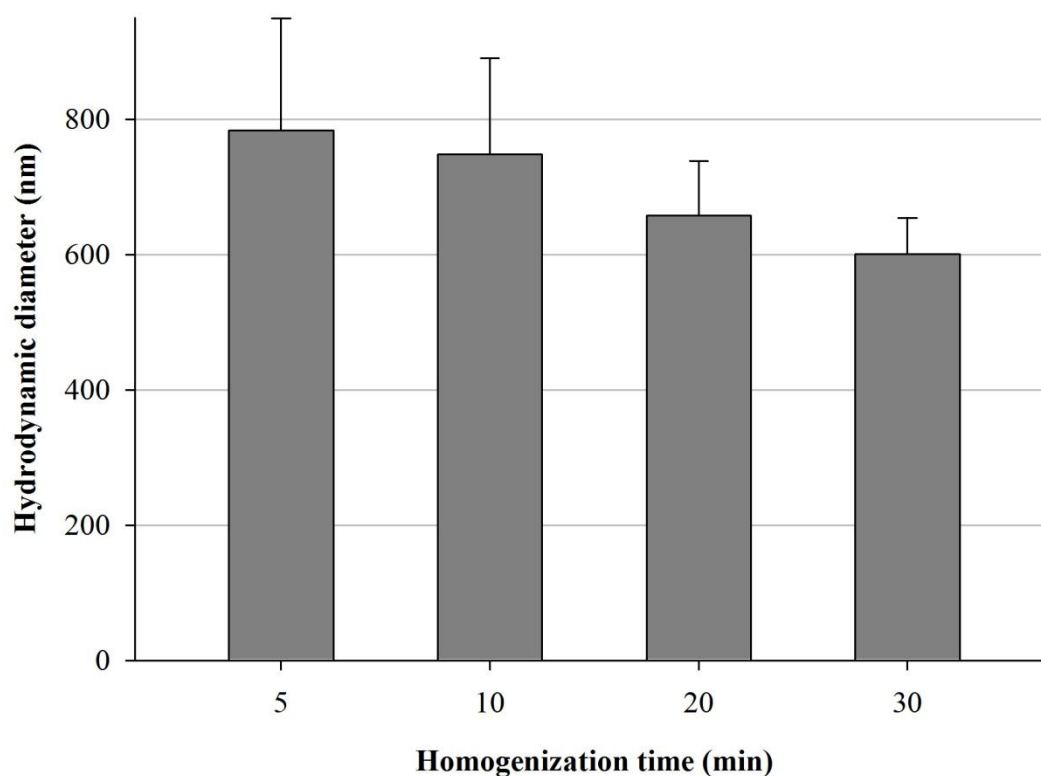


Figure 3.6: Effect of homogenization time on nanonization efficiency. (Albumin CLPA was homogenized at 20 krpm)

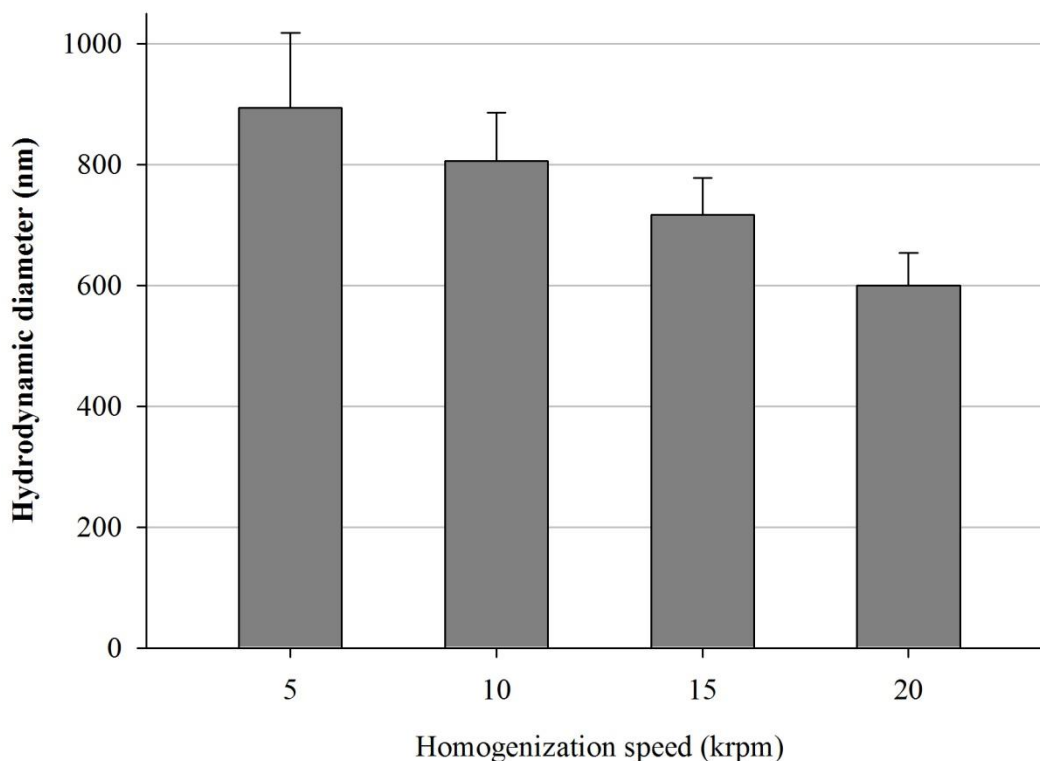


Figure 3.7: Effect of homogenization speed on nanonization efficiency. (Albumin CLPA was homogenized for 30 min)

Higher concentrations of protein per medium volume were tested, in attempt to increase the yield of homogenization, but did not result in improved efficiency. Furthermore higher protein suspension densities often led to decrease in quality of the resultant sample and occasional clogging of the homogenizer propeller.

All attempts to separate particles into size fractions through sieves and membrane filtration has failed even with the finer quality samples. It could be derived that clogging occurs not only due to highly heterogeneous distribution and presence of residual micron sized particles of the lower quality samples, but rather due to intrinsic properties of CLPA material. Centrifuge separated nano particle fractions also appeared to clog the sieves.

Therefore, the only technique employed herein and throughout the further optimization experiments was centrifugation ranging from 1 to 4.5 krpm, assuming complete precipitation of the particles at higher speeds. All DLS measurements were conducted on

the supernatants of homogenized samples centrifuged at 1 krpm in preliminary studies described above, in order to eliminate large portion of residual micron sized particles.

3.4.2. Optimization of nanonization conditions in terms of nanonization yield and size reduction efficiency and consequent final product catalytic activity

The initial study has established the general technique, and proved the merit of unprecedented top-down approach. Yet, while one of the argued benefits of the developed material was the high synthesis yield of the precursor CLPA, dramatically low efficiency of nano-particle generation seemed to defeat the purpose. Therefore further research has focused on overall yield enhancement, along with narrowing the range of desired particle size distribution for any given CLPA formulation.

3.4.2.1. Homogenization medium effect on yield and size reduction efficiency

One of the benefits of hydrodynamic shear versus mechanical shear could not be accounted for during initial trials: that is the benefit of using homogenization medium composition in order to manipulate fine tuning of particle size, and enhance overall nanonization efficiency and provide convenient size separation out of nanonized mixture.

Incorporation of aqueous glycerol solutions into homogenization medium was first attempted aiming to provide more efficient size fraction separation through centrifugation of generated polydispersed nano-particles⁴¹. The encountered result has exceeded expectations, addressing the problem of low overall sub-micron particle generation yield during the homogenization process.

Figure 3.8 summarizes the hydrodynamic diameter of nano-CLPAs of albumin as a function of the wt% glycerol in water. For a particular CLPA preparation, homogenization time, shear speed, salt concentration and %wt range, the mean hydrodynamic diameter varied from 600 nm in 0wt% glycerol to 230 nm in 70wt% glycerol. Within these extremes, a steady, monotonic decrease of mean diameter was noted as a function of increasing wt% glycerol. Glycerol values of 10-50wt% appeared to yield a linear profile, with slight concave-up deviations being noted at both wt% extremes.

In addition to the decrease of particle diameter, the error bars, or absolute size distribution, had also narrowed with increasing glycerol concentration. In some cases, optimized nanonization media had afforded size variations of less than 100nm (data not shown). Viewed in relative terms (i.e., size distribution / mean diameter), the homogenized albumin CLPA revealed constant product polydispersity over the full range of glycerol trials. Similar downsizing trends were noted for other CLPA preparations, with particle sizes and size distributions showing variation according to the different protein types and CLPA protocols. Most importantly, increased glycerol content had significantly improved yields in the sense that more sub-micron particles could be generated for a given amount of CLPA.

The near-linear trend between mean particle diameter and wt% glycerol indicated near-ideal weight-averaged contributions of water and glycerol in the homogenization medium. The correlation also implied that protein CLEA preparations, properly calibrated at a fixed homogenization temperature, rate and time, could be downsized with good predictability simply by adjusting the ratio of components of the homogenization medium.

The basis for yielding smaller particles in higher glycerol loadings was not systematically investigated, but it can be supposed that higher-viscosity media would invoke stronger shear forces, thus facilitating fragmentation. Hydrodynamic cavitation was also a likely contributor, but its effect on downsizing was likely secondary to hydrodynamic shearing in view that cavitation is less pronounced in viscous media, which in fact yielded the smaller particles. In addition to the fragmentation events, it follows to suppose that nanoparticles, once formed, would be less likely to re-associate in glycerol-rich media, as higher viscosities would slow Brownian motion. For overlapping double layers, it would follow to

also reason that osmotic flow of the denser glycerol-water media would presumably separate the near-agglomerated particles more easily⁴².

In addition to the above, steric and electrokinetic effects were also considered as having potentially contributed to the observed particle size distribution, since both are known to influence dispersion stabilities. Steric repulsion could not have applied herein, as each nano-CLPA surface was solvated with water or glycerol as opposed to large chains such as PEG. In contrast, various electrokinetic effects could have resisted re-agglomeration, but their relative contribution was difficult to rank, particularly in transcending from water to the less understood water-glycerol system. In any case, what is expected was a decrease of the dielectric constant in proceeding from water to glycerol-rich media, reflecting a weight-averaged contribution of both liquids. The near-equivalent hydrogen bonding of water and glycerol also implied spatial homogeneity of the weight-averaged dielectric constant, with potential enrichment of glycerol, in view of its chelating ability, being conceivable only along the immediate nano-CLPA surface. For aqueous-polar organic mixtures, established electrokinetic theories are expected to hold true⁴³, permitting some analysis as a function of the decreased dielectric constant. For instance, the Henry equation as well as measurements reported for alumina dispersions in water-glycerol systems⁴⁴ would predict an increased magnitude of the zeta potential. Hence, nano-CLPAs placed in glycerol-rich media would be expected to take on improved stability. That being said, a decrease of the dielectric constant could also conceivably prompt re-agglomeration, as implied by a decreased Debye-Hückel screening strength⁴², which would serve to thin the double-layer and permit closer approach of dispersed particles. Even so, it was not clear if the double layer thickness had dropped beneath the average inter-particle separation in glycerol-rich media. Hence, both scenarios could have contributed, or a high zeta potential alone might have established a stable dispersion of small nano-CLPAs in 70 wt% glycerol.

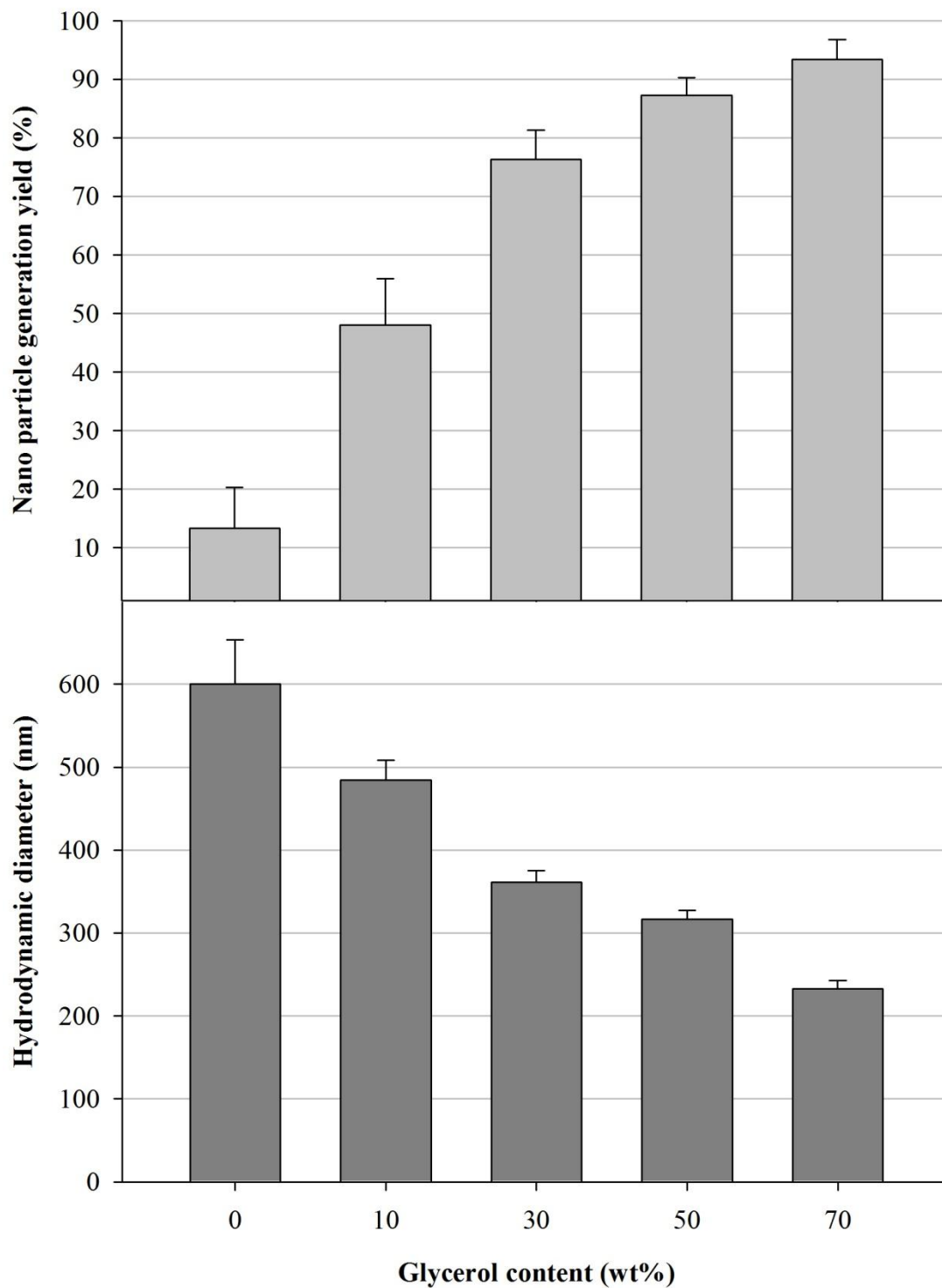


Figure 3.8: Effect of glycerol incorporation in aqueous homogenization medium on nanonization efficiency and nano-particle generation yield. (Albumin CLPA was homogenized at 20 krpm, 30 min)

Preparation of nano-CLPA for initial *in vitro* cell internalization studies, described in the next chapter, has indirectly led to use of ethanol as homogenization medium. These trials, initially intended as disinfection pre-treatment, have posed a plausible alternative to aqueous glycerol medium.

At 70 wt% aqueous ethanol solution the nanonization data has not differed substantially from results obtained in double distilled water medium homogenization. On the other hand, use of absolute ethanol, while following more or less comparable scale as that of the aqueous homogenization in achieved particle size, has resulted in a dramatic increase in overall efficiency and much higher precision in resultant nanoparticle size distribution.

As opposed to the rationale of increased shear forces applied to material due to high viscosity of the glycerol containing homogenization medium, herein it appears that the induced nanonization yield arises from change in intrinsic mechanical behavior of the material, induced by the medium. Given the specific efficiency of anhydrous ethanol, it may be assumed, that the effect of desiccation by highly hygroscopic solvent leads to elevation of T_g (glass transition temperature) leading to embrittlement of the material⁴⁵. Indeed, even trace amounts of water in pharmaceutical lyophilizates are known to undergo much more rapid deterioration due to the strongly plasticizing effect of residual water. In short, the highly efficient stabilization of generated nano-particles could be rationalized by induced “dryness” of the system. In contrast, the presence of any highly hygroscopic solvent like water reduces the kinetic barrier for structural reorganization such as those prompted by the temporary separation of inter-particle hydrogen bonds and salt bridges.

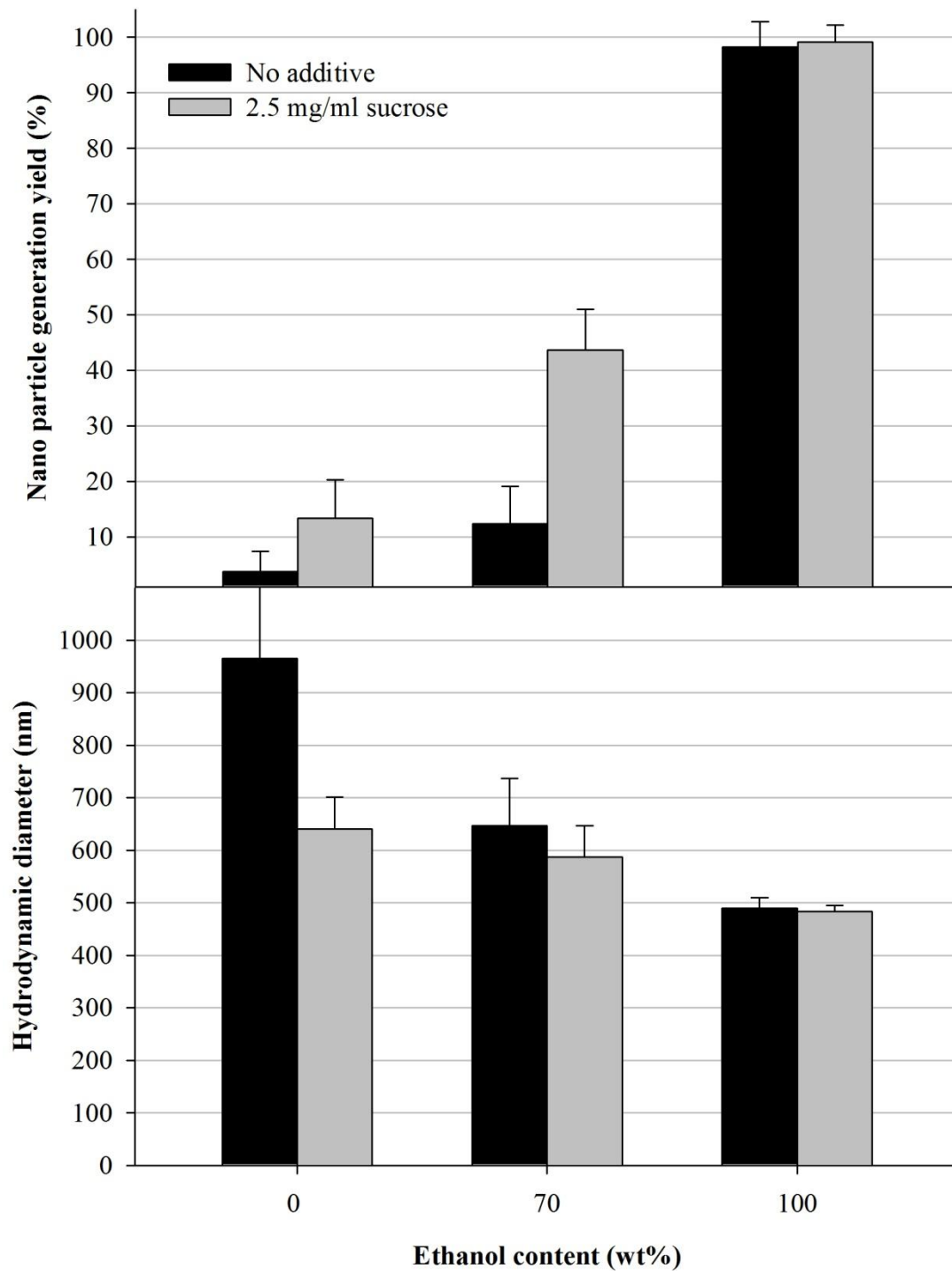


Figure 3.9: Effect of ethanol incorporation in homogenization medium on nanonization efficiency and nano-particle generation yield. (Albumin CLPA was homogenized at 20 krpm, 30 min)

Introduction of both aqueous glycerol solution and ethanol into homogenization medium has resolved the overall yield issue encountered in the preliminary work to a large extent.

The application of each method has separate advantages. While homogenization in glycerol medium possesses the benefit of further ease of finer particle size separation through centrifugation, lacking in case of ethanol medium. Therefore, glycerol incorporation might prove beneficial for applications requiring very high precision of particle size distribution. With that in mind, the crude size separation precision of ethanol as homogenization medium exceeds that of glycerol even at highest concentrations of the later.

Furthermore glycerol concentration by itself is a powerful tool in adjustment of particular size range for a given CLPA formulation and protein type, which obviously is only achieved in ethanol medium by manipulation through homogenization rate and time.

The most important advantage of ethanol appeared to be the observed preservation of less brittle formulations such as dehydrothermally crosslinked and dextran polyaldehyde crosslinked CLPL. These softer formulation, would fail under high shear rates (over 9-10 krpm) applied in aqueous and glycerol incorporated media, which could be directly observed by foaming resembling native protein solution property and smeared appearance. This effect was most likely unrelated to cavitative damage as described earlier in the text, since the behavior occurred to higher degree in glycerol rich media, but rather due to intolerable plastic deformation of the material matrix under high shear conditions. This resulted in rapid irreversible agglomeration of the large portion of nano-particle content generated and generally in significant to complete loss of catalytic activity. The tightened matrix of ethanol submerged material, leads to minimization of plastic deformation, facilitating brittle fracture therefore preserving the integrity of the material while facilitating covalent bond rupture, under greatly decreased shear conditions.

Further discussion on relationship of synthesis protocol and nanonization efficiency is included further in this chapter.

Both methods require eventual transfer of the nanosized material into an aqueous environment for most applications aimed. Complete precipitation out of the medium through centrifugation followed by re-suspension in buffers resulted in irreversible agglomeration of larger part of formed nanoparticles. Air drying of particles suspended in ethanol had the same consequence. As mentioned earlier, filtration was ruled out due to

clogging of the membrane once again leading to agglomeration. Therefore, the only feasible method appeared to be dialysis against the desired final medium, which has proved sufficiently easily applicable, and resulted in successful preservation of nano-particle content. Here once again, the use of ethanol as homogenization medium appears beneficial due to readier diffusion of ethanol as compared to glycerol, which has required longer dialysis times and at least 5 dialysis medium changes. Moreover, for attempted *in vitro* experiments (see Chapter 4.) ethanol medium has also served the sterilization purposes of the material prior to incubation with cell culture, only requiring dialysis against sterile PBS or cell culture medium.

3.4.2.2. Homogenization speed on yield and size reduction efficiency

Just as observed through preliminary screening data homogenization speed forms the main size reduction parameter, higher shear rates generating lower size particles, that is, in the range prescribed by the CLPA formulation and protein type given. Combined with the medium composition variable it was possible to fine tune the desired particle size range at high yields.

Applied in combination with varying medium compositions, lower rates could not be efficiently applied to more viscous homogenization medium formulations, due to insufficient mixing of the sample at higher viscosity values. 50 wt% and higher glycerol concentrations could only be successfully incorporated at speeds of 15 krpm and higher.

Furthermore homogenization speed of 22 krpm and higher, has been observed to result in re-agglomeration of generated nano-particles, even in case of most mechanically stable CLPA formulations.

Figures 3.10-12 represent the effect of homogenization rate on nanonization efficiency in protein type specific manner, on albumin, trypsin and Savinase® CLEA (CLEA Technologies) examples respectively.

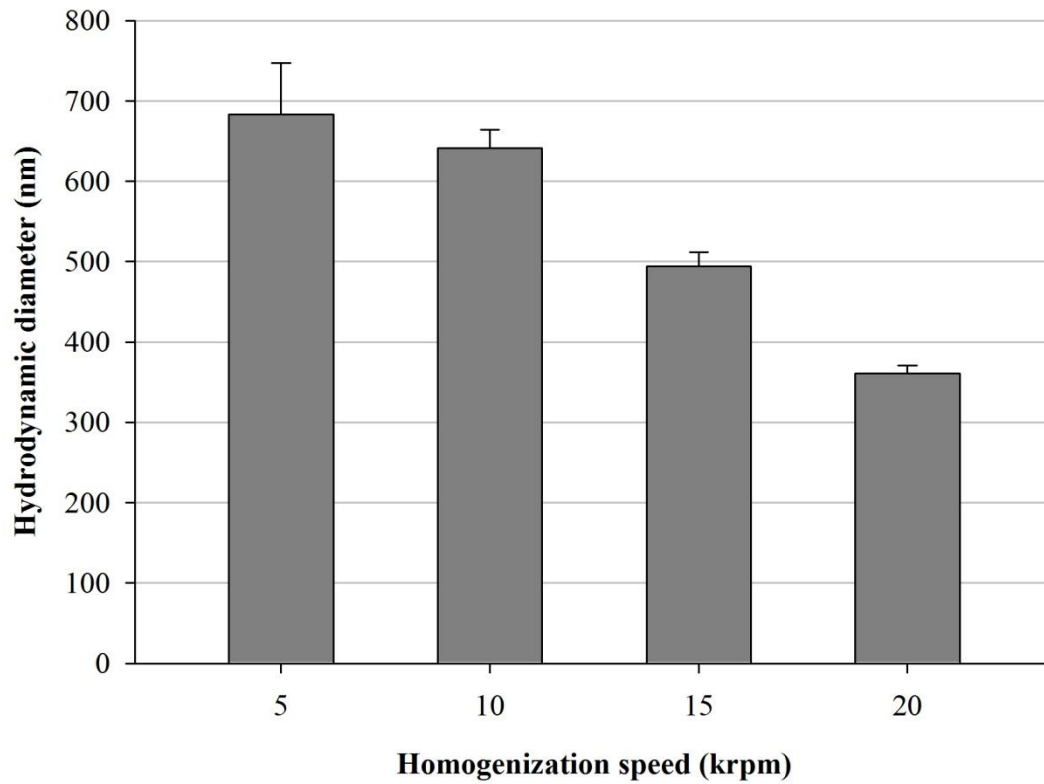


Figure 3.10: Effect of homogenization speed on nanonization efficiency of albumin CLPA. (homogenized in 30 wt% glycerol for 30 min)

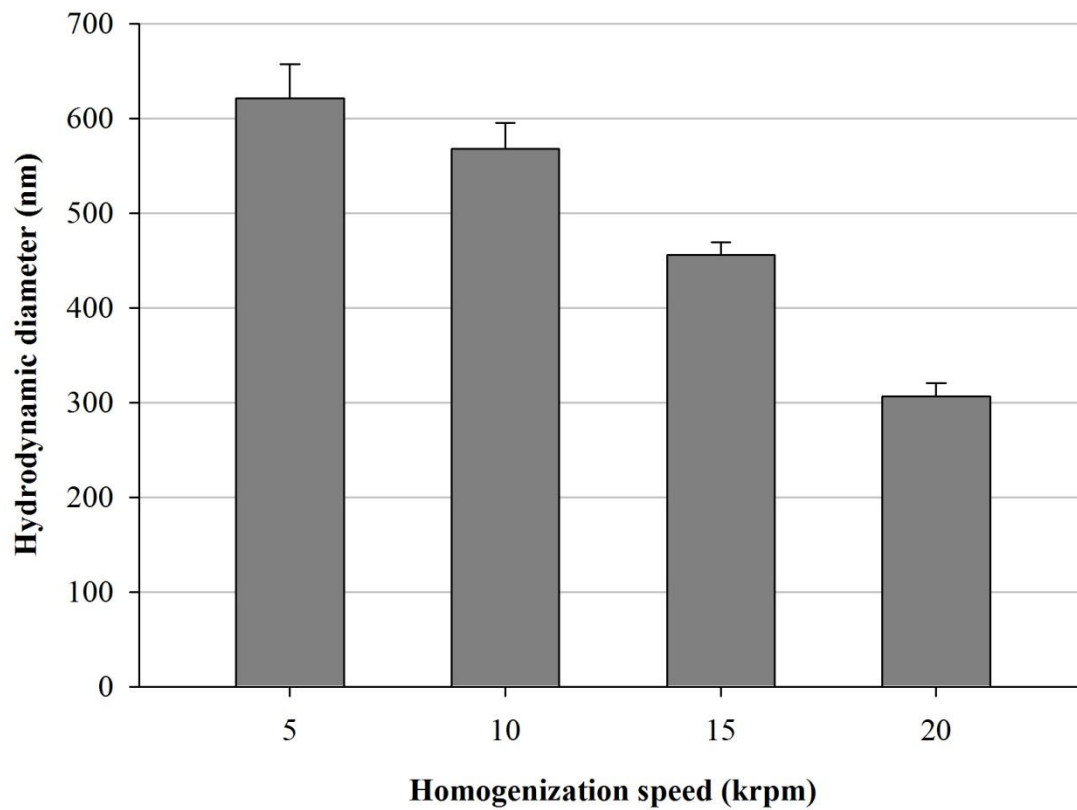


Figure 3.11: Effect of homogenization speed on nanonization efficiency of trypsin CLPA. (homogenized in 50 wt% glycerol for 30 min)

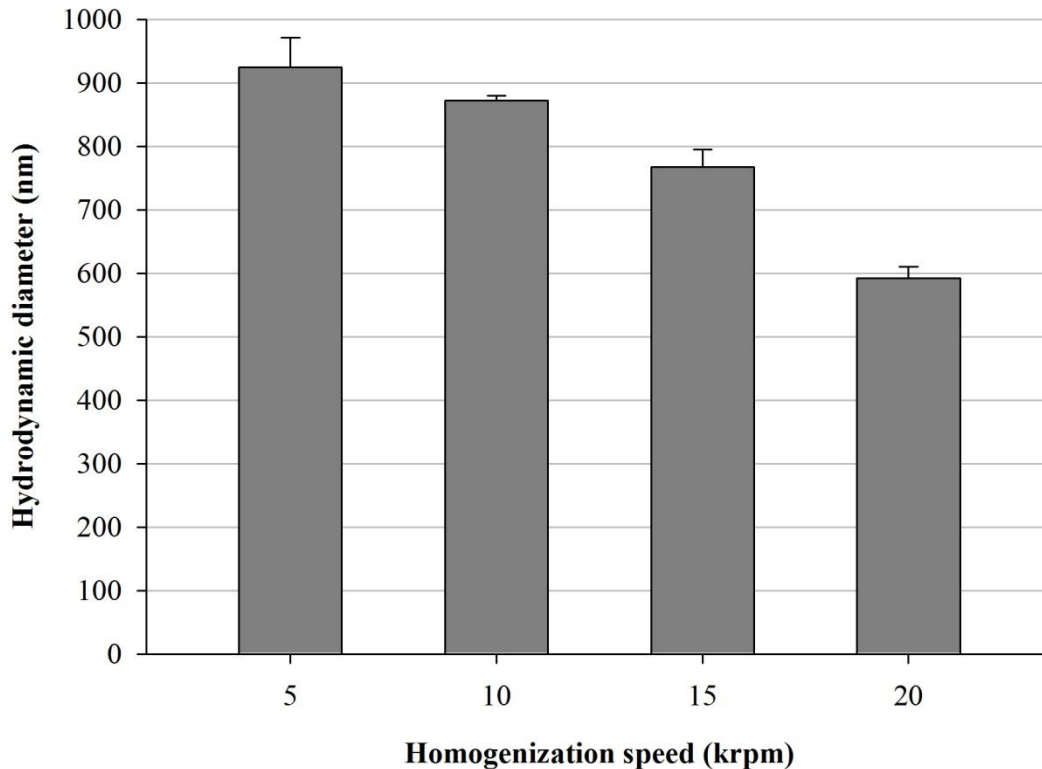


Figure 3.12: Effect of homogenization speed on nanonization efficiency of Savinase® CLEA (CLEA Technologies). (Homogenized in 50 wt% glycerol for 30 min)

3.4.2.3. Homogenization time on yield and size reduction efficiency

Nanonization could be achieved after periods as short as 5 min, but in order to achieve size distribution homogeneity longer homogenizations times were required. While some decrease in overall particle size was observed with increasing homogenization time, in glycerol medium homogenizations this parameter is best used to optimize size homogeneity quality and overall yield, rather than size fine tuning tool (Figure3.13). All nano-CLPA shown bellow were achieved as a result of at least 30 min homogenization, in order to minimize the particle distribution error.

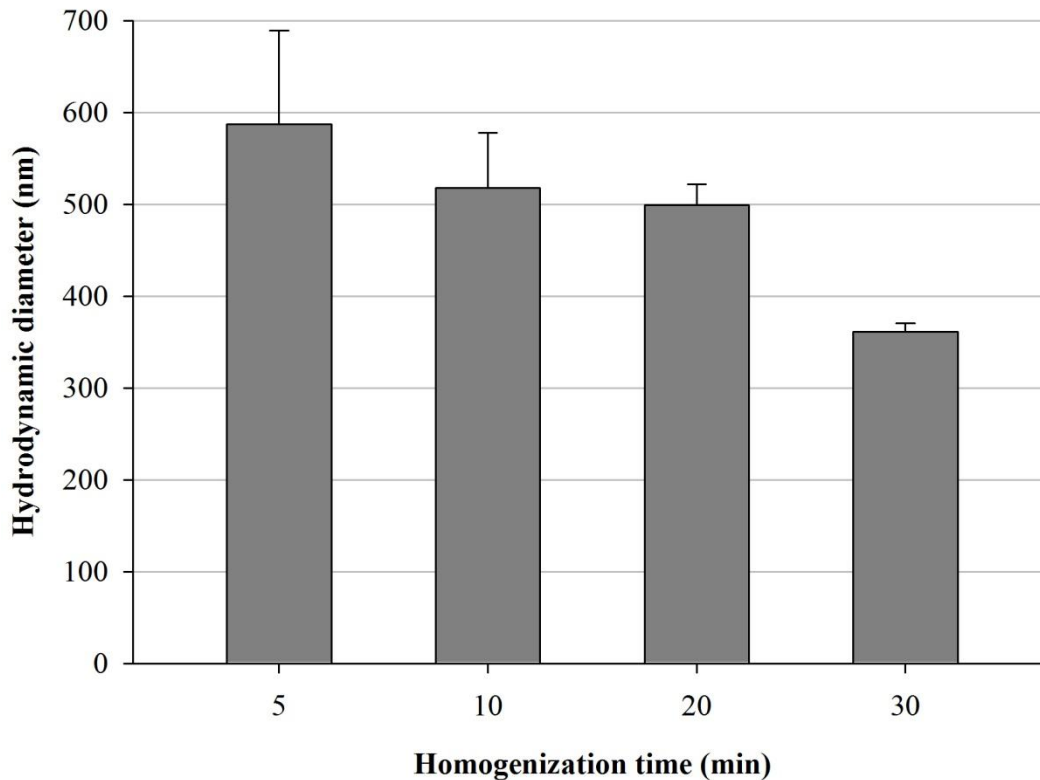


Figure 3.13: Effect of homogenization speed on nanonization efficiency of albumin CLPA. (Homogenized in 30 wt% glycerol at 20 krpm)

In case of ethanol homogenization, homogeneous particle distribution was achieved significantly more rapidly (15-20 min) and extended homogenization times were, to some extent, utilized to fine tune the desired particle size of a given CLPA formulation.

3.4.2.4. Particle size versus catalytic activity

All data demonstrated versus defined particle size was obtained as a result of repeated homogenization in sequence with DLS measurements. The data presented here is gathered from repeatable trials, as can be observed from the standard deviation data included. Unfortunately this wasn't always the case, and approach has not always been optimal, re-agglomeration would occasionally occur upon second or third homogenization, observably

related to human error. Furthermore, decrease in reproducibility of resultant catalytic activity was observed even where predicted particle size could be established.

The main factor was observed to be the immersion depth, and particularly location of the hole on the homogenization tool with respect to the medium surface (Figure 3.14), of the homogenization rode, arranged manually and affecting all formulations independent of protocol and conditions, therefore rendering the process repeatability highly dependent on gathered experience applied within the limits of human error, rather than engineering controlled. This mainly reflected on unanticipated increase in homogenization medium temperature.

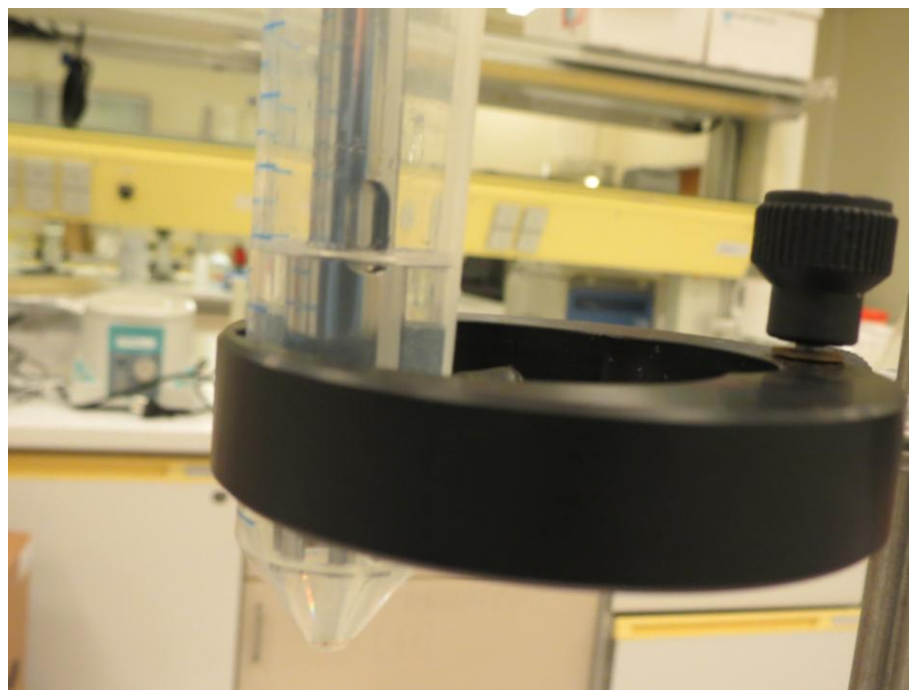


Figure 3.14: Visualization of sample placement prior to homogenization

Raise in temperature of the medium during homogenization was a factor not fully investigated. Main controllable parameters were medium composition, where most viscous mediums led to highest increase, and homogenization rate, where temperature raise would increase with increasing rate. The temperature rise fluctuations could also be observed in case of any specific CLPA formulation. The general temperature increase prescribed by

these parameters was up to 30-50 °C with the device operated at laboratory temperature conditions (20 °C).

Significant rapid increase in temperature up to 70-90 °C, was occasionally observed unrelated to the intrinsic material and homogenization medium formulations. The resultant samples of different formulations were analyzed and while the nanonization efficiency would generally correspond to the given formulation and protocol, the dramatic decrease in catalytic activity (results not shown, due to lack of systematic appearance of the issue). Obviously, on formulations described earlier as more susceptible to plastic deformations, were affected to greater extent, nevertheless unlike the described earlier effect of glycerol and ethanol media incorporation, in this case significant loss of catalytic activity was general for all formulations, independent of the protocol.

It can be assumed, that slight changes in positioning of the rotor tool components with respect to medium surface has led to alteration of flow character. The observed increase in turbidity of the sample, pointing to increased air bubble incorporation within the medium, could lead to conclude a sudden cavitation number increase, in which case further increase in hydrodynamic cavitation portion would be expected with increasing temperature.

These observations occurred under limitations of laboratory scale design, and could be overcome with development of a fully automated system, in order to eliminate the human error factor and optimize the reproducibility. A system equipped with thermostat controlled cooling jacket could prove further beneficial for both repeatability improvement and preservation of integrity in certain CLPA formulations.

Observed on Figure 3.15 is a relationship of particle size to catalytic activity of sub-optimal formulation of trypsin CLPA (excessive crosslinking degree). This example is chosen here, since the highly brittle nature of the formulation allowed easily adjustable very precise nano-particle size generation. As has been shown in the preliminary study discussion, altering of the diffusion limitation in large substrate involving catalysis significantly affects the resultant activity.

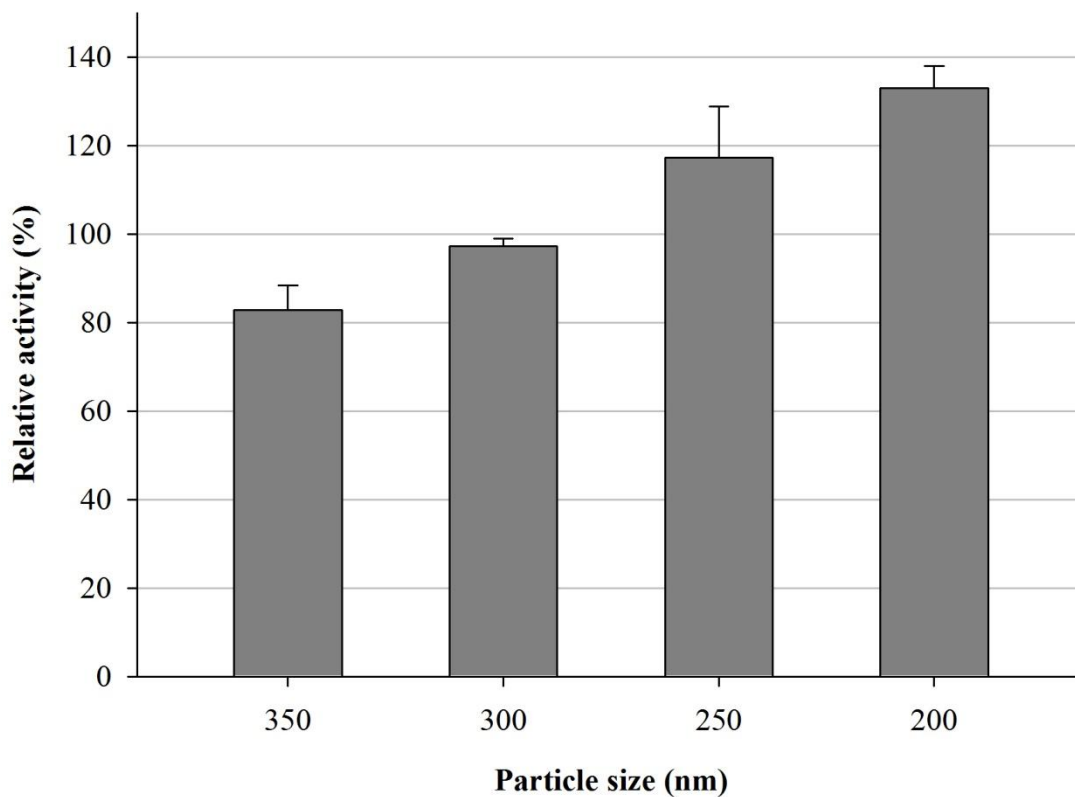


Figure 3.15: Effect of particle size on catalytic activity of trypsin CLPA. (sub-optimally formulated CLPA)

The similar pattern was observed on the example of the Savinase® CLEA (CLEA Technologies) (Figure 3.16), demonstrating generality of this approach. The significant gap between macroscopic and sub-micron size particle catalytic activity is observed, followed by further gradual change amongst different size fractions.

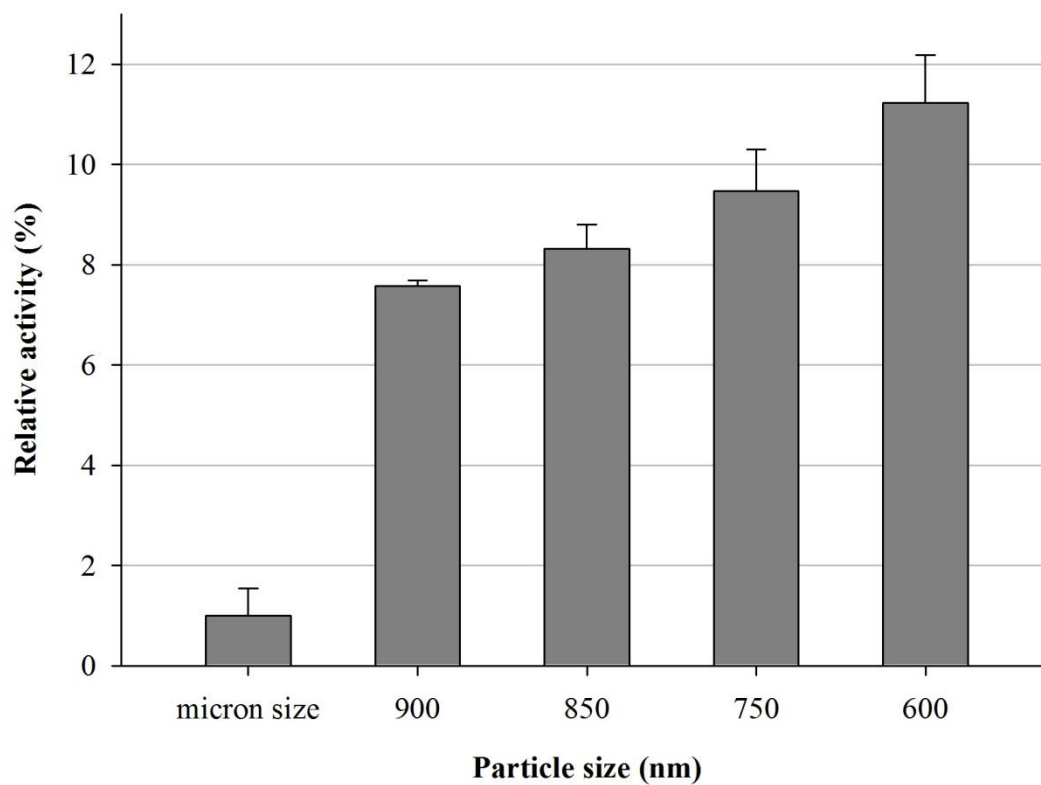


Figure 3.16: Effect of particle size on catalytic activity of Savinase® CLEA (CLEA Technologies).

3.4.3. Optimization of CLPA synthesis steps in terms of nanonization yield, size and final product catalytic activity

CLPA preparation was influential in terms of downsizing efficiency, as the particular manipulations used to enforce aggregation ultimately defined the packing and crosslinking densities of the protein aggregates. Effective packing as well as sufficient crosslinking served to “stiffen” the crosslinked precursor, enabling size-reduction at length scales where soft materials generally become self-plasticizing and increasingly difficult to downsize.

Furthermore, the catalytic activity of downsized material, while generally increased to the extent defined by the protocol and resultant particle size, clearly bared the pattern established of its corresponding macroscopic precursor.

This trend is nicely demonstrated on the model of trypsin nano-CLPA (Figure 3.17), which follows the pattern described in Chapter 2. Here despite much more efficient size reduction of glutaraldehyde crosslinked material, catalytic activity of dehydrothermally crosslinked CLPA still exceeds, although to somewhat less ratio degree than that of macroscopic precursors. This effect can be attributed both to the difference in aggregation and lyophilization techniques as well as potentially activity degrading effect of glutaraldehyde crosslinking. Furthermore, increase of catalytic activity of dehydrothermally crosslinked nano-CLPA, as compared to its macroscopic precursor, demonstrates that increase in the surface area is a separate parameter acting additionally to the improved accessibility provided by intrinsic high porosity of the material, further decreasing diffusion limitations on the nanoscale.

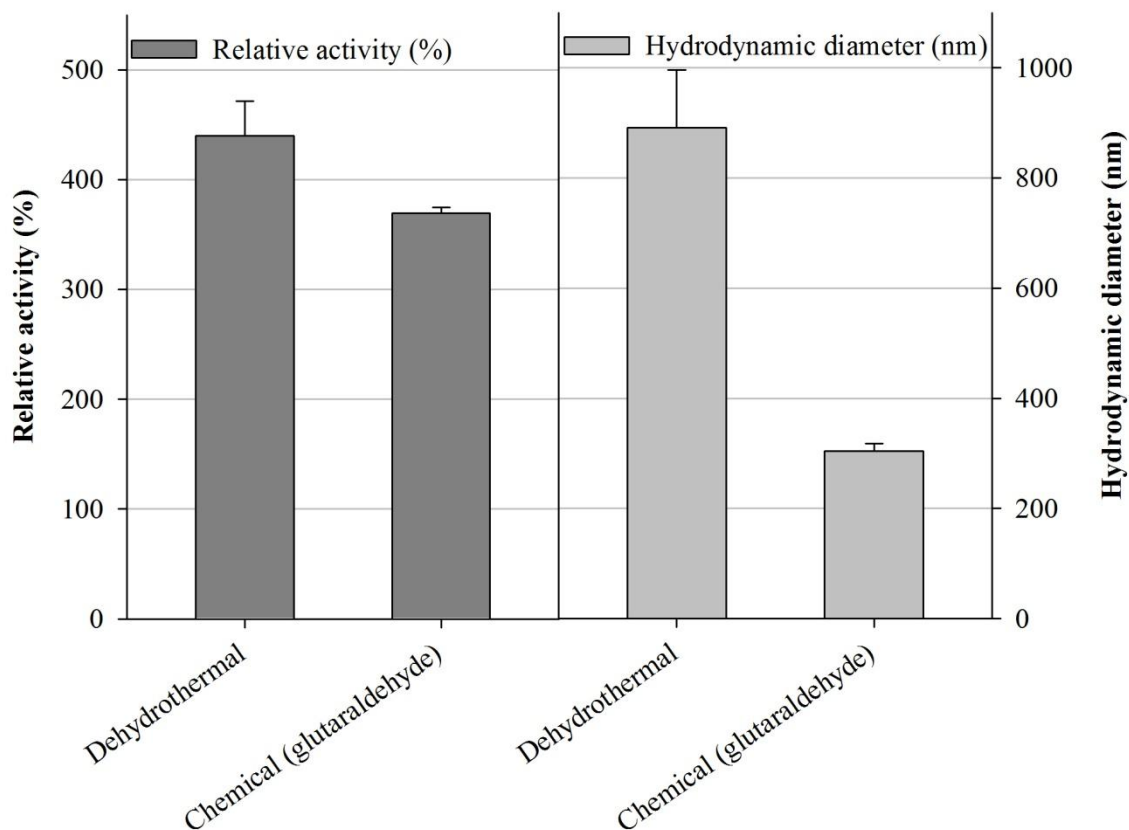


Figure 3.17: Comparison of chemically and dehydrothermally crosslinked CLPA nanonization results

This method, although highly efficient, is not exploited in the following nanonization studies, for the same reasons earlier mentioned in favor of increased catalytic activity: fewer crosslink formation and higher porosity is leading to a very soft material which is also less mechanically stable, compared to chemically crosslinked CLPA. Homogenization in absolute ethanol was employed, preventing loss of catalytic activity due to material deformation, but nano-particle size generation capacity was rather limited. Instead CLPL formulations described in Chapter 2, were preferred due to chemical crosslinking induced rigidity, while still preserving increased activity associated with high porosity prescribed by the precursor lyophilizate.

3.4.3.1. Effect of precursor solution conditions

No independent relevance could be established between nano-particle generation and precursor solution, rather it was realized through crosslinking efficiency determined by the precursor solution.

In terms of catalytic activity, the effect trend demonstrated on macroscopic precursor can be obviously observed herein with 3-4 fold increase implemented by size reduction.

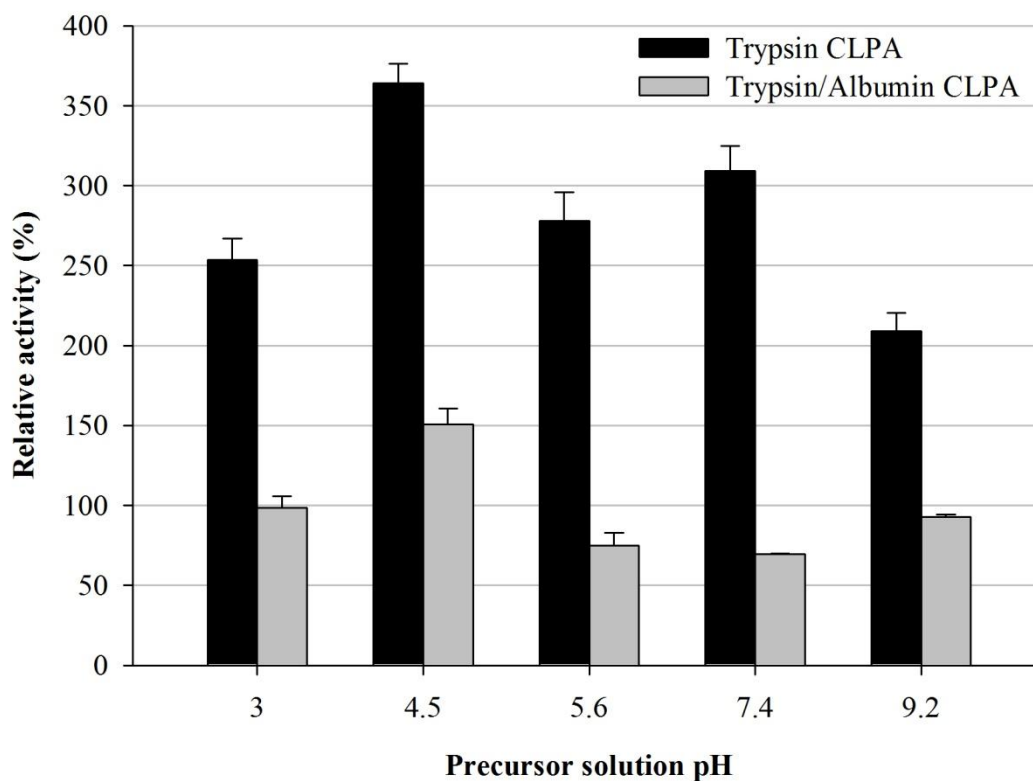


Figure 3.18: Precursor solution effect on 300 nm nano-CLPA catalytic activity. Trypsin CLPA (aggregated in acetone, glutaraldehyde crosslinked)

3.4.3.2. Effect of aggregation method

While not confirmed directly, it could be supposed that among the available protein aggregation methods, those leading to greater inter-protein packing or ordering would better facilitate nanonization, much like crystalline material is more easily ground compared to amorphous forms. For example, trypsin CLPA of otherwise same protocol

obtained from aggregation with saturated ammonium sulfate and 2-propanol, have led to readier downsizing of the later

That being said, as discussed in Chapter 2., aggregation method has incremental effect on final product catalytic activity. This and facilitation of efficient crosslinking were predominant parameters of choice in optimizing nano-CLPA formulation protocol, rather than as the particle size distribution fine tuning tool. The results of nano-CLPA analysis were found to parallel to those of CLPA with respect to aggregation method versus relative activity.

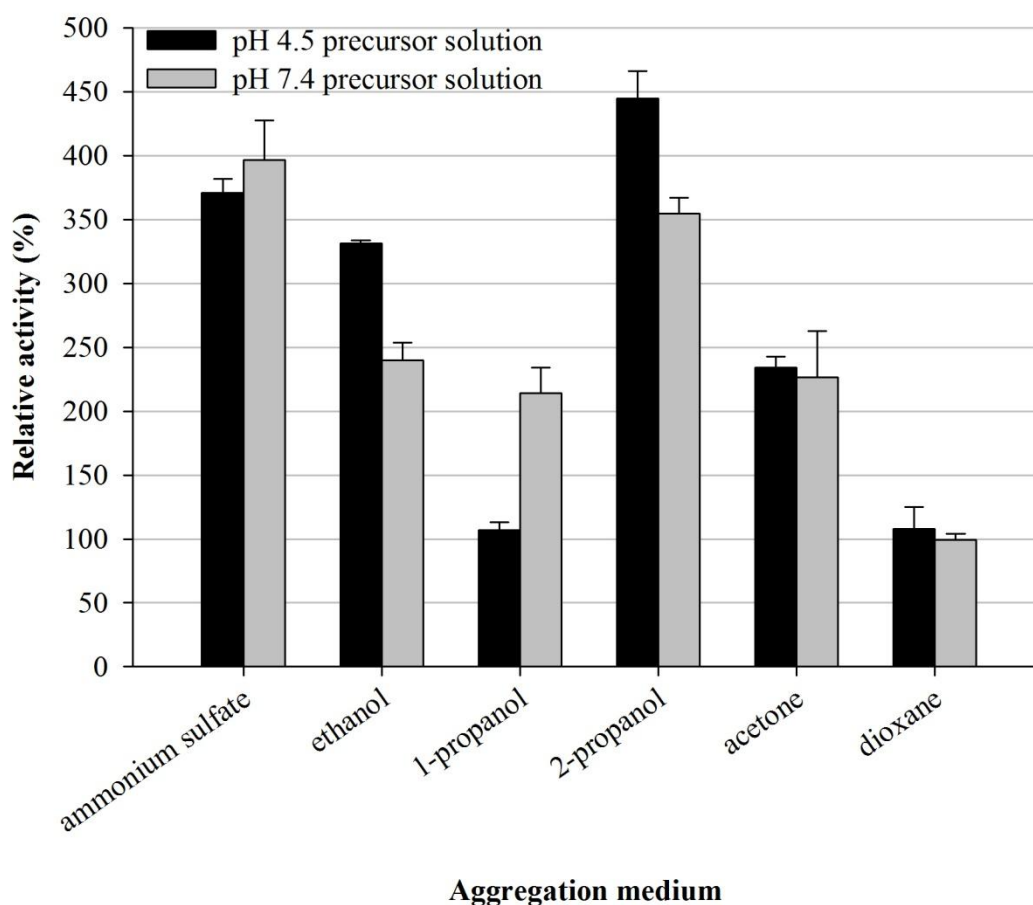


Figure 3.19: Aggregation medium effect on 300 nm nano-CLPA catalytic activity. Trypsin CLPA (glutaraldehyde crosslinked)

As mentioned earlier, chemically crosslinked CLPL provided much improved nanonization capacity, as compared to dehydrothermally crosslinked lyophilizates. Nano-CLPL as observed from its dextran polyaldehyde crosslinked precursor earlier resulted in plausible activity yields, when combined with optimum starting solution conditions (example in the next section). The method was further supported by 100% synthesis yield.

3.4.3.3. Effect of crosslinking method

Examples of most chemically crosslinked CLPA, assuming formulations providing sufficient covalent crosslinking, which blocks any possibility of inter-protein reorganization of shear-stressed material, enforcing bouts of catastrophic mechanical failure as opposed to gradual stress-to-strain changes. Macroscopically speaking, the covalent crosslinking of densely-packed aggregates paralleled the effects of metal embrittlement, as evidenced by lack of malleable deformation, namely, CLPA smearing, in favor of brittle-fracture-like fragmentation.

The fact that catalytic activity of nano-CLPA compared to corresponding precursor CLPA, while numerically increased in statistically significant fashion, poses almost identical trends, further supports the above claiming, showing that the only effect implemented by downsizing treatment is the reduction of diffusion limitation catalytic activity. This trend is demonstrated on the same CLPA formulations provided in Chapter 2. In comparison of crosslinking reagent pH effect (Figures 3.20 and 3.21)

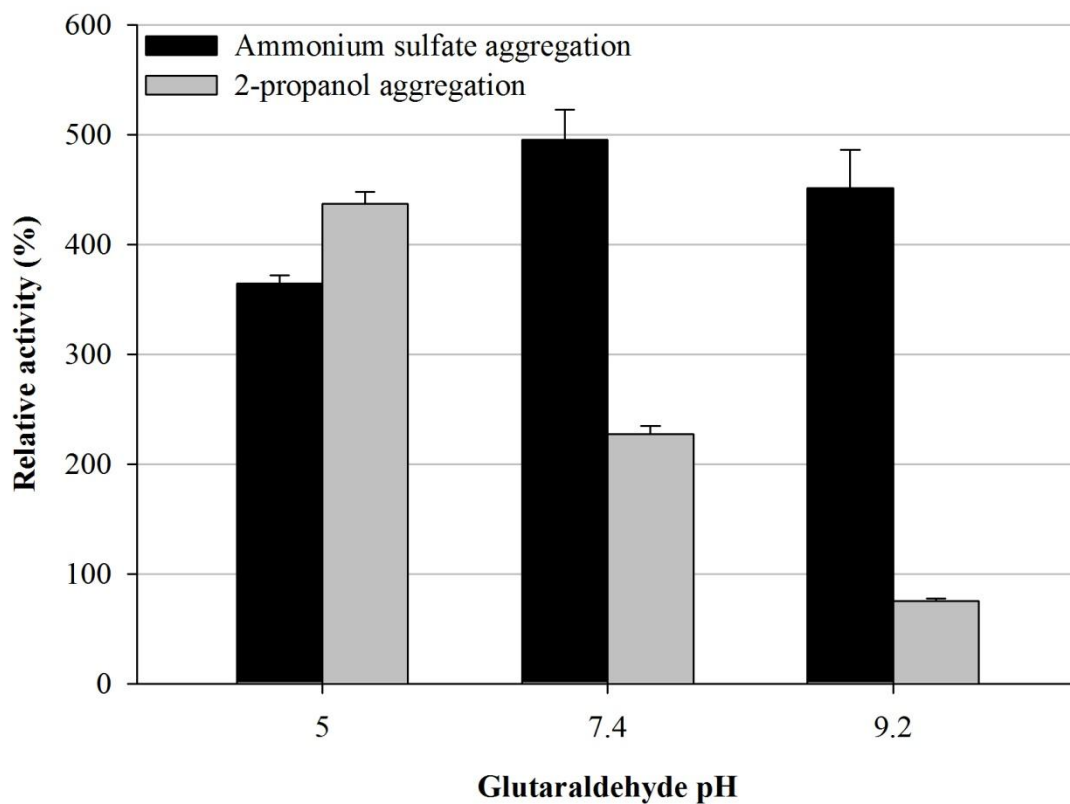


Figure 3.20: Crosslinking reagent (glutaraldehyde) pH effect on 300 nm nano-CLPA catalytic activity. Trypsin CLPA (pH 4.5 precursor solution, aggregated in 2-propanol)

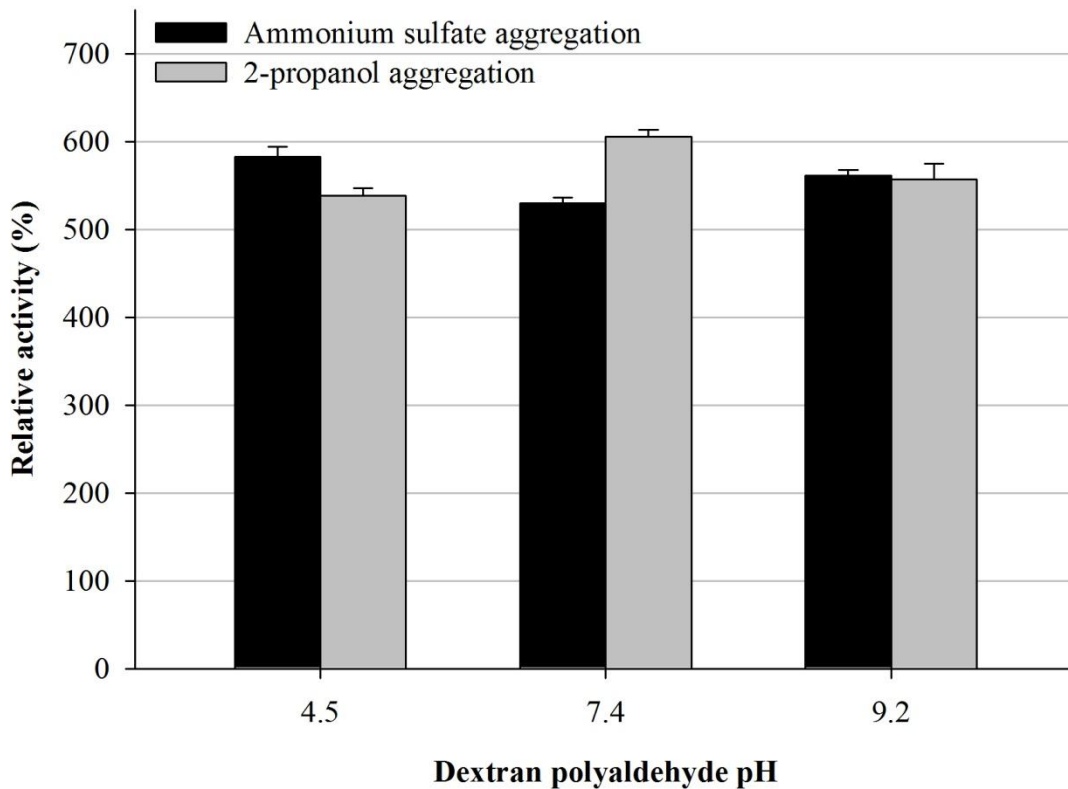


Figure 3.21: Crosslinking reagent (dextran polyaldehyde) pH effect on 300 nm nano-CLPA catalytic activity. Trypsin CLPA (pH 4.5 precursor solution, aggregated in 2-propanol)

As it has been demonstrated earlier, during homogenization medium discussion, particular formulations do not withstand high shear rates in high viscosity medium, namely aqueous glycerol solutions. These include much softer formulations: dehydrothermally crosslinked and dextran polyaldehyde crosslinked lyophilizates. This does not apply to glutaraldehyde crosslinked CLPL, which appears to perform as a robust material closely resembling CLPA formulations, but the results for these formulations are not presented herein, due to unsuitability of this formulation in case of protease examples demonstrated here. Efficient downsizing procedure was achieved through absolute ethanol homogenization medium employment for dextran polyaldehyde CLPL, as described earlier, yet while readily nanosized, no particles under 200 nm could be generated in these formulations. As can be observed from Figure 3.22, this did not cause a serious concern, since the catalytic activity fluctuation appears to be greatly reduced between 300 and 200 nm particles.

This trend could be explained by two scenarios, the plausible case being that at around 300 nm catalyst approaches, reaction limited rates rather than diffusion limited. Unfortunately, this could not be verified, since kinetic studies, initially being within ambition of this work, could not be conducted due to technical difficulties. And will present the main subject of further research on the topic.

Less desirable scenario involves incremental deformation under highest shear rates leading to some degradation of activity expected from a smaller size particle.

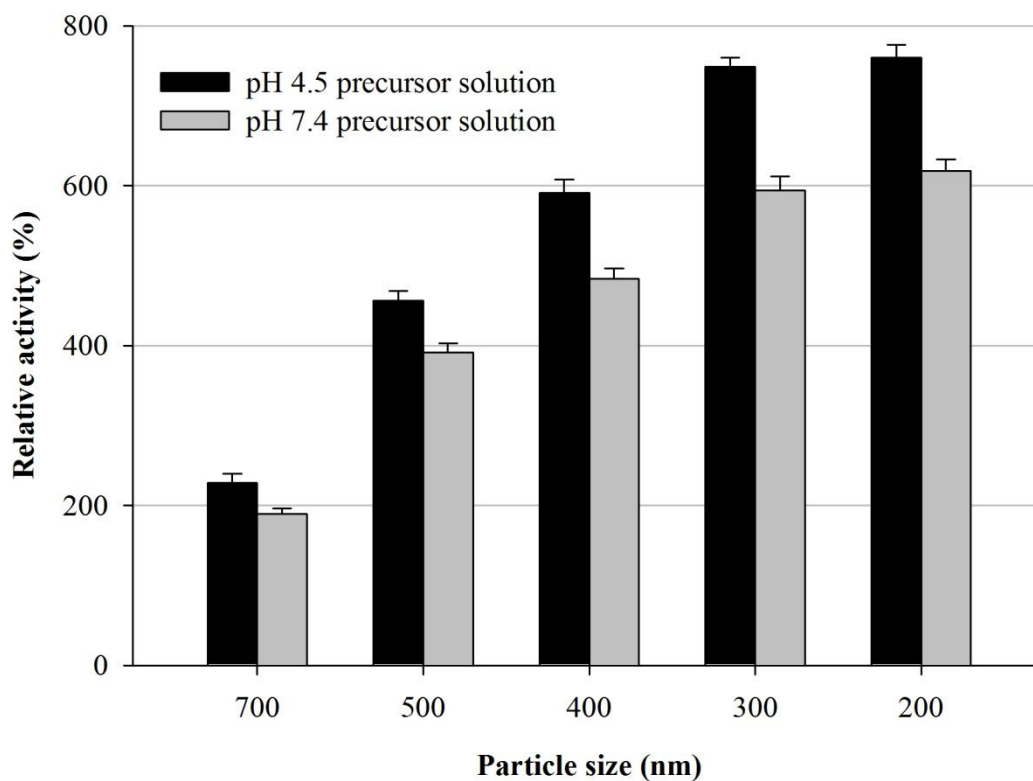


Figure 3.22: Effect of particle size on catalytic activity of trypsin CLPL

3.4.3.4. Effect of crosslinking degree

Given the main rationale, that increased robustness implemented by covalent crosslinking facilitates brittle fracture of CLPA in homogenization medium, it is not surprising to observe that higher crosslinking degree would provide lower nano-particle size under same

downsizing conditions (Figure 3.23). Nevertheless, as described in Chapter 2., excessive crosslinking dramatically affects the CLPA activity, which is directly reflected on corresponding nano-CLPA formulations and must be optimized with caution (Figure 2.24). Data for 1. and 2. crosslinking formulations could not be obtained, due to inability to downsize these softer materials to the common scale with the rest of the formulations.

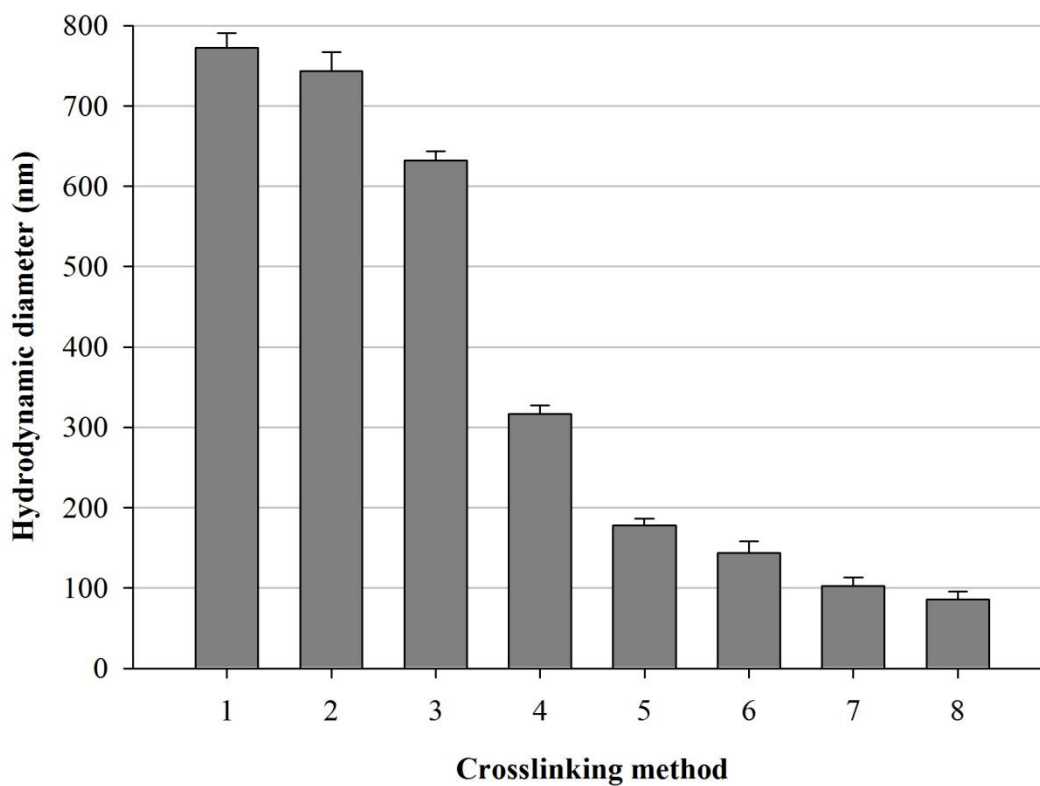


Figure 3.23: Effect of precursor CLPA crosslinking degree on nanonization efficiency. (Albumin CLPA homogenized in 50 wt% glycerol at 20 krpm)

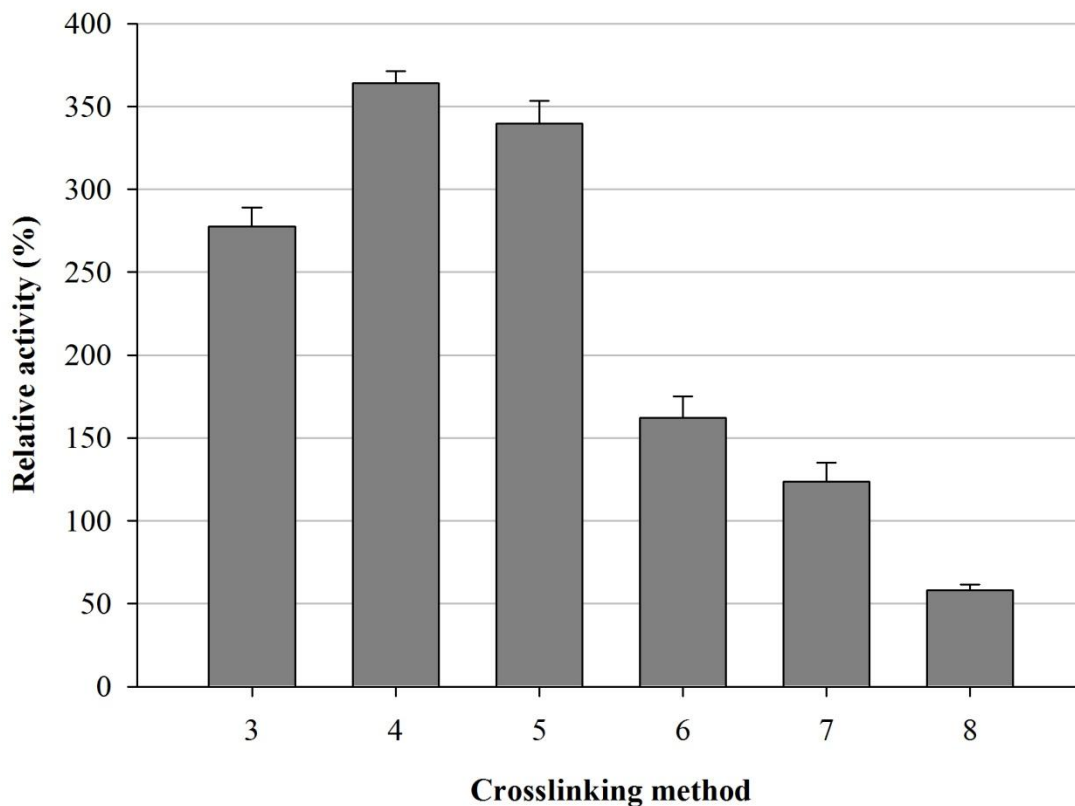


Figure 3.24: Effect of precursor CLPA crosslinking degree on catalytic activity of 300nm trypsin nano-CLPA.

3.4.4. Stability of nano-CLPA

3.4.4.1. Comparison of operational and hydrolytic stability of CLPA and nano-CLPA

CLPA/CLPL synthesized in house and generated nano formulations have been tested for operational stability in a manner that would facilitate comparison to CLEA data provided by Sheldon *et al*⁴⁶. The results for both macroscopic and nano materials have been shown comparable. These experiments were performed on macroscopic and 300 nm trypsin

formulations generally described as optimized in this Chapter, namely optimal formulations of glutaraldehyde, dextran polyaldehyde crosslinked CLPA and dextran polyaldehyde crosslinked CLPL.

It was observed that nano-CLPA bared the continued activity of the precursor CLPA, and is suitable for continuous processes. CLPA and nano-CLPA incubated in PBS under mild agitation at 50 °C for 1-14 days resulted in identical residual catalytic activity (results not shown).

Furthermore, recyclability of nano-CLPA was realized by repeatedly dialyzing of the particles out of previous reaction medium. 10 consequent trials have led to statistically insignificant alterations in catalytic activity results. This result was not surprising based on the established reusability of CLPA precursors mentioned in the literature⁴⁶. Successful repeated dialysis, on the other hand, has provided evidence of suspension stability.

3.4.4.2. Storage stability

Storage stability of CLPA formulations is conventionally accepted, stability of nano-CLPA suspensions overtime, in different 2.5 mg/ml potassium chloride containing aqueous glycerol concentrations, absolute ethanol and PBS buffer was established here. Suspensions left to sit at room temperature and 4 °C for as long as 4 month were all readily re-suspended upon agitation. DLS measurements have shown increase hydrodynamic diameter in 0-30 wt% glycerol solution with lowest concentrations approaching 1 micron, after periods as short as a week. 40-70 wt% glycerol solutions, absolute ethanol and PBS buffer suspensions have retained the initial particle size upon the whole incubation period.

Stabilization of nano-particles in high glycerol concentrations and absolute ethanol have been discussed earlier. So was the effect of salts in arresting re-agglomeration of nano-particles in homogenization medium, apparently this effect upon prolonged periods of incubation required higher ionic strength, such as provided by the isotonic PBS solution, in order to establish sufficient zeta potential of suspended particles.

No evidence was obtained on storage stability exceeding 4 month period, but eventual irreversible agglomeration at some point is suspected for all above medium compositions.

Surprisingly enough, given the complexity and unpredictability of freezing process conditions, nano-CLPA lyophilized in PBS buffer, upon re-suspension formed the same nano-particle distribution suspension achieved in a matter of seconds, as verified by DLS measurement (results not shown). This discovery provides a much more convenient storage alternative to suspension. Furthermore, for potential synthesis applications in various organic media, this could serve as an alternative to dialysis, particularly with less water miscible solvents.

3.4.5. Applicability of the scale up process

The applicability of scale up process was assessed using industrial grade protease mixture Palkofeed (Mapa Enzymes) in a pilot scale trial. Aggregation and crosslinking steps were performed in the same reactor started by gradually pouring Palkofeed solution into 35L volume aggregation medium. The obtained CLPA was subsequently dried and ground using Gelimat compounder with addition of potassium chloride, as performed in the initial trials. The same synthesis formulation applied Palkofeed CLPA synthesis was performed on laboratory scale, and homogenized under same shear rates as Gelimat compounder provided, in order to compare the efficiencies of different scales. As can be observed from Figure 3.25 the results appeared closely comparable.

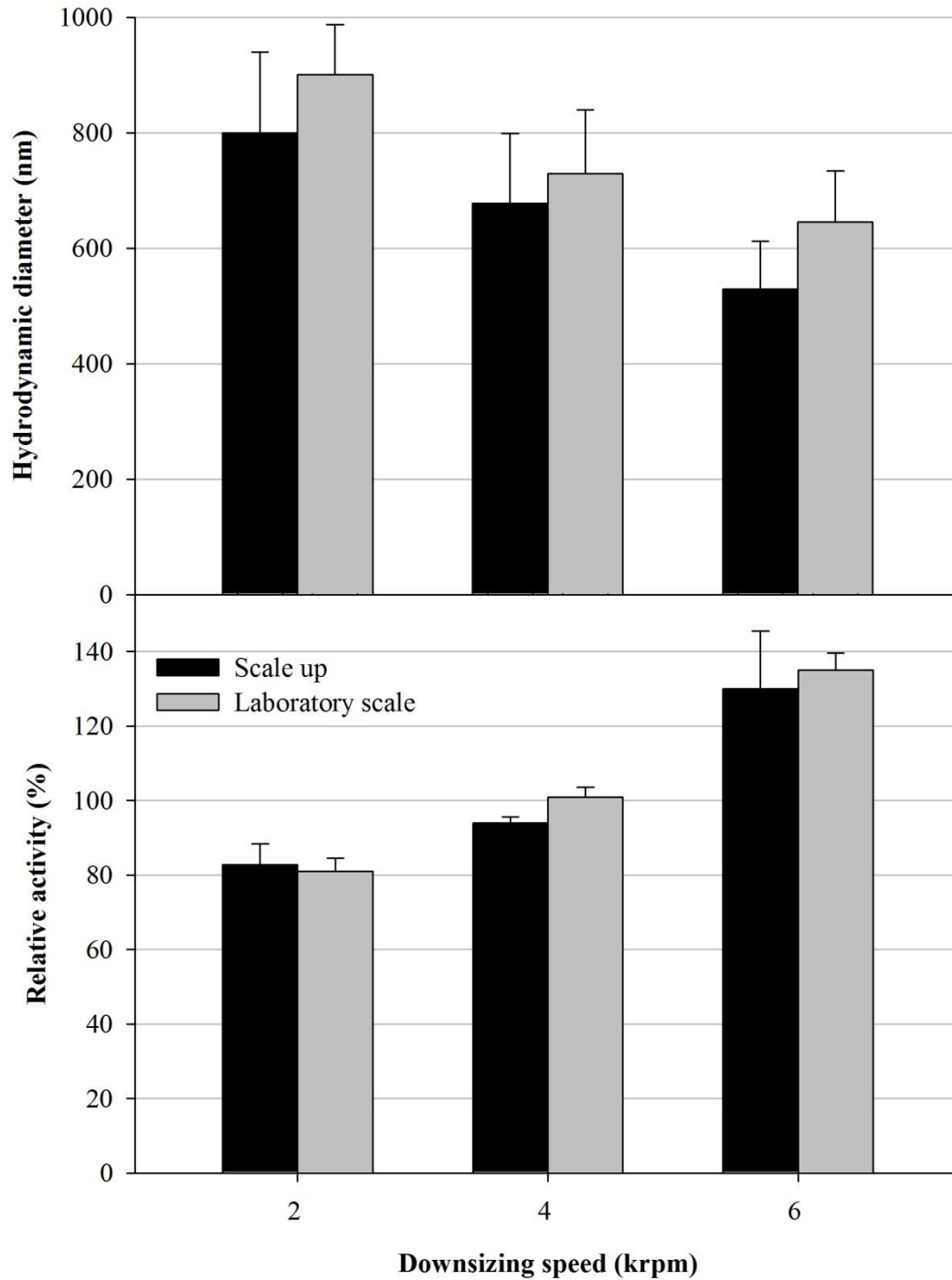


Figure 3.25: Comparison of scale up and laboratory scale nano-CLPA synthesis efficiency

4. Nano/Micro-CLEA Formulations for Potential Biomedical Applications

4.1. Introduction and Rationale

The aim of this chapter is to introduce of nano-CLPA as potential alternatives to commercially available conventional formulations.

Examples of generally used products include antimicrobial powders, wound healing aids and digestive aids^{31,47}. Plausible alternative to these products could be formed by lysozyme CLPA, lysozyme/hemoglobin nano-CLPA and a complex of hydrolytic enzyme CLPA respectively.

Hemoglobin based oxygen carriers (HBOC) provide a more specific example. Many formulations have been attempted in the field but none are applicable yet. Along with optimization of oxygen affinity and release, renal filtration in case of particles under 100nm, and hepatic/spleen clearance for larger particles is one of the main concerns. This leads to short half life of the particles, and toxicity^{48,49}. This problem could potentially be addressed by hemoglobin nano-CLPA, by maintained particles around 150nm.

Another example is an alternative formulation for enzyme replacement therapy approach to lysosomal storage disorders⁵⁰, in form of long-term therapy, stable enzyme powders with rapid mass transfer traits.

Herein, feasibility of co-aggregate complex formulations is represented on the example of hemoglobin/lysozyme nano-CLPA. Furthermore, internalization studies are performed on generated albumin and alpha-galactosidase nano-CLPA, later as a representative of lysosomal deficient enzymes. This preliminary work merely induces a discussion of potential utilization of nano-CLPA as a systemic therapeutic.

4.2. Materials

Alpha galactosidase was obtained from Sigma Aldrich. α -Galactosidase from green coffee beans, ammonium sulfate suspension, ≥ 9 units/mg protein

Other proteins were obtained as described in Chapter 2.

Trypsin solution (Trypsin-EDTA (0.05%), phenol red), Dulbecco's modified Eagle medium (DMEM) (+4.5g/L D-Glucose, + L-Glutamine, - Pyruvate, phenol red), heat inactivated Fetal Bovine Serum (FBS), antibiotic solution (Penicillin-Streptomycin; 10,000 U/mL) were obtained from Gibco®.

Dulbecco's modified Eagle medium (DMEM) (+4.5g/L D-Glucose, + L-Glutamine, - Pyruvate, - phenol red) was obtained from Pan Biotech GmbH.

Human Epithelial Cervix Adenocarcinoma (HeLa; ATCC® Number: CCL-2™), Human Epithelial Colorectal Carcinoma (HCT 116; ATCC® Number: CCL-247™), Human Embryonic Kidney (HEK-293; ATCC® Number: CRL-1573™) and Mouse Embryonic Fibroblast (NIH/3T3; ATCC® Number: CRL-1658™) cell lines were kindly donated by Dr Batu Erman of Sabanci University, Biological Sciences and Bioengineering Program.

All other reagents were obtained from commercial suppliers as analytical grade and were used without further purification.

4.3. Methods

4.3.1. Synthesis of albumin, lysozyme, hemoglobin, lysozyme/hemoglobin co-aggregate and alpha-galactosidase CLPA

4.3.1.1. Precursor protein solutions

Protein solutions described in this chapter were generally of the following composition:

Protein(s)	Concentration (mg/ml)	Solution composition	pH
Hemoglobin	50	100mM potassium chloride in 10mM sodium acetate buffer	5,6
Lysozyme	100	100mM potassium chloride in 10mM sodium acetate buffer	5,6
Hemoglobin/ Lysozyme	50/50	100mM potassium chloride in 10mM sodium acetate buffer	5,6
Albumin	100-200	100mM sodium phosphate buffer	7,4

4.3.1.2. CLPA synthesis and nano-particle generation

Precursor CLPA formulations were synthesized as described in Chapter 2.

Alpha-galactosidase, obtained in the form of suspension in ammonium sulfate solution, was an exception. Precursor solution and further aggregation procedures have not been performed and dialysis was not attempted; crosslinking was performed directly in the commercially obtained suspension medium.

Size reduction was performed via homogenization as described in Chapter 3, the corresponding procedures are specified in the text.

Modification of CLPA with PEG was realized through addition of 1:1 and 1:10 (protein: PEG) molar ratio of monofunctional PEG amine (600 MW) or aqueous solution of bifunctional PEG amine (1900 MW) into unreduced crosslinking medium. Reaction was conducted on the resultant mixture for 30 min under homogenization conditions at 10 krpm. The suspension was thereafter reduced by incubation with 0.1 % sodium borohydride solution for 30 min at mild agitation. Suspension was diluted with glycerol solution, to

obtain the desired glycerol wt% of the medium and further size optimization was performed where needed, through additional homogenization.

4.3.2. *In Vitro* Cell Culture Study

4.3.2.1. Preparation of nano-CLPA for cell culture incubation

Nano-CLPA suspension of optimized size has been modified with dansyl chloride, for visualization purposes in florescent microscopy experiments, through the following procedure:

0.6 ml of 2.5mg/ml nano-CLPA suspension obtained after homogenization was diluted with 0.8 ml pH 9.2 0.1M carbonate buffer and incubated for 1 hour at room temperature with agitation (550 rpm) upon addition of freshly prepared 0.1ml 3mg/ml dansyl chloride/dimethyl formamide solution.

Upon dansylation the labeled nano-CLPA samples were transferred into 1.5 ml eppendorf tubes with the dialysis membrane replacing the top of the tube cap, tubes were further secured with parafilm tape to avoid any leakage. All samples prepared as described were dialyzed against pH 7.4 PBS buffer, with constant agitation, for the period of 6 hours, repeated 4 times.

Material disinfection has been performed by dialysis against 70 wt% ethanol solution containing 5 wt% sucrose and subsequently dialyzed against sterile PBS, for the period of 6 hours, repeated 3 times. Buffer exchanges were performed in the laminar flow hood. All subsequent dilutions were performed with sterile PBS.

4.3.2.2. Cell culture preparation

HeLa, HCT116, HEK-293, NIH/3T3 cell lines were maintained in complete DMEM - supplemented with 10% heat inactivated fetal bovine serum, 100 unit/ml penicillin and 100 unit/ml streptomycin. For cell viability assays phenol red free DMEM was used.

4.3.2.3. Internalization/localization study

HeLa and NIH3T3 cells were cultured on 6-well plates at a density of 4×10^4 cells per well with unmodified cover slips placed on the bottom of each well in complete DMEM and incubated at 37 °C in a tissue culture incubator under a 5% CO₂ atmosphere. Internalization trials were performed upon 24 hour incubation.

Lysosome staining

Where applicable, lysosome staining was performed using Cell Navigator™ Lysosome Staining Kit (Red Fluorescence), reagent was prepared as prescribed in the manufacturer protocol (AAT Bioquest®, Inc). Medium was removed and replaced with 1ml medium supplemented with 10 v% of the fluorescent reagent and incubated for 30min in tissue culture incubator. Upon incubation, medium was removed and wells were washed thrice with warm PBS buffer, 2 ml of complete DMEM was replaced.

Nano-CLPA internalization

20 µl 1mg/ml Nano-CLPA suspension were directly introduced into 2ml cell culture medium and incubated for 3 h, if not stated differently in the text. Upon incubation, medium was removed and wells were washed thrice with warm PBS buffer. After the last wash, cells were fixed using 3% paraformaldehyde solution, washed thrice with PBS and placed on the slide.

Subsequent analysis was conducted using Zeiss confocal microscope. Visualization of dansylated nano-particles was conducted by excitation with 405nm laser and lysosomal staining dye by excitation with 561 nm laser. All images compared were obtained under

same conditions and images processed identically. Image processing was performed using Zeiss software.

4.3.2.4. Viability upon internalization

HeLa, HCT116, HEK-293, NIH/3T3 cells were cultured on 96 well plates at a density of 4×10^3 cells per well in complete DMEM. Nano-particle incubation was performed upon 24 hour incubation for HeLa and HCT116 cell cultures and upon 36 hour incubation for HEK-293 and NIH/3T3.

Nano-CLPA suspensions were directly delivered into the cell culture medium at corresponding dilution in 20 μ l aliquots per 180 μ l medium and incubated for 3 hours. Upon incubation, medium was removed and wells were carefully washed thrice with warm PBS buffer. After washing, 100 μ l of phenol red complete DMEM medium is replaced.

Control wells were supplemented with 20 μ l aliquots of PBS.

MTT test was performed at 0, 24 and 48 hour time points upon nano-particle incubation.

10 μ l of MTT labeling reagent was added and incubated for 4 hours in tissue culture incubator. Upon incubation 100 μ l MTT solubilizing solution was added and incubated overnight at 37 °C. Absorption values were measured at 570 nm using a reference wavelength of 665nm in accordance with the Roche Applied Science Cell Proliferation Kit I (MTT) protocol (Roche Applied Science; apoptosis, cell death and cell proliferation 3d edition, 85-86).

4.3.3. Characterization

4.3.3.1. Relative bioactivity assays

Lysozyme

Assay method 1. The assay is based on lysozyme catalyzed hydrolysis of synthetic substrate, 4-Methylumbelliferyl β -D-N,N',N''-triacetylchitotrioside ((GlcNAc)₄-MeU). Hydrolytically liberated MeU amount is detected fluorimetrically upon 360nm excitation at 455 nm emission.

The reaction was conducted as follow: 10 μ l 5×10^{-4} M reagent solution was added into 190 μ l 1 mg/ml lysozyme solution or nano-CLPA suspension in 100mM potassium chloride in 10mM acetate buffer solution. Reaction was conducted for 30 min at 37 °C under 450 rpm agitation. Reaction was terminated with pH 11 buffer and fluorimetrically measured at λ_{ex} = 360 nm, λ_{em} = 455 nm. The established pH was established to favor fluorescent anionic form of MeU.

Native protein solution measurements were assigned a value of 100% and CLPA measurements were calculated relative to this value.

Assay Method 2. *Micrococcus luteus* cell wall digestion assay was performed as described in Chapter 2.

Bovine Serum Hemoglobin assay was performed as described in Chapter 2.

Alpha-galactosidase

The assay is based on alpha-galactosidase catalyzed hydrolysis of synthetic substrate, p-Nitrophenyl α -D-Galactopyranoside Solution (PNP-Gal). Hydrolytically liberated p-nitrophenol amount is detected spectrophotometrically at A_{405nm} . The reaction was conducted as follow: 200 μ l 10 mM reagent solution and 100 μ l 1 mg/ml alpha-galactosidase solution or nano-CLPA suspension was added to 700 μ l reaction buffer in 80mM potassium phosphate pH 6.5 buffer. Reaction was conducted for 30 min at 25 °C under 450 rpm agitation. Reaction was terminated by addition of 9.8 pH buffer. Amount of

liberated p-nitrophenol was assessed spectrophotometrically at $A_{405\text{nm}}$. Native protein solution measurements were assigned a value of 100% and CLPA measurements were calculated relative to this value.

4.4. Results and Discussion

4.4.1. Lysozyme, hemoglobin and lysozyme/hemoglobin co-aggregate nano-CLPA

4.4.1.1. Nano-CLPA optimization

Hemoglobin solutions were readily aggregated in all attempted media, generally described in Chapter 2. That being said significant loss of catalytic activity appeared in most of the formulations, with an exception of ammonium sulfate aggregation provided CLPA. Crosslinking was readily achieved through all conventionally described techniques; Figure 4.1 represents crosslinking method effect on catalytic activity of hemoglobin. Herein, hemoglobin is assessed in terms of its oxidase catalytic activity.

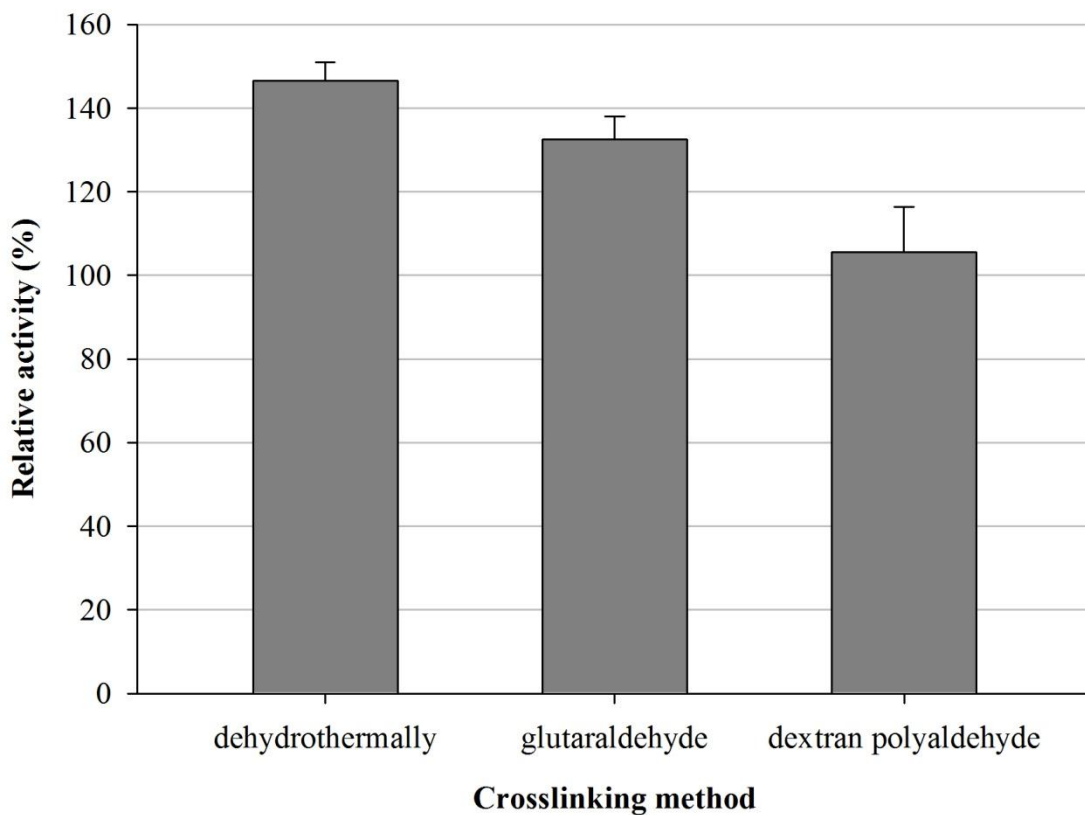


Figure 4.1: Crosslinking method effect on 200 nm hemoglobin nano-CLPA catalytic activity.

Downsizing procedures were conducted without apparent structural damage, as would be expected from brittle appearance of obtained CLPA. That being said, gradual particle size adjustment has posed a challenge, since CLPA homogenized even in low concentrations aided rapid decrease in size. The issue was not successfully addressed herein.

Given the particularly small molecular weight of substrates in the applied activity assay, the small fluctuations between different size catalyst is not surprising (Figure 4.2)

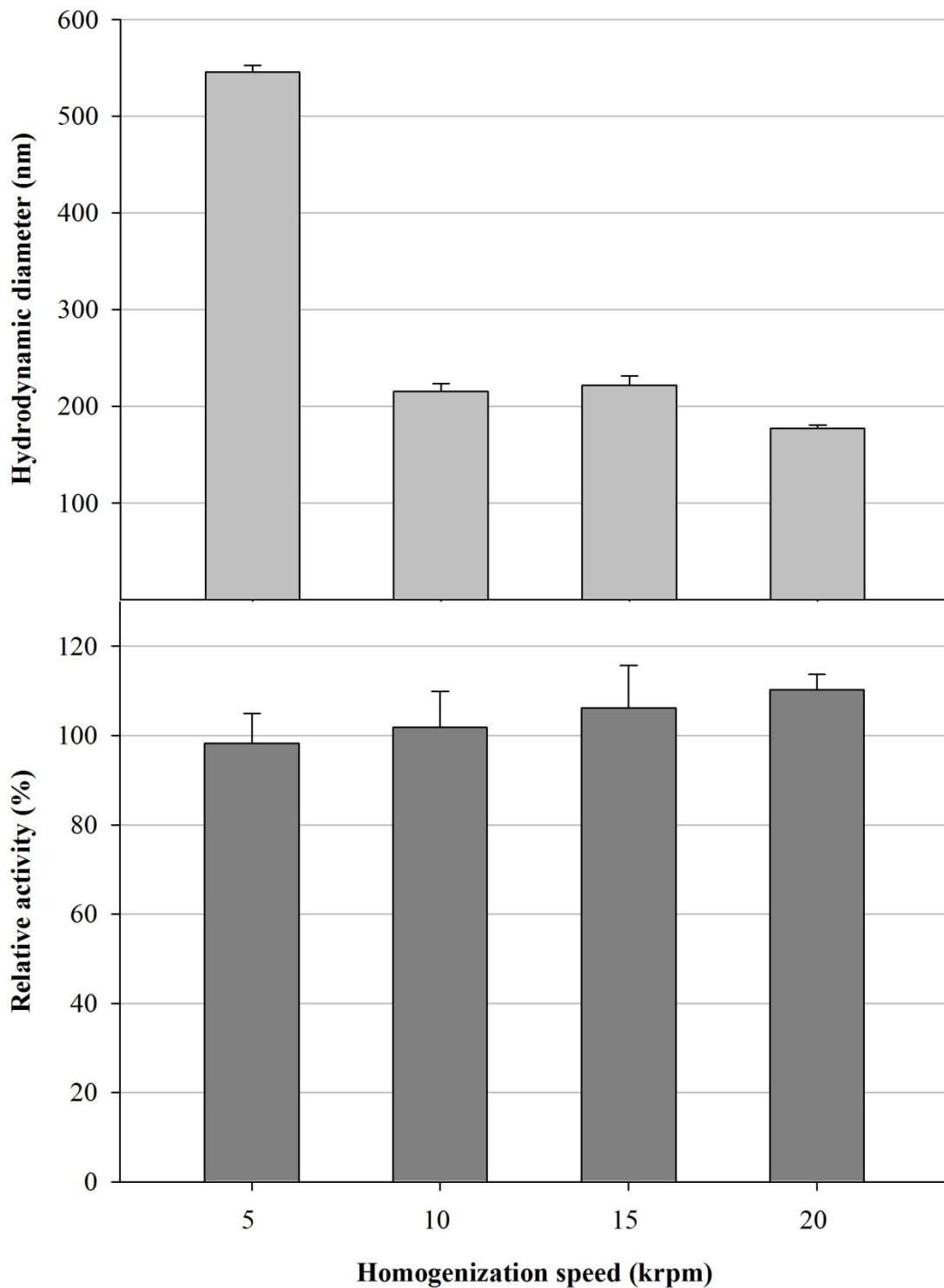


Figure 4.2: Effect of homogenization speed on size reduction and resultant catalytic activity of dextran polyaldehyde crosslinked hemoglobin CLPA. (CLPA was homogenized in 30 wt% glycerol for 30 min)

Ethanol, acetone and ammonium sulfate has appeared highly efficient for lysozyme precipitations, but some degradation of catalytic activity has been observed in ethanol and acetone aggregated formulation. Ammonium sulfate aggregation has been established optimum and was utilized thereof.

Figure 4.3 presents crosslinking method effect on lysozyme nano-CLPA catalytic activity. Remarkably, as has also been noted in the initial studies, generally highly efficient dehydrothermal crosslinking method has yielded the lowest activity in case of lysozyme CLPA. Apparent much lower crosslinking degree of CLPA formulation was noted, both from much softer appearance of lysozyme CLPA, and from qualitatively observed milder fluctuations in amideI/amideII bands upon FTIR analysis (data not shown) for all obtained crosslinking formulations, as compared to other attempted proteins. Given the generally lower crosslinking capacity of the material, it could be rationalized that very few crosslinks were formed upon dehydrothermal crosslinking, therefore avoiding the earlier discussed thermodynamic constraint, theorized to have caused increase in catalytic activity, with respect to the native enzyme.

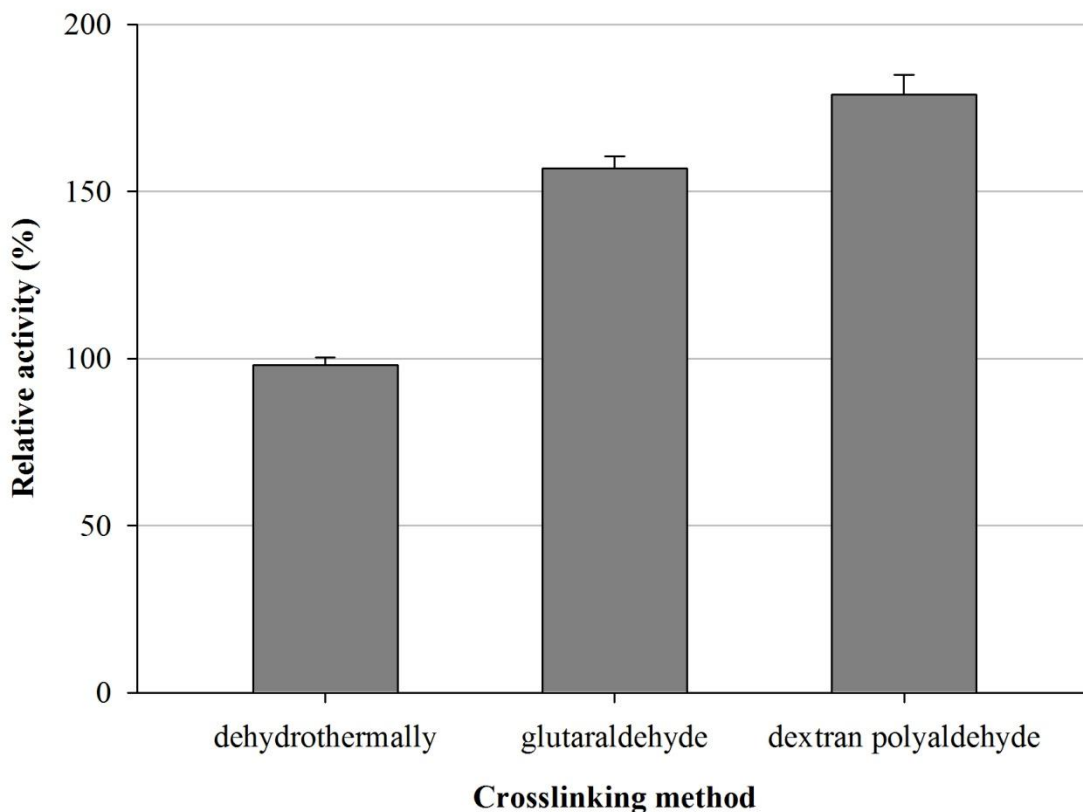


Figure 4.3: Crosslinking method effect on 150 nm lysozyme nano-CLPA catalytic activity

All formulations of lysozyme CLPA appeared particularly challenging in terms of stability during homogenization in high concentrations of glycerol, leading to obvious extensive structural damage. This could be attributed to presumably lower crosslinking degree achieved through conventional crosslinking methods, as could be visualized by the relatively soft appearance. Material had to be mechanically ground with 1:1 weight of potassium chloride prior to transfer into glycerol containing medium, in order to avoid clogging of homogenizer tool. Nevertheless, successful size reduction yield could be achieved at 30 wt% glycerol medium (Figure 4.4), with plausible catalytic activity yields. Since, this study has been conducted way before discovery of absolute ethanol alternative as a homogenization medium, the corresponding efficiency is not provided herein. It can be rationalized that given its performance on softer materials, discussed in Chapter 3., this alternative would be successfully applied here, with potential further increase in catalytic activity of the formed nano-particles.

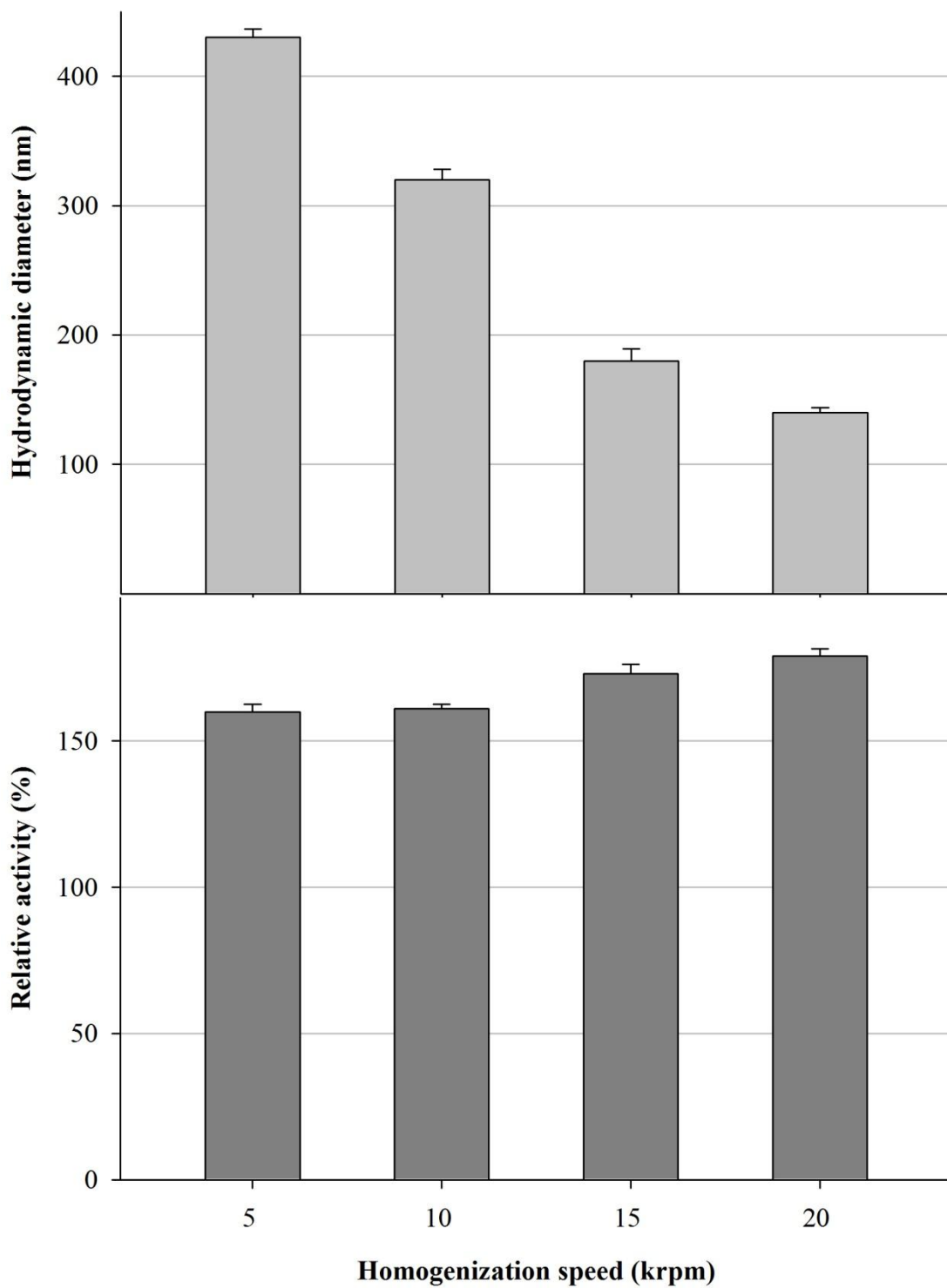


Figure 4.4: Effect of homogenization speed on size reduction and resultant catalytic activity of dextran polyaldehyde crosslinked lysozyme CLPA. (CLPA was homogenized in 30 wt% glycerol for 30 min)

Lysozyme nano-CLPA has provided a nice model for demonstration of substrate size and catalyst size relationship. The two substrates chosen herein, are posing two extremes in size, first: low molecular weight, synthetic substrate and the micron scale natural substrate. The predicted slight fluctuations in low molecular weight substrate and gradual increase in size dependant manner in case of large substrate can be observed on Figure 4.5. Much higher affinity of lysozyme nano-CLPA to its natural substrate could also be noted from the provided results.

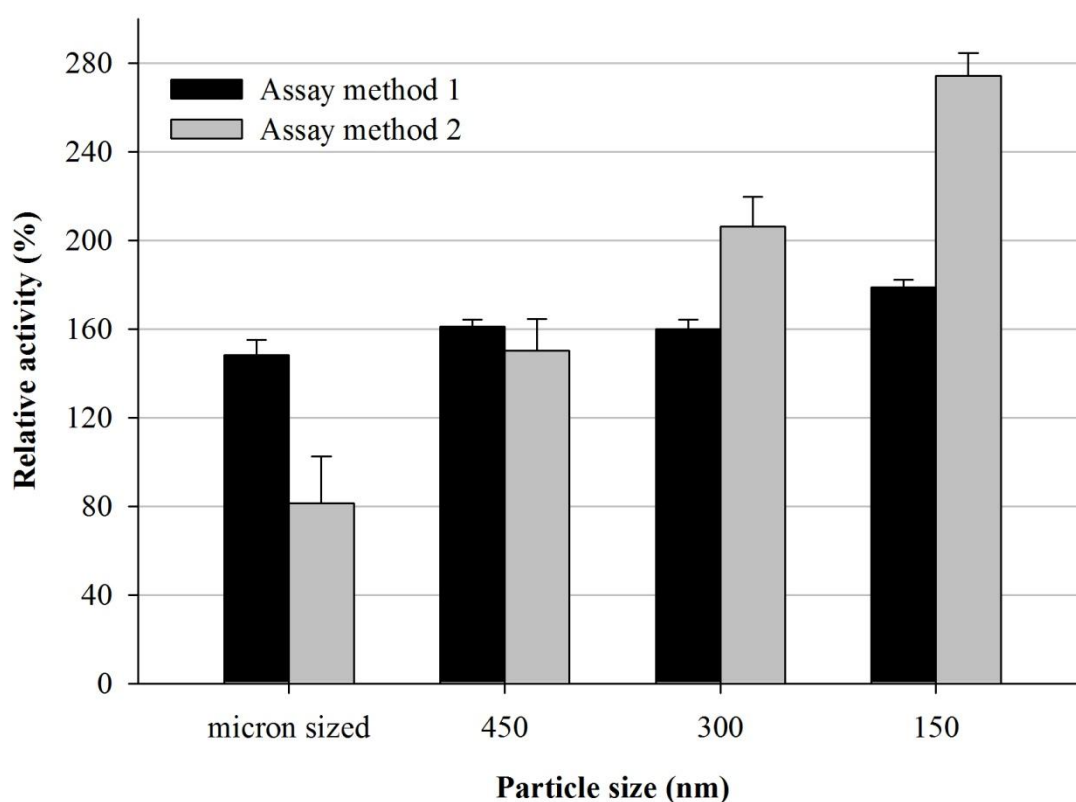


Figure 4.5: Assessment of substrate size versus catalyst particle size relationship on model of dextran polyaldehyde crosslinked lysozyme CLPA. Method 1.: Fluorimetric analysis of small substrate degradation; Method 2.: Optical density detection of bacterial wall degradation. (please see Methods section for detail)

4.4.1.2. Co-aggregate nano-CLPA

Given the general compatibility of precursor CLPA techniques developed separately for both proteins, co-aggregates and subsequent crosslinking procedure were easily achieved. Dextran polyaldehyde was chosen as crosslinking reagent for these formulations, as to benefit lysozyme catalytic activity. As observed from Figure 4.6, the given downsizing protocol yielded an average comparable particle size in hemoglobin, lysozyme and hemoglobin/lysozyme co-aggregate formulations. The retention of CLPA formulation dictated catalytic activity is also observed. The slight increase in lysozyme catalytic activity of hemoglobin/lysozyme co-aggregate nano-CLPA could be noted, and might be explained by more efficient preservation of lysozyme CLPA fraction during homogenization procedure in this case. Potentially higher crosslinking degree provided by supplementation of juxtaposed functional groups due to hemoglobin incorporation can be considered the first plausible factor. Furthermore, stabilization of proteins in solution by addition of another globular protein is a well established technique.

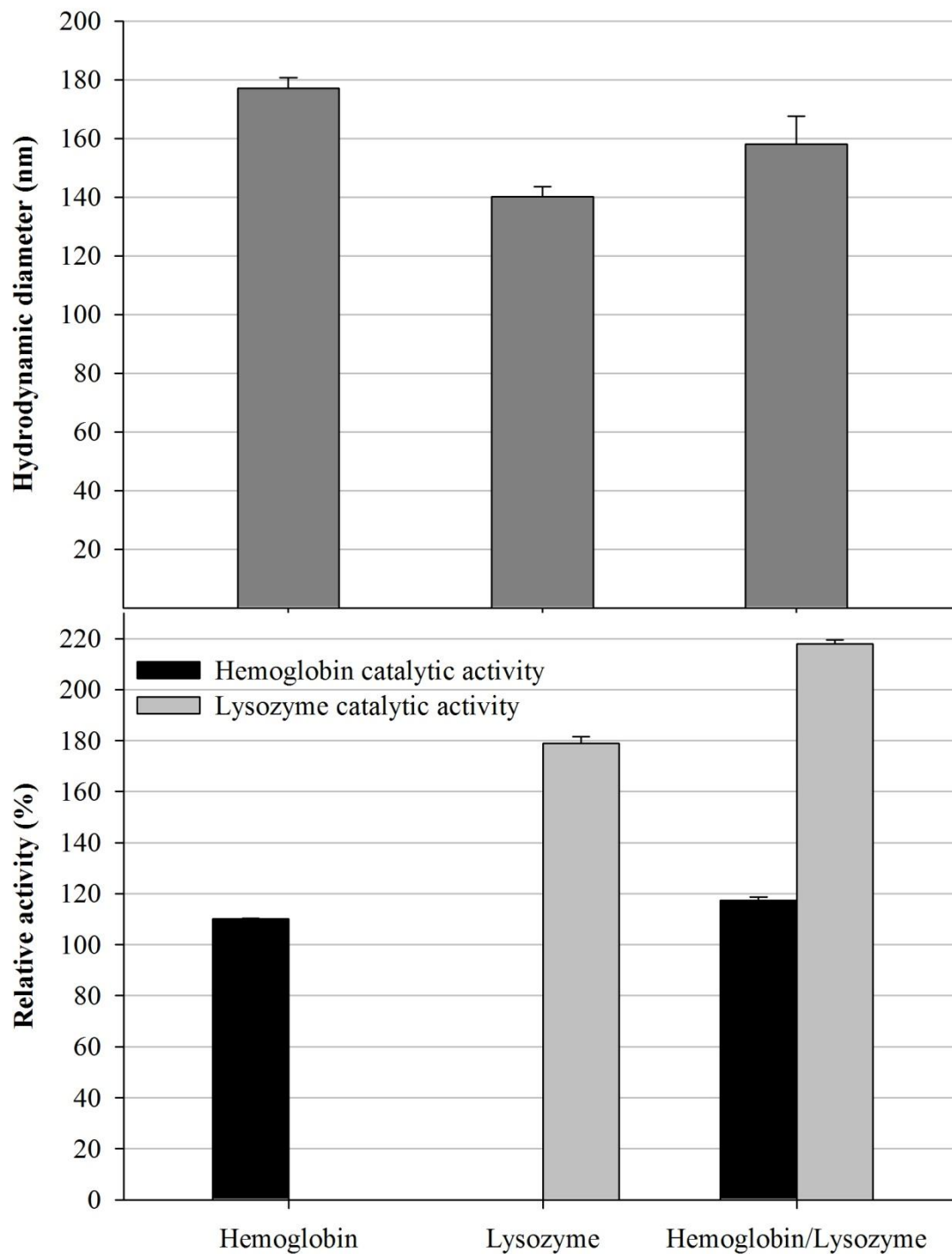


Figure 4.6: Comparison of hemoglobin, lysozyme and hemoglobin/lysozyme CLPA size reduction and resultant activity trends

4.4.2. *in vitro* internalization study on the model of albumin and alpha-galactosidase nano-CLPA

Due to rather limited amounts of available alpha-galactosidase stock most of the parameters, namely, CLPA protocol, surface modification and particle size, in this study had to be assessed through albumin nano-CLPA internalization. Only one formulation of alpha-galactosidase could be assessed which was utilized through the effect of particle size concentration – cell viability relationship.

4.4.2.1. Nano-CLPA optimization

Albumin nano-CLPA particle size optimization was performed via general techniques described in Chapter 3. Higher glycerol concentrations (50-70%) were employed in order to ensure maximum size distribution homogeneity. Samples were homogenized at approximate conditions prescribed to achieve a given particle size, analyzed with DLS and further homogenized at modified speed/time in order to obtain the desired nano-CLPA size with minimum particle size distribution error. The error up to 40 nm has been tolerated.

Two alpha-galactosidase nano-CLPA formulations were generated and assessed using the same CLPA formulation: both brought to 400 nm particle size through 50 wt% glycerol and absolute ethanol medium homogenization. Homogenization modes employed here proved readily applicable on alpha-galactosidase CLPA formulation.

50 wt% glycerol and absolute ethanol homogenized alpha-galactosidase nano-CLPA catalytic activity was assessed, relative to native enzyme solution, yielding 173% (± 8) and 198% (± 7) relative activity, respectively.

All nano-CLPA samples have been modified with dansyl chloride for further visualization purposes. It has been observed that both modification of precursor CLEA material and final size nano-CLEA material results in efficient and equivalent modification extent (results not shown). All data shown herein is acquired from samples modified post-homogenization procedure.

Since nano-CLPA formulations have been prepared in either glycerol or ethanol medium, particles purposed for internalization experiments had to be re-suspended in PBS. Dialysis has proved a viable technique, with the nano-particle content completely preserved. DLS and SEM analysis has been performed on each sample to verify the retained nano-particle composition prior to internalization experiments.

Material disinfection, after homogenization in aqueous glycerol medium, has been performed by dialysis against 70 wt% ethanol solution containing 5 wt% sucrose. Sucrose was incorporated in order to prevent potential agglomeration of nano-particles. After ethanol treatment samples were dialyzed against sterile PBS buffer, buffer exchange was performed inside the laminar flow hood, and further introduced into cell culture upon protocol prescribed dilution with the same buffer. Samples homogenized in absolute ethanol medium were directly dialyzed against sterile PBS buffer, not requiring disinfection step.

Although further disinfection using UV radiation has been avoided in order to preserve the fluorophore degradation, ethanol disinfection has been found to be sufficient. Even throughout prolonged trials (up to 4 days) in antibiotic free medium, no contamination has been observed upon particle incubation (results not shown).

The overall preparation procedures proved reliable for all nano-CLPA formulations and appeared rather user friendly.

4.4.2.2. Cell internalization pattern as a function of CLPA synthesis method and nano-CLPA generation protocol

General cell internalization trends of nano-particles have been assessed on HeLa cell line. Results did not provide sufficient resolution to conclude effect of variable parameters quantitatively, but appear sufficient to raise a preliminary discussion.

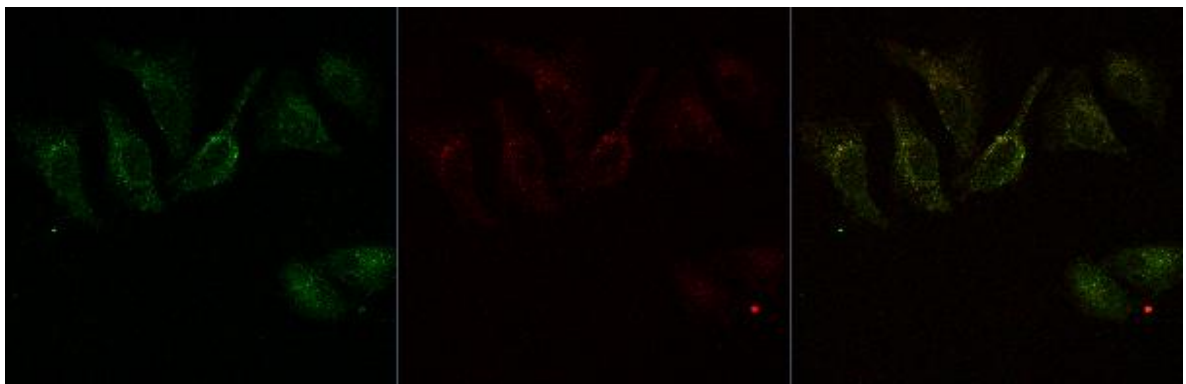
Incubation time

Rapid internalization of glutaraldehyde crosslinked 400 nm sized albumin nano-CLPA can be observed on Figure 4.7, throughout 0.5-6 hour incubation periods. Some internalization

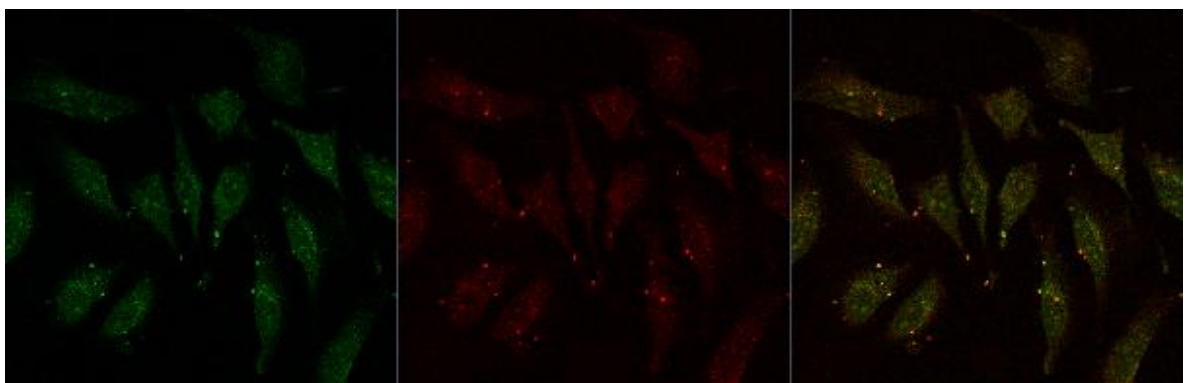
could be observed upon incubation period as short as 30 min (b), followed by gradual increase at prolonged periods, as could be visualized through increase in fluorescence intensity.



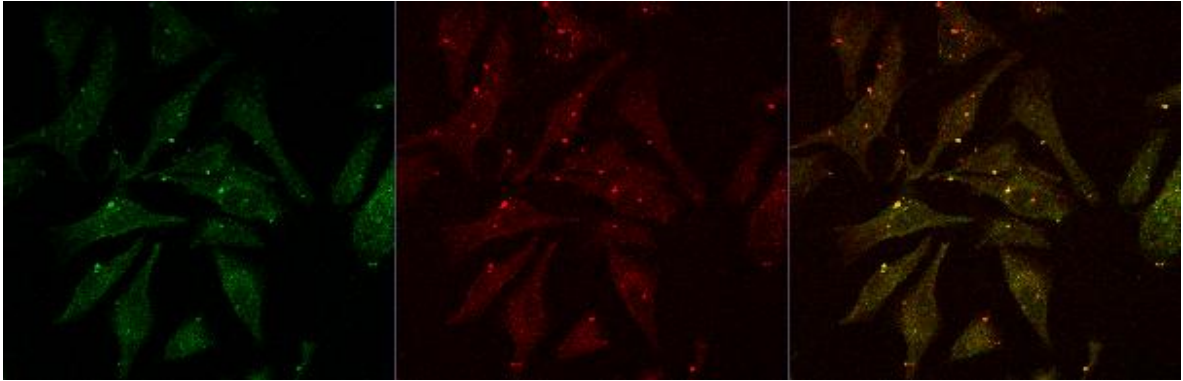
a) Control



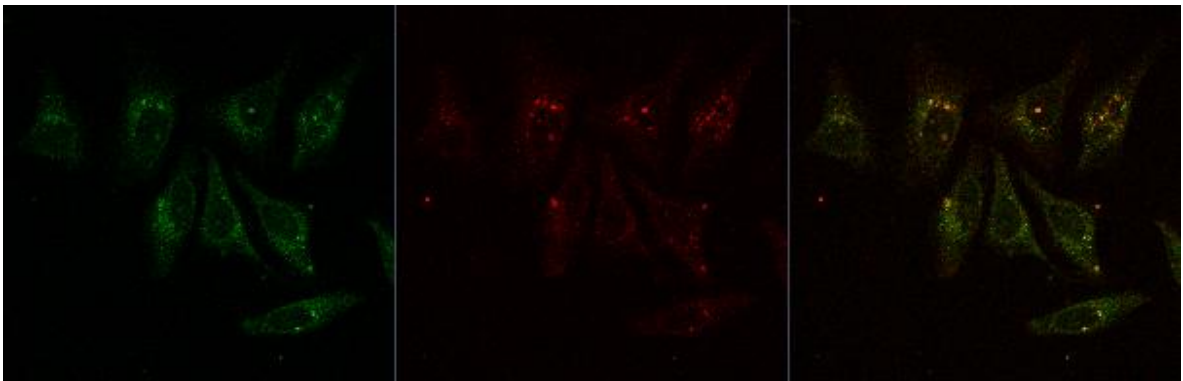
b) 0.5 h



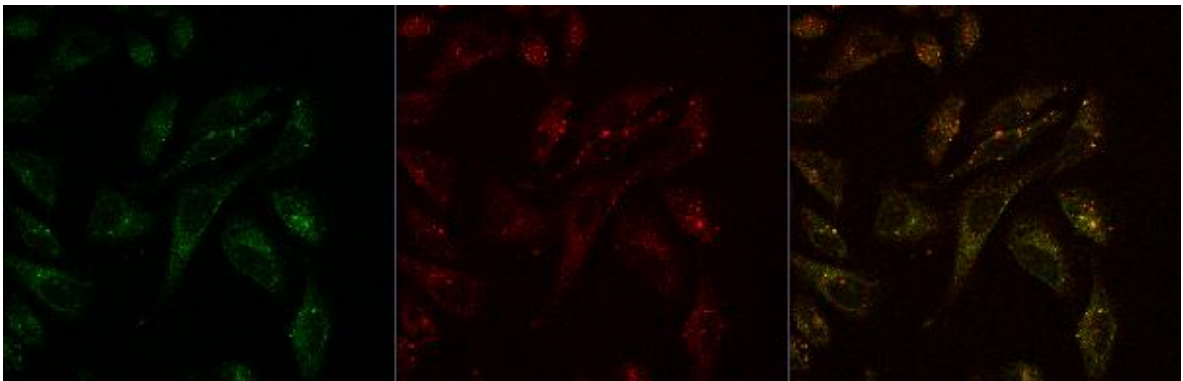
c) 1 h



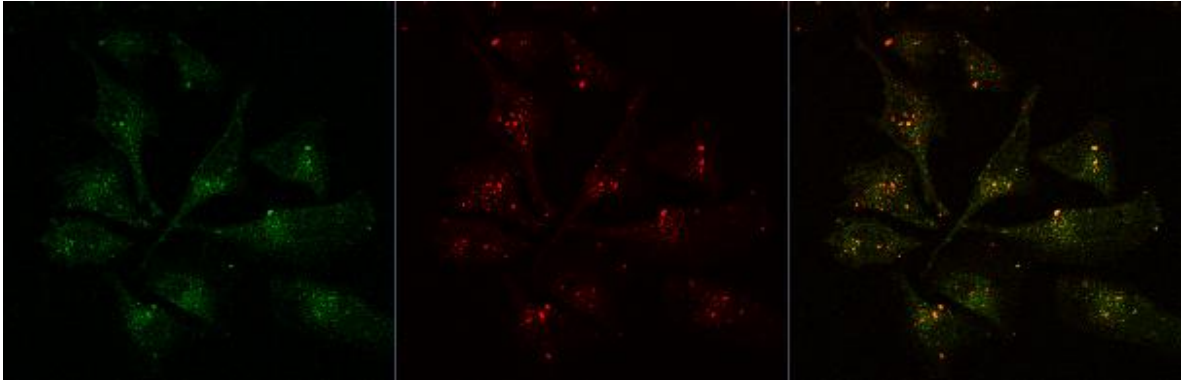
d) 2h



e) 3h



f) 4h



g) 6h

Figure 4.7: Internalization upon incubation with albumin nano-CLPA. HeLa cell culture (glutaraldehyde crosslinked, homogenized in glycerol medium to establish size of 400 nm particle size)

Co-localization analysis was performed using CoLocalizer Pro 1.0 software and Manders Overlap Coefficient (MOC) was used to estimate the degree of colocalization. Analysis was performed on the image corresponding to 6 hour incubation of nano-CLPA. 68.4% overlap of dansylated particles with lysosomal dye was detected (Figure 4.8).

The localization of engulfed particles was suspected to be dominantly located in lysosomes. Endocytosis of nano-particles through phagocytic and else pathways, both generally result in compartmentalization in lysosome⁵¹.

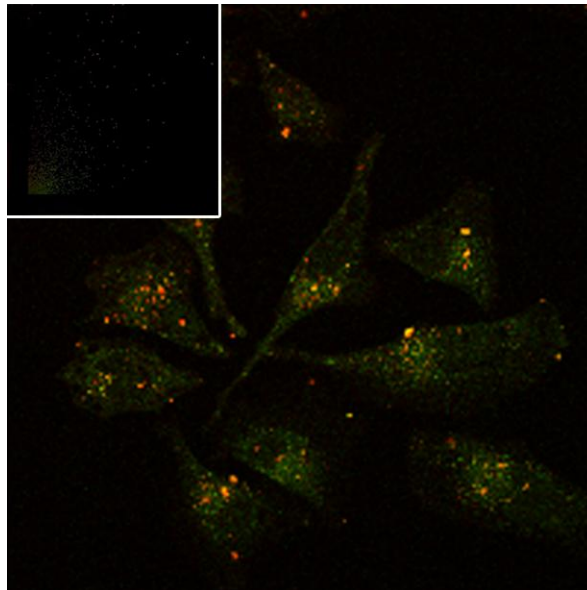


Figure 4.8: Co-localization analysis illustration upon incubation with albumin nano-CLPA and lysosomal staining dye. HeLa cell culture

Nano-CLPA particle size

Figure 4.9 demonstrates internalization of different particle size albumin nano-CLPA. Interestingly enough, no internalization is observed of 100 nm particles. Behavior of nano-CLPA, otherwise shown stable in PBS, was not investigated for FBS containing DMEM environment. It could be suspected, that irreversible re-agglomeration of higher surface area particles occurs rapidly preventing cell internalization. It could otherwise be explained by ability of smaller sized particles to escape the compartment, which was precedent through pumping out⁵².

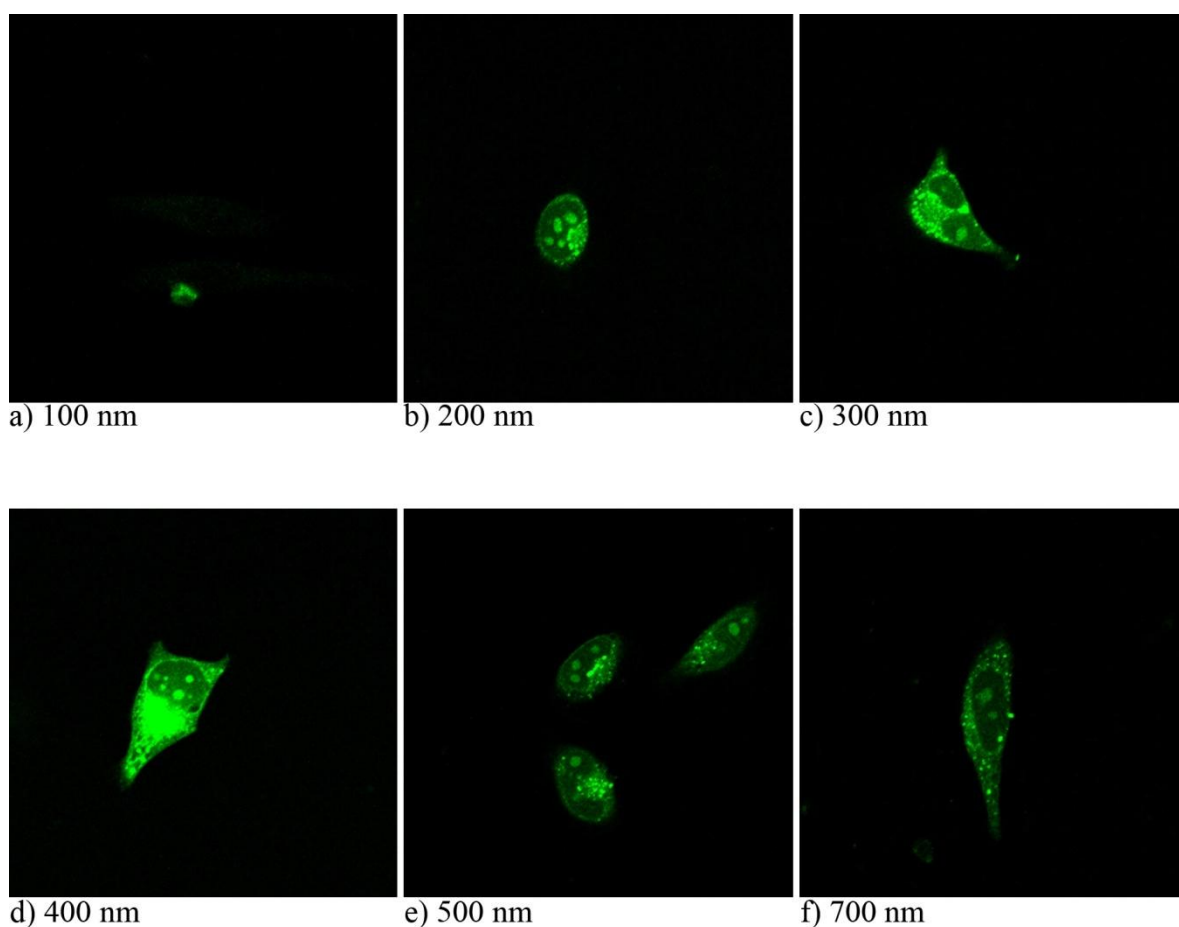


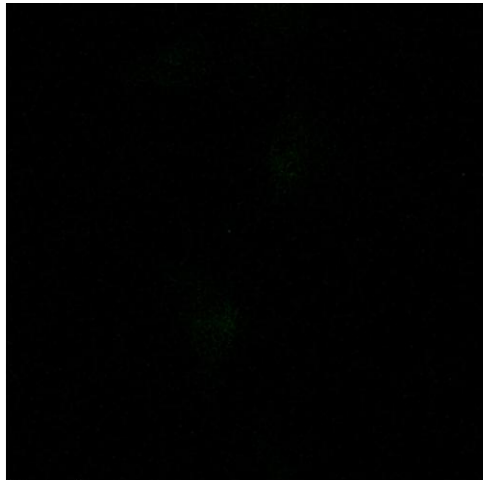
Figure 4.9: Size dependant internalization of albumin nano-particles. HeLa cell culture

Nano-CLPA surface modification

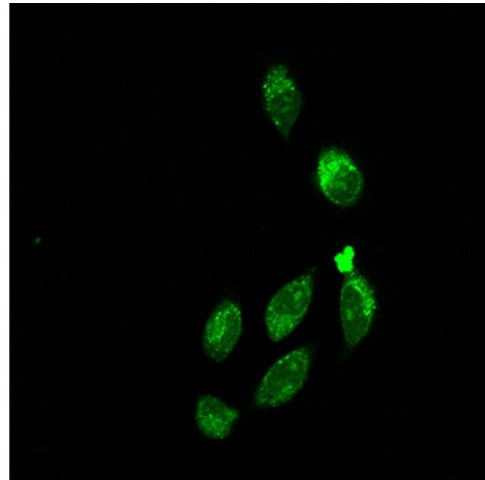
Modification of albumin nano-CLPA with monofunctional PEG amine 600, appeared to only slightly alter internalization, as monitored by fluorescence intensity. Some relative

decrease in intensity can be observed in case of higher PEG amine surface density, which could be readily explained by increase in overall hydrophobicity of the surface.

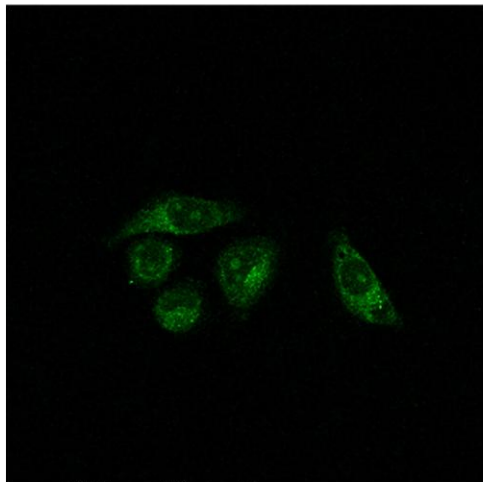
Modification with bifunctional PEG amine 1900, on the other hand, resulted in untraceable internalization at low PEG amine surface area, and much improved at higher PEG amine amounts. It could be rationalized, that suboptimal conformation of longer PEG amine chain on the surface due to lack of steric constraint took place in the case of low polymer distribution over particle surface, which was optimized by increase in the amount of the later. Internalization of the described particles is visualized on Figure 4.10. Furthermore, the comparable pattern can be observed upon incubation of the same particles in NIH/3T3 cell culture (Figure 4.11), therefore providing generality to the above observation.



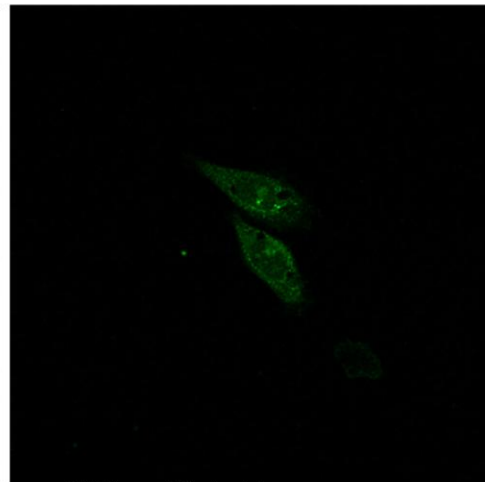
Control



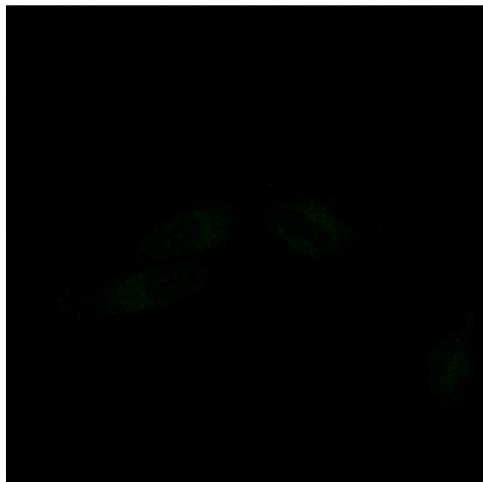
Unmodified nano-CLPA



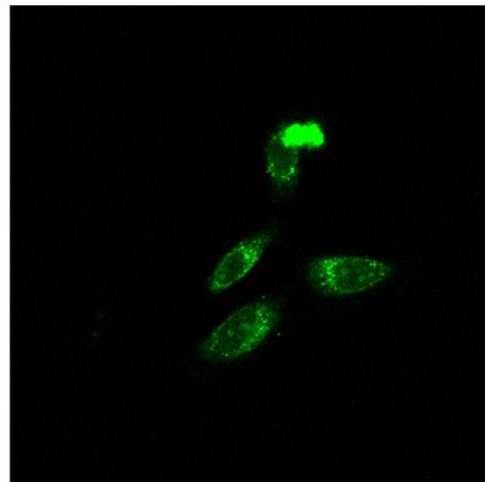
nano-CLPA modified with
monofunctional PEG amine (1:1 molar ratio)



nano-CLPA modified with
monofunctional PEG amine (1:10 molar ratio)



nano-CLPA modified
with bifunctional PEG amine (1:1 molar ratio)



nano-CLPA modified with
bifunctional PEG amine (1:10 molar ratio)

Figure 4.10: Internalization of PEGilated albumin nano-CLPA observed HeLa cell culture

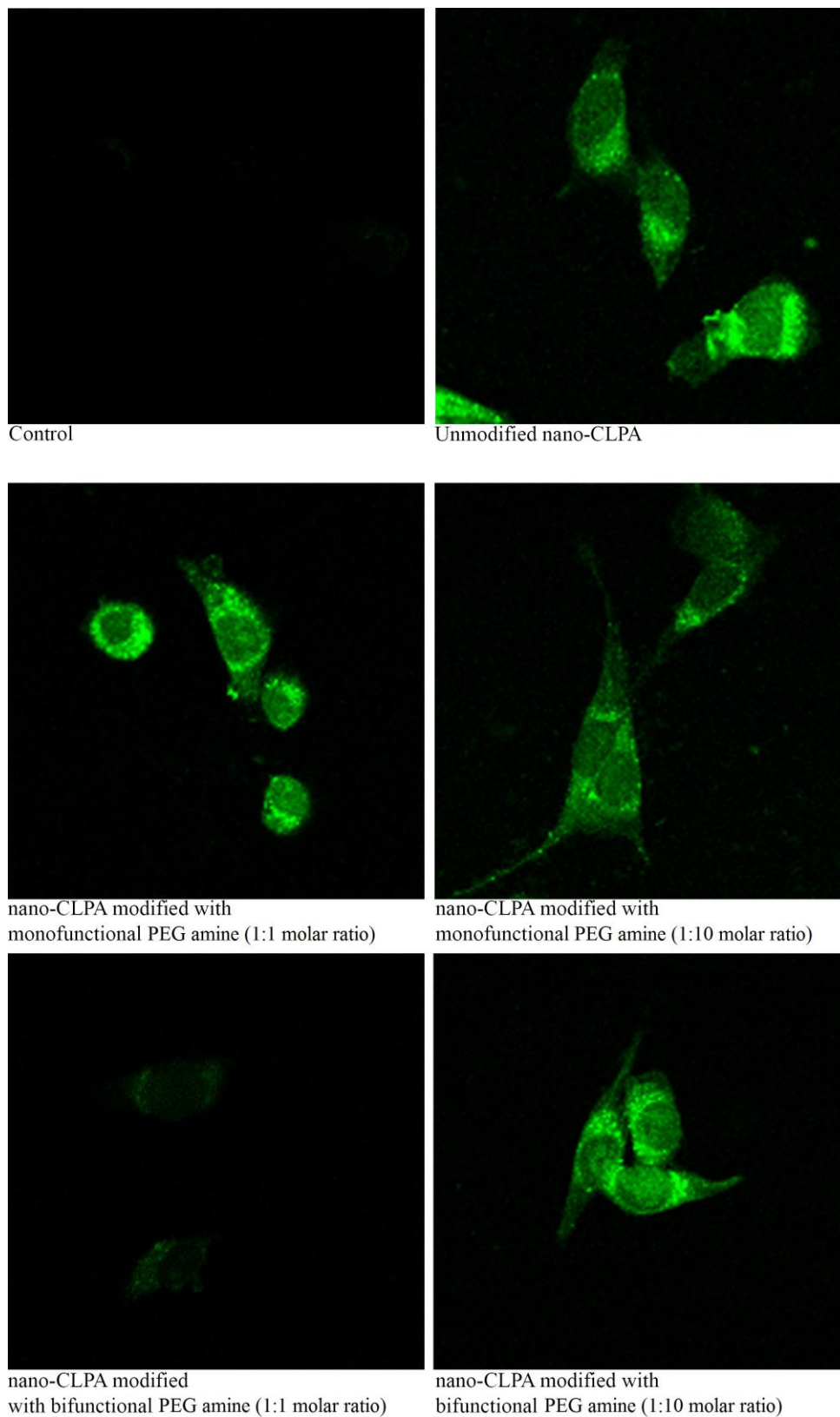


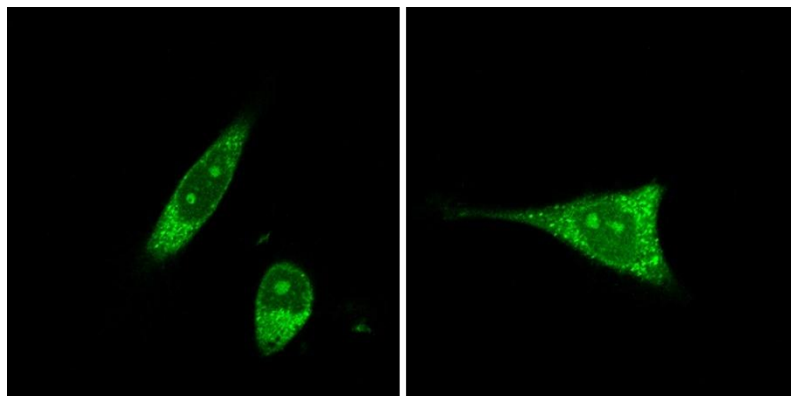
Figure 4.11: Internalization of PEGilated albumin nano-CLPA observed NIH3T3 cell culture

There has been precedence that in coating of nano-particles with amine functionalized PEG, polymer chain length hasn't significantly affected the internalization behavior⁵³. Nevertheless, parameters such as polymer chain length, and charge effect of functional groups on the surface and density of surface modification, must be further analyzed. These initial observations lead to conclude, that modification of nano-CLPA surface could be a plausible way to obtain desired internalization trend or otherwise, where necessary for a certain application, prevent internalization.

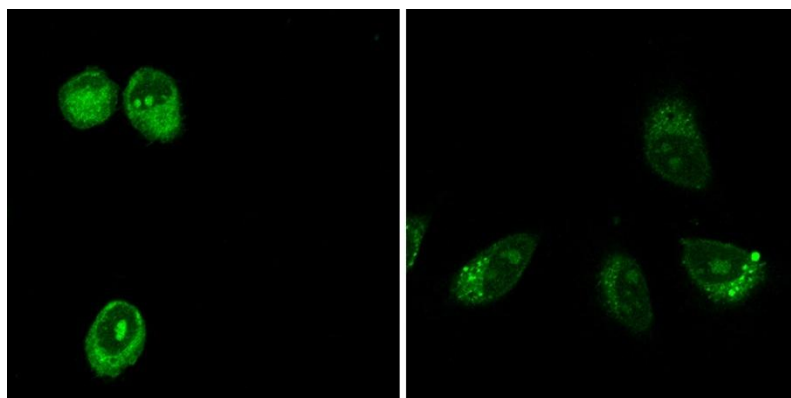
Homogenization medium

It has been initially suspected that particle shape and mechanical behavior may be the responsible parameters governing internalization. No evidence to this assumption has been observed throughout the results, including internalization of PEGylated nano-particles presented above.

Parameter suspected to effect the particle shape, namely homogenization medium, has been utilized here, furthermore presenting evidence rejecting the initial assumption. No detectable difference could be observed upon internalization of different protocol albumin alpha-galactosidase nano-CLPA (Figure 4.12)



a) albumin nano-CLPA internalization



b) alpha-galactosidase nano-CLPA internalization

Figure 4.12: Internalization of nano-CLPA upon homogenization in glycerol (left) and ethanol (right). HeLa cell culture

4.4.2.3. Cell viability upon nano-CLPA internalization as a function of particle concentration

Cell viability upon nano-CLPA internalization has been additionally assessed on HCT116, HEK293 and NIH3T3 cell lines, afforded by MTT cell viability assay.

Particle concentration dependant cell viability upon 3 hour incubation was assessed over the course of 2 days, on glutaraldehyde crosslinked albumin homogenized in glycerol medium and dextran polyaldehyde alpha-galactosidase nano-CLPA homogenized in absolute ethanol medium, to aid 400 nm particle sizes.

Confocal microscope imagery was obtained on additional cell cultures, upon internalization of the particles subsequently used for dose dependent proliferation study, in order to confirm that the effect is indeed related to internalization (Figures 4.13-15).

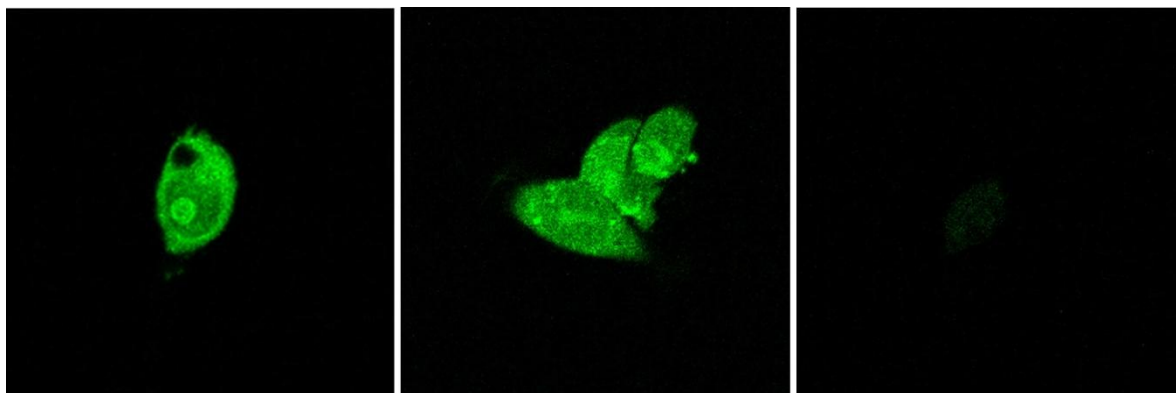


Figure 4.13: Confocal microscope images of internalized albumin (left) and alpha-galactosidase (centered) nano-CLPA presented against control cells (right) in HCT116 cell culture

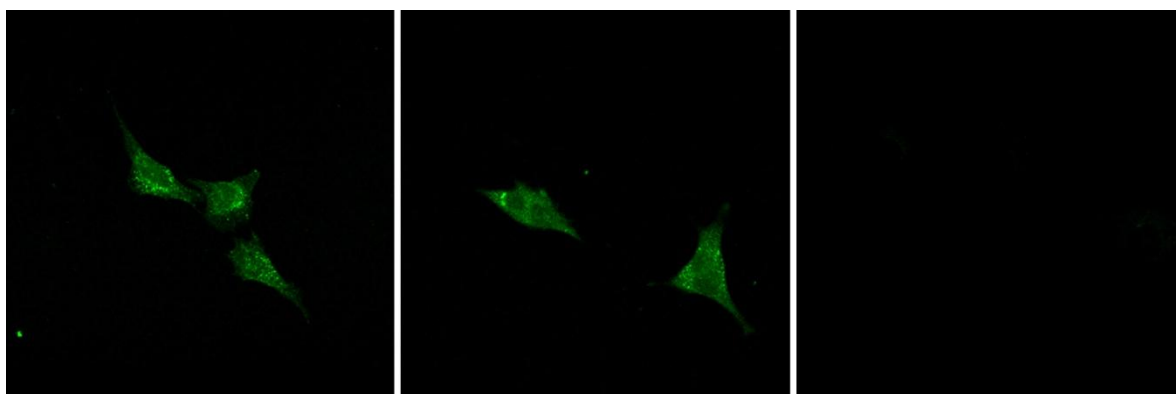


Figure 4.14: Confocal microscope images of internalized albumin (left) and alpha-galactosidase (centered) nano-CLPA presented against control cells (right) in NIH/3T3 cell culture

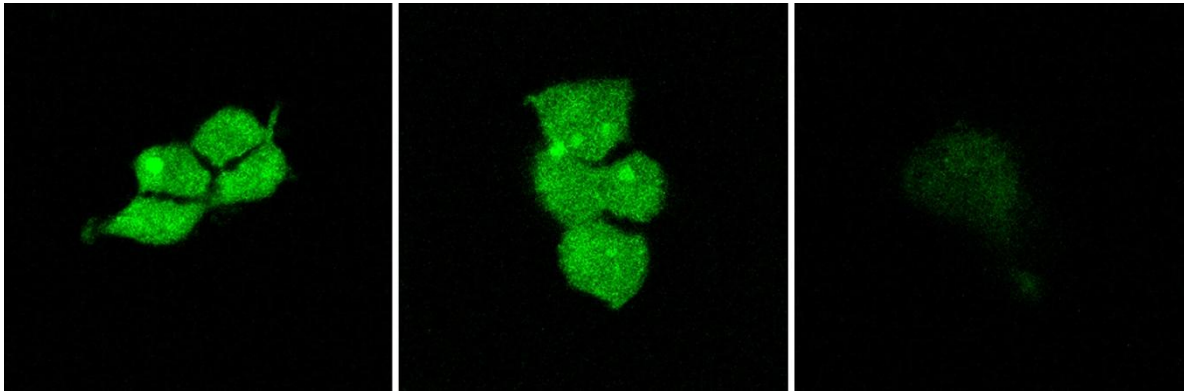


Figure 4.15: Confocal microscope images of internalized albumin (left) and alpha-galactosidase (centered) nano-CLPA presented against control cells (right) in HEK293 cell culture

Upon incubation with albumin nano-CLPA, reversible increase in proliferation could be observed at small dosage treatment and some cytotoxicity effect was detected at higher doses in HeLa cell culture (Figure 4.16). Somewhat more consistent dosage dependent trend was observed in alpha-galactosidase nano-CLPA treated culture, with observed proliferative induction of 20% 0.0 $\mu\text{g/ml}$ dose (Figure 4.17).

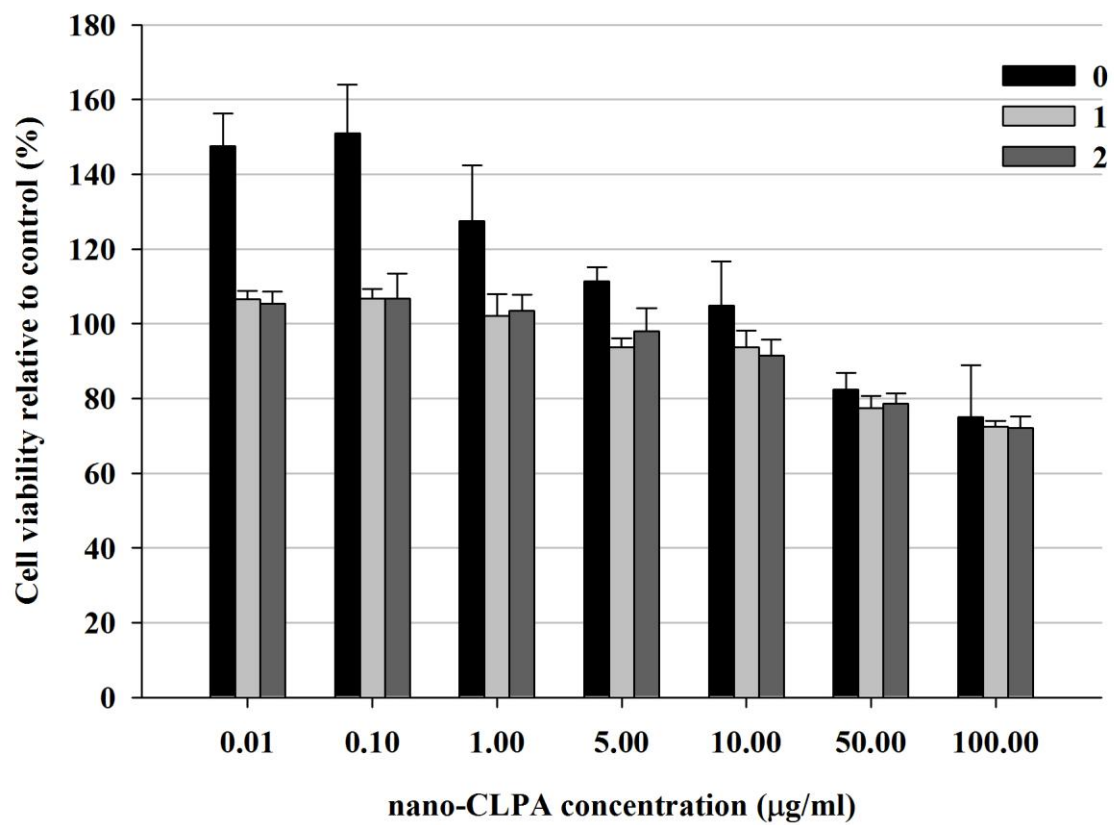


Figure 4.16: Dosage dependent effect of albumin nano-CLPA on HeLa cell proliferation

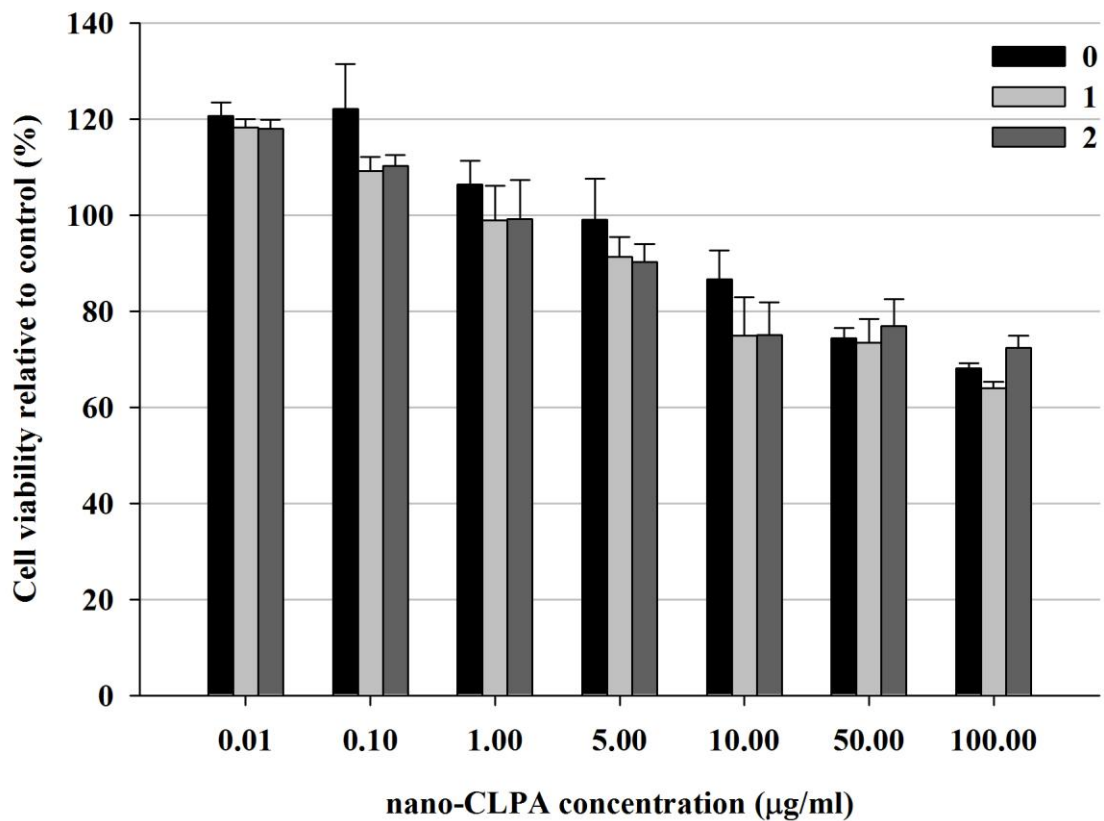


Figure 4.17: Dosage dependent effect of alpha-galactosidase nano-CLPA on HeLa cell proliferation

The pattern observed above resembled that of HCT116 cell culture, with the difference of proliferation increase in small doses more pronounced upon 24 hours after nano-particle treatment (Figure 4.18). This difference was assigned to different metabolic activities in between cell cultures. Furthermore, more pronounced cytotoxicity effect with increasing dosage was observed in both albumin and alpha-galactosidase nano-CLPA treatment (Figure 4.19) as opposed to although minor but prolonged proliferation induction of small doses in HeLa cell culture.

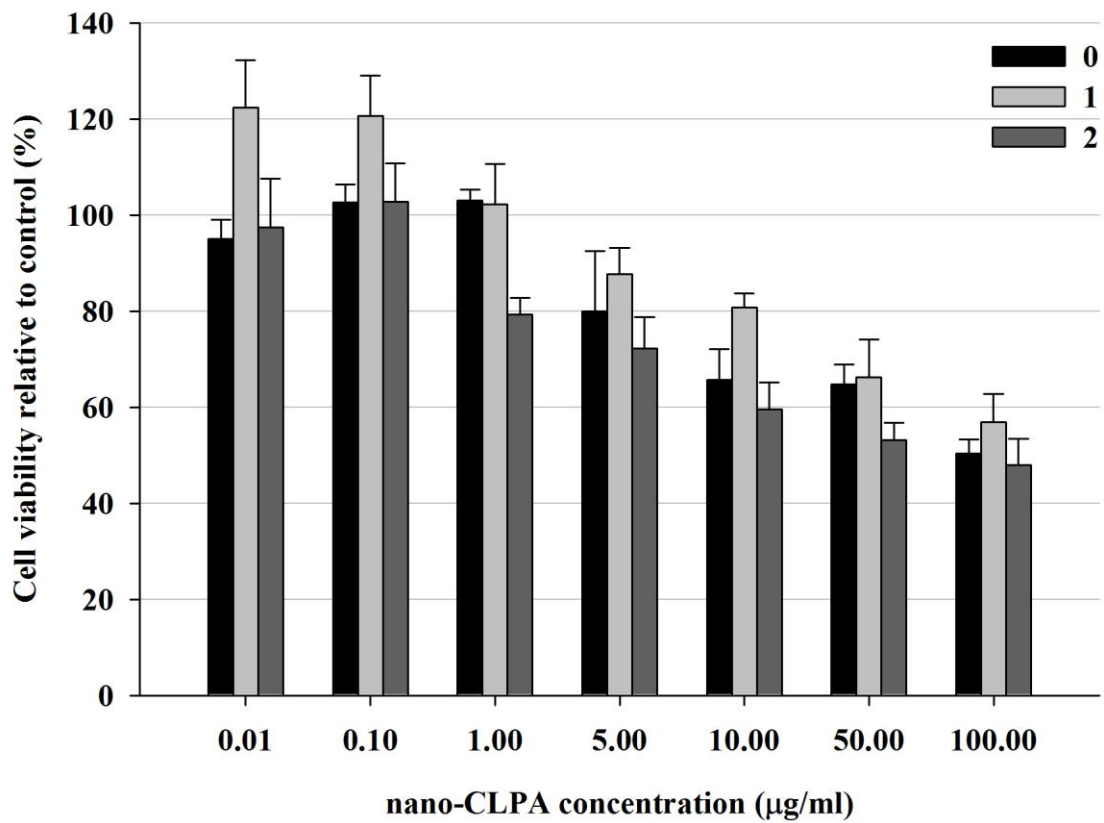


Figure 4.18: Dosage dependent effect of albumin nano-CLPA on HCT116 cell proliferation

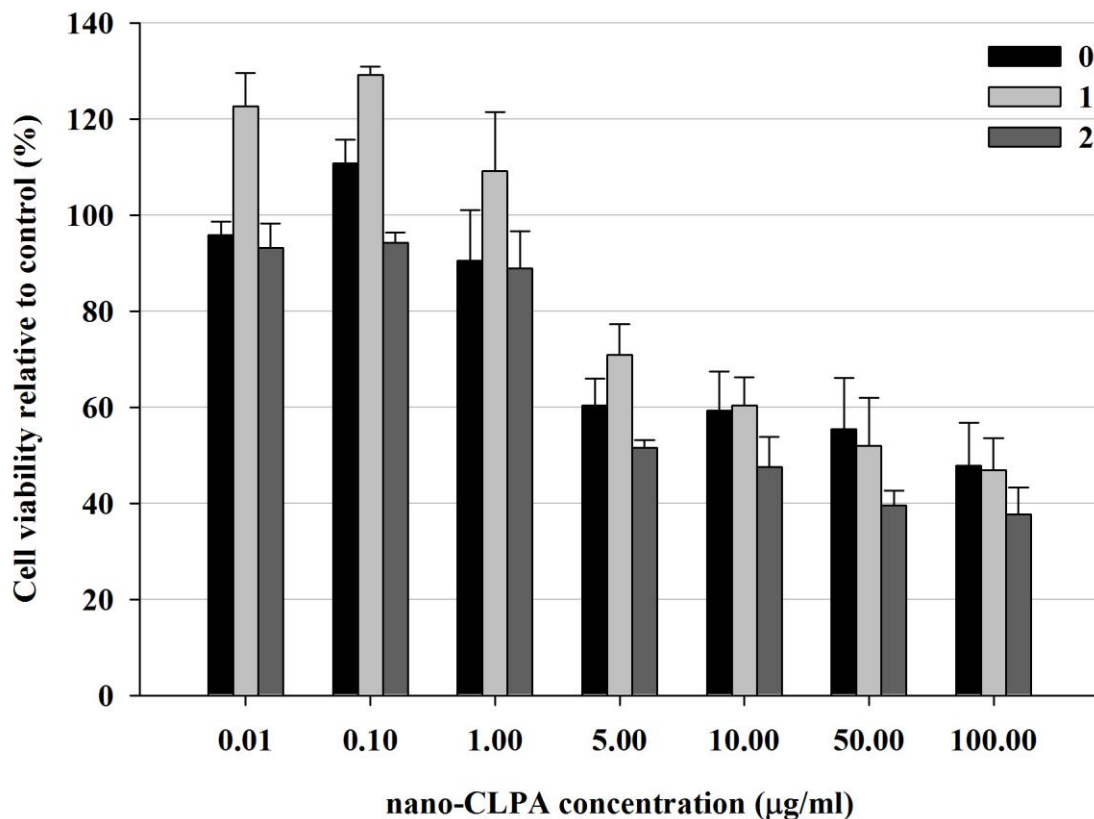


Figure 4.19: Dosage dependent effect of alpha-galactosidase nano-CLPA on HCT116 cell proliferation

Trials were also conducted on non cancerous cell lines, in order to further assess generality of effect of dosage related proliferation behavior.

Surprisingly enough, statistically insignificant cytotoxicity was detected upon treatment with high doses of both albumin and alpha-galactosidase nano-CLPA of NIH/3T3, as opposed to cancer cell lines assessed above. Slight proliferative induction could be observed upon internalization with albumin nano-CLPA, particularly at concentration of 0.1µg/ml.

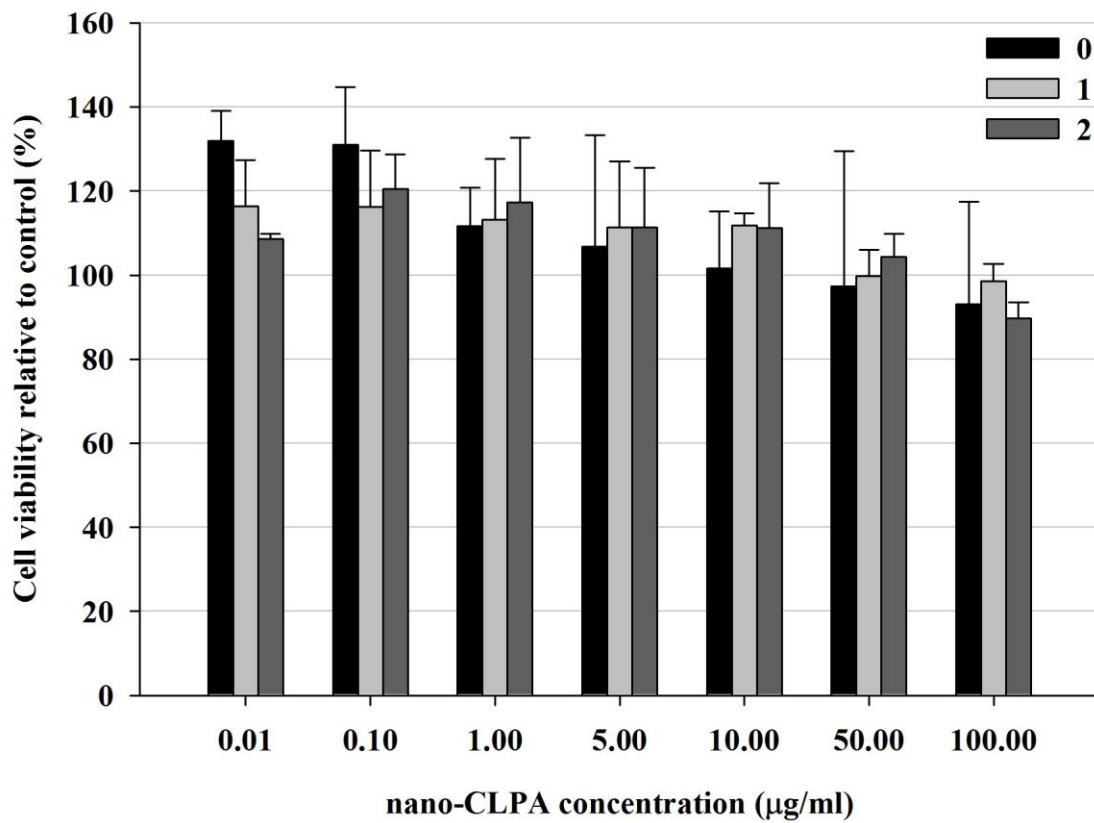


Figure 4.20: Dosage dependent effect of albumin nano-CLPA on NIH/3T3 cell proliferation

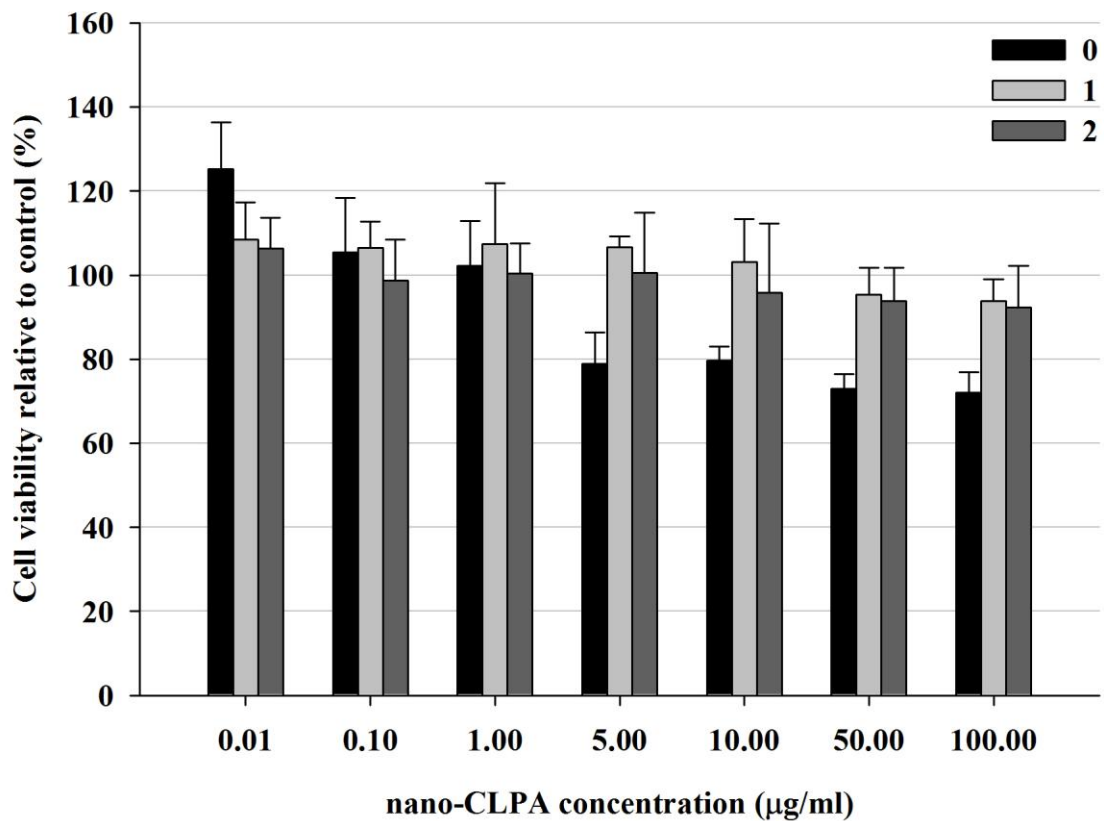


Figure 4.21: Dosage dependent effect of alpha-galactosidase nano-CLPA on NIH/3T3 cell proliferation

Highest proliferative induction could be detected in the case of small dosage treatment of HEK293 cell culture, once again most pronounced at 0.1 µg/ml nano-particle concentration. Some cytotoxicity was observed in case of high alpha-galactosidase nano-CLPA concentrations.

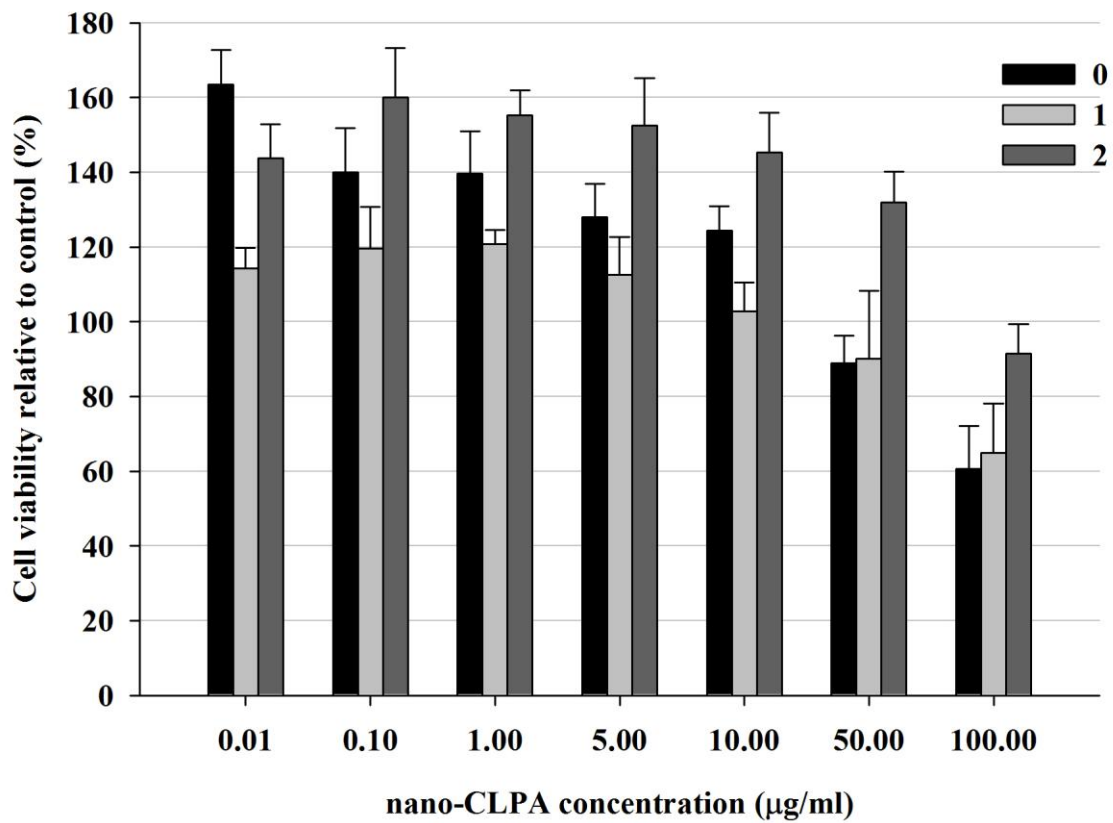


Figure 4.22: Dosage dependent effect of albumin nano-CLPA on HEK293 cell proliferation

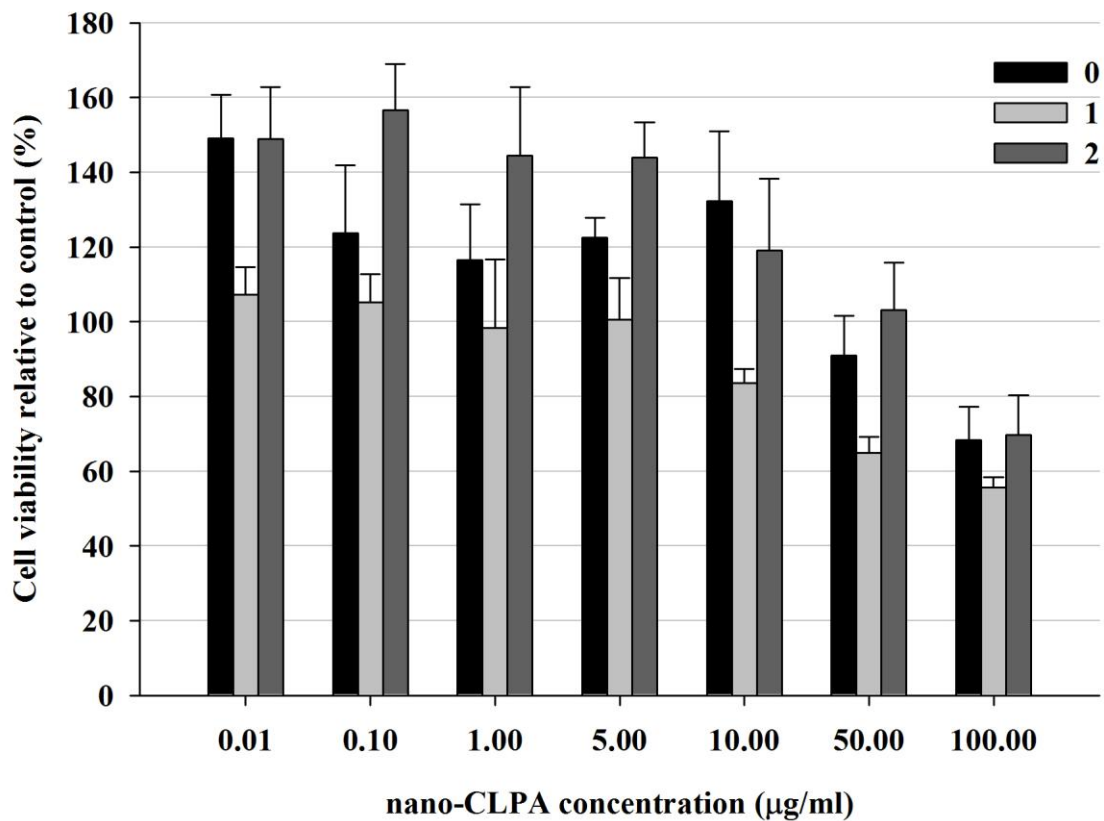


Figure 4.23: Dosage dependent effect of alpha-galactosidase nano-CLPA on HEK293 cell proliferation

The above results show good reproducibility upon 4 independent experiment repetitions, of triplicated measurements. Nevertheless, since viability was only assessed by MTT assay, the increase in color yields in cases of small dosages observed could actually be the result of increased mitochondrial enzymatic activity, rather than assumed proliferation induction. Alternative proliferation assessment techniques must be utilized in order to verify the above data.

5. Conclusion

Over the course of this study general methodology leading to crosslinked protein aggregates (CLPA) has been assessed on a number of proteins and optimized in detail on albumin, trypsin, chymotrypsin, lysozyme and hemoglobin. Furthermore, crosslinked protein lyophilizates (CLPL) were developed on the example of trypsin and chymotrypsin. Downsizing procedures were developed on the basis of the results obtained from precursor CLPA. The approach was utilized through mechanic and hydrodynamic shear modes. While successful utilization of both methods in generation of nano-particle species was established, hydrodynamic shear realized through homogenization was employed in further downsizing optimization, due to convenience and operating precision on the laboratory scale. Homogenization conditions, ie. homogenization medium composition, homogenization rate and time, along with precursor CLPA/CLPL synthesis protocol have formed operational parameters in conducted optimization.

Homogenization in salt and small sugar solutions have resulted in nano-particle generation, but with insignificant yield of approximately 10 %. Homogenization yield issue was resolve by incorporation of 10-70 wt% glycerol in homogenization medium, leading to nanonization yields approaching 100%. Furthermore, smaller particle generation capacity (nanonization efficiency) and homogeneous particle distribution have been greatly improved. Alternatively homogenization in absolute ethanol while retaining high nanonization yield has provided much milder conditions, shown necessary in the case of less rigid CLPA/CLPL formulations.

Homogenization rate formed the major parameter in adjusting the desired particle size, combined with appropriate glycerol concentration precision of 10 to 20 nm distribution could be achieved. Time of homogenization, on the other hand determined the quality of particle distribution, with at least 30 min homogenization required for glycerol medium and slightly reduced time of 20 min for absolute ethanol homogenizations in order to achieve higher quality of particle distribution homogeneity described.

CLPA/CLPL protocol effect could be generally described as more brittle formulations nanosized more readily, implying rigidity of precursor aggregate formation and higher

crosslinking degree. That being said, successful nanonization was achieved for all optimized CLPA/CLPL formulations through appropriate adjustment of homogenization parameters, with an exception of dehydrothermally crosslinked lyophilizates.

Finally, potential biomedical applications have been suggested on the example of hemoglobin, lysozyme and complex CLPA of the resultant co-aggregation. Preliminary *in vitro* studies have been performed on the model of albumin and alpha-galactosidase nano-CLPA. Successful internalization was demonstrated on particles of 200 nm and larger. No internalization occurred upon incubation with 100 nm particles. Internalization rapidly occurred within 30 min of incubation increasing with prolonged incubation times. Pegilated nano-particle appeared to modify internalization efficiency, and can be further explored as a parameter in achieving desired nano-particle - cell interaction. Viability assay showed some cytotoxicity upon treatment with higher nano-particle doses (in general 10-100 $\mu\text{g/ml}$ final concentration in the medium) dependant on cell culture involved. Higher cytotoxicity was observed in HeLa and HCT116 cultures, as compared to NIH/3T3 and HEK293 cultures. Some increase in cell proliferation was observed at low dose treatments (0.01-0.1 $\mu\text{g/ml}$) in some cases.

Much more extended studies are required to quantitatively assess the results, but this initial work provides an overview of nano-CLPA behavior.

It can be concluded that development of successful alternative to conventional nano-scale immobilized protein formulation has been achieved. The main benefit of the developed method is convenience and rapid synthesis mode of nano-particle generation. General applicability of the method has been demonstrated and can be further readily applied to desired protein type formulations.

The main focus of the future work involves analysis of detailed heterogeneous catalyst systems on the model of nano-CLPA, targeting to form a better understanding of the theoretical basis of kinetic and reaction limitations in the particle as a function of protocol and particle size. Particularly, construction of a working model for Michaelis-Menten enzyme kinetics under heterogeneous reaction conditions at fixed size distribution, thereby establishing the threshold size of the particle and substrate to avoid diffusion control and to ensure reaction control.

REFERENCES

- (1) Schmid, A.; Dordick, J. S.; Hauer, B.; Kiener, A.; Wubbolts, M.; Witholt, B. *Nature* **2001**, *409*, 258.
- (2) Zhang, D. H.; Yuwen, L. X.; Peng, L. J. *J Chem-Ny* **2013**.
- (3) Levitsky, V.; Lozano, P.; Gladilin, A.; Iborra, J. L. In *Progress in Biotechnology*; A. Ballesteros, F. J. P. J. L. I., Halling, P. J., Eds.; Elsevier: 1998; Vol. Volume 15, p 417.
- (4) Tran, D. N.; Balkus, K. J. *Acs Catal* **2011**, *1*, 956.
- (5) Jesionowski, T.; Zdarta, J.; Krajewska, B. *Adsorption* **2014**, *20*, 801.
- (6) Liu, W. S.; Wang, L.; Jiang, R. R. *Top Catal* **2012**, *55*, 1146.
- (7) Means, G. E.; Feeney, R. E. *Chemical modification of proteins*; Holden-Day: San Francisco, 1971.
- (8) Payne, J. W. *The Biochemical journal* **1973**, *135*, 867.
- (9) Mateo, C.; Palomo, J. M.; van Langen, L. M.; van Rantwijk, F.; Sheldon, R. A. *Biotechnol Bioeng* **2004**, *86*, 273.
- (10) Valdes, E. C.; Soto, L. W.; Arcaya, G. A. *Electron J Biotechn* **2011**, *14*.
- (11) Migneault, I.; Dartiguenave, C.; Bertrand, M. J.; Waldron, K. C. *Biotechniques* **2004**, *37*, 790.
- (12) Quicho, F. A.; Richards, F. M. *Proceedings of the National Academy of Sciences of the United States of America* **1964**, *52*, 833.
- (13) Haring, D.; Schreier, P. *Curr Opin Chem Biol* **1999**, *3*, 35.
- (14) Zelinski, T.; Waldmann, H. *Angew Chem Int Edit* **1997**, *36*, 722.
- (15) Zelinski, T.; Waldmann, H. *J Prak Chem-Chem Ztg* **1997**, *339*, 394.
- (16) Lalonde, J. *Chemtech* **1997**, *27*, 38.
- (17) Wang, Y. F.; Yakovlevsky, K.; Zhang, B. L.; Margolin, A. L. *J Org Chem* **1997**, *62*, 3488.
- (18) Cao, L. Q.; van Rantwijk, F.; Sheldon, R. A. *Org Lett* **2000**, *2*, 1361.
- (19) Cao, L.; Lopez, S. P.; Sheldon, R. A.; Van, R. F.; Google Patents: 2002.
- (20) Jansen, E. F.; Tomimatsu, Y.; Olson, A. C. *Archives of biochemistry and biophysics* **1971**, *144*, 394.
- (21) Goldstein, L.; Katchalski-Katzir, E. In *Applied Biochemistry and Bioengineering*; Lemuel B. Wingard, E. K.-K., Leon, G., Eds.; Elsevier: 1976; Vol. Volume 1, p 1.
- (22) Arruebo, M.; Fernandez-Pacheco, R.; Ibarra, M. R.; Santamaria, J. *Nano Today* **2007**, *2*, 22.
- (23) Martin, R. W.; Zilm, K. W. *J Magn Reson* **2003**, *165*, 162.
- (24) Lipscomb, W. N. *Proceedings of the National Academy of Sciences of the United States of America* **1973**, *70*, 3797.
- (25) Falkner, J. C.; Al-Somali, A. M.; Jamison, J. A.; Zhang, J. Y.; Adrianse, S. L.; Simpson, R. L.; Calabretta, M. K.; Radding, W.; Phillips, G. N.; Colvin, V. L. *Chem Mater* **2005**, *17*, 2679.
- (26) Mohamad, N. R.; Marzuki, N. H. C.; Buang, N. A.; Huyop, F.; Wahab, R. A. *Biotechnology, Biotechnological Equipment* **2015**, *29*, 205.
- (27) Simons, B. L.; King, M. C.; Cyr, T.; Hefford, M. A.; Kaplan, H. *Protein Sci* **2002**, *11*, 1558.

- (28) Kise, H.; Shirato, H. *Enzyme and Microbial Technology* **1988**, *10*, 582.
- (29) Costantino, H. R.; Griebenow, K.; Langer, R.; Klivanov, A. M. *Biotechnol Bioeng* **1997**, *53*, 345.
- (30) Vakos, H. T.; Kaplan, H.; Black, B.; Dawson, B.; Hefford, M. A. *J Protein Chem* **2000**, *19*, 231.
- (31) Liang, J. F.; Li, Y. T.; Yang, V. C. *Journal of Pharmaceutical Sciences* **2000**, *89*, 979.
- (32) Hoshino, Y.; Koide, H.; Urakami, T.; Kanazawa, H.; Kodama, T.; Oku, N.; Shea, K. J. *Journal of the American Chemical Society* **2010**, *132*, 6644.
- (33) Fang, Y.; Yan, S.; Ning, B.; Liu, N.; Gao, Z.; Chao, F. *Biosensors and Bioelectronics* **2009**, *24*, 2323.
- (34) Zhang, K.; Mao, L. Y.; Cai, R. X. *Talanta* **2000**, *51*, 179.
- (35) Govardhan, C. P. *Curr Opin Biotech* **1999**, *10*, 331.
- (36) Menfaatli, E.; Zihnioglu, F. *Artificial cells, nanomedicine, and biotechnology* **2015**, *43*, 140.
- (37) Kong, J.; Yu, S. *Acta Biochimica et Biophysica Sinica* **2007**, *39*, 549.
- (38) Al-Azzam, W.; Pastrana, E. A.; Ferrer, Y.; Huang, Q.; Schweitzer-Stenner, R.; Griebenow, K. *Biophysical Journal* **2002**, *83*, 3637.
- (39) Kaplan, H.; Taralp, A. *Tech Prot Chem* **1997**, *8*, 219.
- (40) Werth, J. H.; Linsenbuhler, M.; Dammer, S. M.; Farkas, Z.; Hinrichsen, H.; Wirth, K. E.; Wolf, D. E. *Powder Technol* **2003**, *133*, 106.
- (41) Qiu, P. H.; Mao, C. B. *Adv Mater* **2011**, *23*, 4880.
- (42) Cao, G.; World Scientific Publishing Company,; Singapore, 2004, p 1 online resource (448 p).
- (43) Delgado, A. V.; González-Caballero, F.; Hunter, R. J.; Koopal, L. K.; Lyklema, J. *Journal of Colloid and Interface Science* **2007**, *309*, 194.
- (44) Somasundaran, P.; Wang, D. In *Developments in mineral processing*; 1st ed.; Elsevier,; Amsterdam ; Boston, 2006.
- (45) McIntosh, T. J.; Lin, H. N.; Li, S. S.; Huang, C. H. *Bba-Biomembranes* **2001**, *1510*, 219.
- (46) Cao, L. Q.; van Langen, L.; Sheldon, R. A. *Curr Opin Biotech* **2003**, *14*, 387.
- (47) Braue, E. H.; Hobson, S. T.; Govardhan, C.; Khalaf, N.; Google Patents: 2002.
- (48) D'Agnillo, F.; Chang, T. M. S. *Nat Biotech* **1998**, *16*, 667.
- (49) Taralp, A.; Google Patents: 2011.
- (50) Beck, M. *Hum Genet* **2007**, *121*, 1.
- (51) Ma, X. W.; Wu, Y. Y.; Jin, S. B.; Tian, Y.; Zhang, X. N.; Zhao, Y. L.; Yu, L.; Liang, X. J. *Acs Nano* **2011**, *5*, 8629.
- (52) Stern, S. T.; Adiseshaiah, P. P.; Crist, R. M. *Part Fibre Toxicol* **2012**, *9*.
- (53) Chen, R. J.; Yue, Z. L.; Eccleston, M. E.; Williams, S.; Slater, N. K. H. *J Control Release* **2005**, *108*, 63.